

MINISTRY OF SCIENCE AND HIGHER EDUCATION
OF THE RUSSIAN FEDERATION
Federal State Budget Educational Institution of Higher Education
«Ivanovo State Polytechnic University»

Manuscript rights

吴忻舟

Wu Xinzhou

**IMPROVEMENT OF DESIGN TECHNOLOGY
OF WOMEN'S DIVING WETSUITS**

Dissertation
for the degree of candidate of sciences
05.19.04 Technology of garments

Scientific adviser – Prof., Dr.Sc., V.E.Kuzmichev

Ivanovo 2022

CONTENT

	Page
LIST OF ABBREVIATIONS	5
LIST OF FIGURES	7
LIST OF TABLE	11
INTRODUCTION 1	13
INTRODUCTION 2	17
1 REVIEW OF MODERN DESIGN OF FEMALE WETSUIT	18
1.1. Introduction of wetsuit.....	18
1.1.1. A brief history of wetsuit.....	18
1.1.2. The current situation of the wetsuit markets.....	20
1.1.3. Modern wetsuit design style.....	22
1.1.4. Wetsuit technology.....	26
1.2. Current wetsuit material.....	29
1.2.1. Brief classification of wetsuit material.....	29
1.2.2. The relationship between material properties and clothing structure.....	32
1.3. Compression pressure and wearing comfort.....	33
1.3.1. The classification of compression clothing.....	33
1.3.2. Pressure measurement methods.....	34
1.3.3. Clothing pressure distribution on the human body.....	36
1.3.4. Clothing comfortable pressure.....	37
1.4. Anthropometric measurement.....	39
1.4.1. Modern systems of dimensional features.....	39
1.4.2. Influence of dynamic postures on the change in dimensional features.....	41
1.5. Construction of a modern wetsuit drawing.....	43
1.6. Application of 3D technology in clothing design.....	47
1.6.1. Application of scanned body and avatar.....	47
1.6.2. 3D compression clothing design.....	49
The purpose and directions of the dissertation research.....	51

2 ANTHROPOMETRIC DATABASE	53
2.1. Grouping torsos of female bodies	53
2.1.1. The ratio of the front and back half-girths of the body	53
2.1.2. Cross-sections of the female torso	54
2.1.3. New grouping of bodies by shape and torso	55
2.1.4. Improved mannequins of typical bodies	57
2.2. Changing the dimensional features of the human body	59
2.2.1. Body measurements change in static	59
2.2.2. Changing the dimensional features of a body in dynamic	61
Conclusion of Chapter 2	68
3 STUDY OF COMPRESSION OF MATERIALS	69
3.1. Compression of clothing at the levels of girths of a female body. . .	69
3.2. Relationship between body reduction, material elongation and compressive pressure	75
3.2.1. Compressibility of the soft tissues of the human body	75
3.2.2. Tension of materials	77
3.3. Structural additions	79
Conclusion of Chapter 3	81
4 RELATIONSHIP BETWEEN INDICATORS OF MATERIALS MECHANICAL PROPERTIES AND PRESSURE OF CLOTHES ON THE BODY.	83
4.1. Mechanical test of wetsuit materials.	83
4.2. Correlation-regression analysis	87
4.3. Prediction model	88
4.4. Check on prediction mathematical models	89
Conclusion of Chapter 4	90
5 DEVELOPMENT OF WETSUIT DESIGN	91
5.1. Investigation of wetsuit pattern design	91
5.1.1. Initial prototype for tight clothing	91
5.1.2. Basic wetsuit pattern	94

5.2. Development of digital replica	95
5.2.1. Modeling of important parts of the body.	95
5.2.2. Modeling the initial and basic patterns of a wetsuit.	97
5.3. Improving the basic design of the wetsuit.	100
5.3.1. Improvement and verification of the sleeve design	100
5.3.2. Experimental verification of other design improvements	105
5.4. Practical evaluation of the developed design	109
5.4.1. Comparison with existing analog models.	109
5.4.2. Underwater testing and evaluation of results	113
5.4.3. Verification of theoretical pressure values	115
Conclusion of Chapter 5	116
CONCLUSIONS AND SUGGESTIONS	117
RECOMMENDATIONS, PROSPECTS FOR FURTHER DEVELOPMENT OF THE THEME	118
REFERENCES	119
APPENDIX A. Results of anthropometric measurements	131
APPENDIX B. Results of measurements of pressure and tension of materials	136
APPENDIX C. Results of testing wetsuit materials on the KES-F	143
APPENDIX D. Algorithm for constructing a basic wetsuit design and test results	150
APPENDIX E. Act of checking	165

LIST OF ABBREVIATIONS

BG	–	Bust girth
WG	–	Waist girth
HG	–	Buttock/hip girth
BG _F	–	Bust front
BG _B	–	Bust back
WG _F	–	Waist front
WG _B	–	Waist back
HG _F	–	Hip front
HG _B	–	Hip back
TG	–	Thigh
SL	–	Side upper torso length
FNP-WL	–	Neck front point (FNP) to waist line front
BNP-WL	–	Neck back point (BNP) to waist line back
FWP		Waist front point
BWP		Waist back point
Cr	–	Crotch
BP	–	Bust point
P1	–	Standing
P2	–	Standing and arms up
P3	–	Lie prone on a floor with face down, the legs straight backward on a floor
P4	–	The arms stretch forward, and the feet draw up towards the hip, calf 90° with the body on a floor
P5	–	The arms stretch forward, the legs straight backward underwater
P6	–	The arms stretch forward, and the feet draw up towards the hip, calf 90° with the body underwater
DIF	–	Differences between the same body measurements in standing and lying prone postures
ΔG	–	Changes of body girths

- ΔL – Changes of body lengths
- CR – Chloroprene-rubber
- SBR – Styrene-butadiene rubber
- SCR – Styrene-chloroprene rubber
- P_{max} – Maximum acceptable pressure, kPa
- E_{max} – Maximum elongation/ease of the material, %
- E_{min} – Minimum ease of the material for pattern design, %
- ΔG_{max} – Maximum changes of body girths, %
- ΔG_{DIF} – Girth difference between different postures, %
- RC_b – ratio of compressive performance of the human body, %
- RC_m – ratio of material compression, kPa/%
- KES-FB – Japanese KES textile materials test instrument
- EMT – KES index, elongation at 500 cN/cm load on KES-FB1
- F – Force (load) of tension, gf.cm
- LT – The coefficient of completeness of the stretching /relaxation diagram on KES-FB1
- WT – Tension energy on KES-FB1, gf.cm/cm²
- 2HG – Elasticity for minute shear on KES-FB1, gf/cm
- e – Natural base approx. 2.718
- Sig* – The level of statistical significance of the hypothesis
- S.D. – Standard deviation
- DR – Deformed replica, a 3D virtual model
- PW1-S – The mass-production/ purchased wetsuits of small size
- DW-Y1 – The designed wetsuits of Y1 female body type

LIST OF FIGURES

- Fig.1.1 Earliest wetsuit: a – Jack O’Neil wetsuit vest; b – J.S. Foster modeling an early design of the Bradner wetsuit[120]
- Fig.1.2 The history of development of the Olympic suit[74]
- Fig.1.3 Diving suit introduction
- Fig.1.4 Wetsuit types
- Fig.1.5 Protection design: a – different materials and coating craft on knee; b – color design of the arena’s SAMS wetsuit[59]
- Fig.1.6 The methods of wetsuit stitching: a – flatlock with glue; b – blind stitch with glue/tape
- Fig.1.7 Zip locations: a – front zip; b – front upper zip; c – front upper zip, O’Neill Double super seal neck, wide adjustability, and a secure lock down, fully adjustable and watertight; d – back upper zip, O’Neill exclusive F.U.Z.E. (Front Upper Zip Entry) system offers a fresh alternative, closure keeps you dry and allows unrestricted flexibility [43,50]
- Fig.1.8 Wetsuit material: a – different thickness materials; b – the combination of multiple-layer
- Fig.1.9 The relationship between water temperature and wetsuit thickness
- Fig.1.10 Application and researches on female clothing pressure
- Fig.1.11 AMI-3037 airbag contact pressure tester and pressure measuring system (Donghua University Laboratory, Shanghai, China)
- Fig.1.12 Scanned dynamic postures: a – male [104]; b – female [105]
- Fig.1.13 Wetsuit patterns: a – the pattern derived from 3D to 2D [105]; b – a pattern for the standard body type of Korean men [16]
- Fig.1.14 Wetsuit division line options
- Fig.1.15 Rating of problem areas when swimming underwater
- Fig.1.16 Dynamic positions of the wetsuit skin tension during swimming movements ([a [123], b [107], c [98])
- Fig.1.17 3D design of a motorcyclist suit (a) [72] and compression pants (b) [81]
- Fig.1.18 Virtual wetsuit testing: a – digital deformation [105]; b –map of the material strain [125]

- Fig.2.1 Definition of landmarks “a” and “b” for the division of BG into BG_F and BG_B: a – sections of a symmetrical bust; b – section of an asymmetrical bust; c – alignment of the girths of the bust, waist and hips with a common sagittal line and the midpoint “o” (o₁ - point at waist level, o₂ - point at hip level)
- Fig.2.2 Profile of standard torsos (A1 and A2)
- Fig.2.3 Outline of standard torsos: a – sagittal planes of standard torsos (Y, A, B, C) and subtypes; b – cross-sections of the bust and waist
- Fig.2.4 Mannequins B (traditional), B1 and B2 altered to new torso types
- Fig.2.5 Scheme of body measurement by Anthroscan
- Fig.2.6 Probability distributions of Q-Q plots: a – height; b – BG
- Fig.2.7 Change in the cross section of the girth of the bust in statics: a – the initial shape of the section; b – section shape after compression
- Fig.2.8 Dynamic postures
- Fig.2.9 The average differences between measurements for body A
- Fig.2.10 Digital replica mesh of the female body: a – bust cross-sections before and after static compression; b, c – cross-section of chest girth before and after changing the position of the hands in dynamics; d – polygonal mesh editing scheme
- Fig.2.11 Section in the sagittal plane in the position of the upper body tilt forward
- Fig.3.1 The pressure tests: a – test schematic diagram; b – AMI-3037-10 system; c – sensors
- Fig.3.2 Scheme for measuring the deformation of the girth of the figure during elongation of materials
- Fig.3.3 Body girths deformation ΔG_{\max} , -%
- Fig.3.4 Q-Q plots: a – measured pressure P_{\max} ; b – measured elongation E_{\max}
- Fig.3.5 Maximum ease values E_{\max} on seven body girths, %: a – measured under the material course; b – measured under the material wale
- Fig.3.6 Measurements of the average maximum P_{\max} , kPa: a – measured under the material course; b – measured under the material wale
- Fig.3.7 The RC_b values: a – in the material course; b – in the material wale
- Fig.3.8 The RC_m values: a – in the material course; b – in the material wale

- Fig.3.9 The steps of the minimum design ease E_{\min} calculation
- Fig.3.10 The E_{\min} values: a – in the material course; b – in the material wale
- Fig.4.1 Experimental fabric: a –structure of layers; b – Knitted structure of surface
- Fig.4.2 KES tension (500 cN/cm) test M1...M4 in course
- Fig.4.3 Relations between the tension load and the elongation EMT: a – in the course; b – in the wale
- Fig.5.1 Reference lines corresponding to the female body
- Fig.5.2 Drawing of the prototype: a – the top with points marks; b – example of points marks; c – the lower; d – sleeve
- Fig.5.3 Finished drawing of initial prototype
- Fig.5.4 Basic wetsuit pattern modified based on the initial prototype
- Fig.5.5 Flowchart of the wetsuit simulation process
- Fig.5.6 Try on the wetsuit on the initial undeformed avatar: a – virtual connection of parts of the wetsuit prototype; b – areas with misfit, c – compression pressure distribution
- Fig.5.7 Try on test with basic wetsuit (Fig.5.4): a – virtual sewing of basic type wetsuit; b – try on in CLO
- Fig.5.8 The measured virtual pressure values on body part
- Fig.5.9 Raglan line design schemes: a – the position of the raglan line on the body in front (left) and behind (right); b – diagram of the drawing of the best sleeve; c – variants of the studied configurations of raglan lines
- Fig.5.10 The pressure differences of 49 sleeve designs
- Fig.5.11 Stages of designing virtual twins of bodies and virtual try on in the CLO 3D program
- Fig.5.12 Location and allowable configurations of the shape of the side part of the wetsuit
- Fig.5.13 Verification of side part configuration: a – side part optimization; b – pressure map; c – material deformation map
- Fig.5.14 Scheme of the drawing of the front part of the wetsuit: a – the location of the yoke and the central part in the drawing and body; b, c – virtual try on of a wetsuit without and with a yoke

- Fig.5.15 The designed wetsuit pattern blocks
- Fig.5.16 Simulation of designed wetsuit: a – try on in P1; b – try on in P2; c – try on in P3, P4 (P5, P6); d, e – pressure maps; f – material strain mesh maps
- Fig.5.17 The appearance of the existing PW factory-made wetsuits (a – in the Y1 body; b – in the A1 and B1 bodies) and the appearance of problem areas on the existing PW and the developed DW wetsuit (c)
- Fig.5.18 Appearance of the new wetsuits: a – for body Y1 made of material M2; b – for body Y1 from material M3
- Fig.5.19 The static subjective evaluation results
- Fig.5.20 The dynamic subjective evaluation results
- Fig.5.21 Results of body pressure measurements: a – industrial wetsuits PW; b – developed wetsuit
- Fig.5.22 Diving experiment: a – the appearance of the “Wuhan diving center”; b, c, d – scuba diver in different poses
- Fig.5.23 Results of subjective assessment of the fit of DW wetsuits during underwater testing

LIST OF TABLES

Table 2.1	Bodies types involved in the experiment
Table 2.2	Average front and back segments of 8 subtypes
Table 2.3	Main body measurements from 3D body scanner
Table 2.4	The maximum ΔG_{DIF}
Table 2.5	The maximum ΔL_{DIF}
Table 3.1	Experimental wetsuit materials
Table 3.2	Recommendations of other researchers about P_{max} , kPa
Table 3.3	The average E_{max} of material M1...M4, %
Table 3.4	The maximum material P_{max}
Table 3.5	The average materials RC_b on M1...M4, kPa/%
Table 3.6	The average materials RC_m on key body parts, kPa/%
Table 3.7	E_{min} of M1...M4 for 8 body types
Table 4.1	Materials EMT values
Table 4.2	KES-FB1...4 indexes (*Low load 50 gf/cm)
Table 4.3	Correlation coefficients between P_{max} , E_{max} and KES indexes
Table 4.4	Absolute difference between calculated and measured material strips M1...4 pressure
Table 5.1	Variant number
Table 5.2	Absolute difference value between calculated and measured material pressure M2 on 7 body parts

INTRODUCTION 1

The relevance of the work. Diving is becoming more common all over the world and the demand for diving suits is gradually increasing. The use of diving suits includes entertainment, professional work, military use, etc., so the demand for diving suits is constantly increasing. The choice of materials, design of a wetsuit is determined by its area of application. The main indicator of the wetsuit fit is dynamic immersion comfort. To achieve high levels of comfort in a wetsuit underwater, information from various fields of knowledge is needed: human morphology, materials science, the effect of pressure on the human body, and so on.

Positive results for improving wetsuit design were obtained in the research of J.H. Choi, M.M. Naglic, and S. Petrak, etc. Nowadays, some researchers use new information technology as the main means to develop compression clothing. The human body scanner, as a mainstream tool for measuring dimensional characteristics, has been used in many countries (United States, United Kingdom, France, China, etc.) to develop national anthropometric plans and has improved the design process of human body clothing systems, in the works of Lo Yun, Li Yue (IGTA), I.A. Petrosova (MSUDT), I.V. Tislenko (IVGPU). At present, the rise of new 3D simulation software technology has provided beneficial help for rapid design of clothing and objective evaluation, especially in the works of Guo Mengna (IVGPU), Zhe Cheng (IVGPU). These new methods for wetsuit design will humanize the decision-making, increase the clothing comfort, and transfer the designers' opinions to the virtual environment in accordance with the "body-wetsuit" system. Designers can perform virtual fitting and evaluate the quality of art design decisions before actual manufacture.

The research has been done in 2016–2020 at the department of garment design at the Ivanovo State Polytechnic University according to the state assignment No. 2.2425.2017 / 4.6 on the topic **“Development of software for virtual design of static and dynamic systems “body-clothing” and virtual fitting of FashionNet”**.

The work corresponds to the following points of the scientific specialty passport 05.19.04: 1. Development of theoretical foundations and the establishment of general laws for designing clothes for bodies of typical and untypical physique; 5. Improvement of assessment methods and design of clothing with specified consumer and technical and economic indicators.

The degree of problem elaboration. Currently, there is no general design method for female wetsuit, and many aspects have not been studied and systematized, especially the aspect of dynamic fit control for different female morphologies underwater. The existing design mostly simply adds large negative ease to compress the human body, which obviously can not satisfy the different morphologies. From the perspective of optimizing the comfort and functionality of the wetsuit, these aspects need to be considered – female torso, material pressure, wetsuit pattern, and the dynamic fit and comfort.

Currently, there is no general method for designing a women's wetsuit, the problems that arise have not been studied and systematized. One of the main design challenges is to provide freedom of movement underwater for women with various morphologies. With the existing approach, negative ease of allowances is set for the body compression, which, obviously, does not fully take into account its morphology. In order to improve the comfort and functional properties of a wetsuit, it is necessary to take into account the morphology of the human body, its susceptibility to material pressure, ensuring optimal articulation of the parts of the wetsuit, as well as dynamic fit and comfort.

Keywords: female body, wetsuit construction, pressure, dynamic fit

The aim of research is to improve design process of the female wetsuit.

The main tasks of the research are to solve the following tasks:

1. To study the modern design, manufacturing technology, and materials of the female wetsuit, summarize all related information, including material thickness, sewing stitch, and all the possible locations of their contour/internal lines on the surface of female bodies, and make artistic and constructive evaluations and analysis.

2.To develop a new scheme for grouping of female torsos based on the existing female body classification, for the optimal arrangement of division lines.

3.To study female dynamic soft tissue deformation range of different body parts based on basic diving postures and hydraulic pressure under two environments: above and underwater.

4.To study the dependence between the material deformation of the wetsuit, on one side, and the change of the body size, on the other side.

5. Measure the allowable pressure range and deformation limits for different body areas.

6. Develop indexes that allow to identify the comfort of a wetsuit on its design solution.

7. Improve the method of female wetsuit designing.

8. Evaluate and check the design technology of the wetsuit parts templates in accordance with the “deformable avatar - digital wetsuit” system in the CLO virtual environment.

9. Make approbation by evaluating and checking theoretical developments. The rationality of the design process for female wetsuits needs to be tested from a practical point of view and criteria for assessing the quality of the results obtained in the process of virtual modeling should be established.

The objects of research – female bodies of various anthropological types, female wetsuit, wetsuit materials, real and virtual systems “body(avatar) - wetsuit”, the process of construction and virtual simulation.

The subject of research – the process of designing female wetsuit.

Research methods and tools. To measure, read and visualize images of scanned bodies (called scanatars), a VITUS Smart XXL 3D scanner (Human Solutions, Germany, DIN EN ISO 20685 standard) with the Anthroscan program was used. The Kawabata Evaluation System KES (Japan) was used to test the mechanical properties of textile materials. The AMI-3037-10II (Japan) was used to record clothing pressure on the body. The CLO 3D virtual software was used for virtual body modeling and fitting. 3ds Max was used to edit polygon shapes.SPSS

was used to analyze the measurement results using correlation and regression analysis, reliability analysis, and checking the normality of the distribution of the measurement results.

The scientific novelty is establishment of dynamic changes in the sizes of various parts of the female body under the influence of the aquatic environment and ergonomic postures and their application to develop of wetsuit design.

The following scientific results were obtained for the first time.

1. New method of grouping female bodies based on new torsos measurements of front and back.

2. The relationship between the deformation of the wetsuit material and the pressure exerted on the soft tissues, equations for predicting pressure values, and an index of the compression ratio.

3. The permissible boundaries for changing the bodies girths for various parts.

4. The influence of pressure and ergonomic postures on the change in the dimensions of female bodies.

Provisions for the defense.

1. New grouping of female torsos.

2. A method for evaluating the compression of various body girths by the materials.

3. Dynamic changes of female bodies in conditions of being underwater.

4. A new method of designing a female wetsuit.

5. Digital twins of deformed female bodies in a virtual environment to test the design of a wetsuit and determine the compressive ability of materials.

The theoretical significance of the study is to establish the values of critical factors, including a new anthropometric grouping of female torsos, deformation of soft tissues under the influence of typical underwater positions and hydraulic pressure, to create dynamic comfort for a female wetsuit.

The practical significance of the study is to develop a method for measuring human figures and a 3D method for designing a female wetsuit with a simulation of a dynamic landing and a comfortable state underwater. This will help wetsuit

designers to quickly modify and optimize designs, improve productivity and accommodate operating conditions.

The reliability of the results and conclusions is ensured by the convergence of the results of experimental and theoretical studies, the statistical adequacy of the obtained equations, the use of modern and trusted measuring instruments.

Approbation of the results. The results of the research were reported and received a positive assessment at the following conferences: the second international scientific-practical conference "Models of innovative development of textile and light industry based on the integration of university science and industry. Education-science-production" (**Kazan, 2016**); All-Russian scientific student conference "Innovative development of light and textile industry (INTEX-2016)" (**Moscow, 2016**); International scientific and practical conference "Modeling in engineering and economics" (**Vitebsk, 2016**); Information Environment of the University (**Ivanovo, 2017**); AUTEX world textile conference (**Istanbul, Turkey, 2018**); International conference Aegean international textile and advanced engineering conference AITAE 2018 (**Mytilene, Greece, 2018**); International conference on computational modeling and applied mathematics (**Wuhan, China, 2018**). International conference on advanced materials, electrical and mechanical engineering AMEME (**Xiamen, China, 2020**); International conference on technics, technologies, and education ICTTE (**Yambol, Bulgaria, 2020**); in the educational cycle "New opportunities for everyone" of the national project "Education" in the course "Digital bows in virtual space: artistic and industrial design of 3D clothes in virtual reality" (**Ivanovo, IVGPU, 2020**).

The main results of the research were published in 12 papers, including 1 article in a Russian journal from the list of the Higher Attestation Commission (BAK), 6 articles in English-language journals included in the Web of Science database, 5 abstracts and conference papers, the total volume of which is 3.625 printed lists (personal contribution 1.8 printed lists).

The structure of the dissertation. The dissertation consists of 5 chapters, set out on 165 pp., including 18 tables, 65 figures, 5 appendixes, 176 literary sources.

INTRODUCTION 2

Digitalization of the fashion industry, which has been actively taking place in the last decade of the XXI century, significantly expands the opportunities for making scientific design and technological decisions. Increasingly, computer programs are used not only for their intended purpose, but also as a new means of technological research. Thanks to powerful functionality, computer programs allow to model different situations, choose rational solutions from many possible options and predict the consequences of their material implementation.

The experience gained in computerizing the processes of preparing new garments for production allows positive consideration of their possibilities for solving more complex problems. Traditionally, the design of ergonomic compression garments used in specific conditions, and causes difficulties among patternmakers due to the lack of scientific design algorithms. To create such algorithms, an extensive database is needed, including formalized information about all the elements involved in creating a high-quality garment: a human body in static and dynamics, significant indicators of material properties, drawings of garment parts as a prototype of a flattening garment and external conditions. The multi-factorial content of the process and the difficulty of finding a rational combination of factors do not guarantee a single correct solution. Naturally, modern computer technologies that provide such an opportunity open a new direction in industrial clothing design.

The purpose of this scientific and qualification research is to develop a knowledge base and a rule base for the application of existing body scanning technologies and computer 2D and 3D programs for generating virtual twins of female bodies and wetsuits in dynamic conditions underwater.

Chapter 1. REVIEW OF MODERN DESIGN OF FEMALE WETSUIT

1.1. Introduction of wetsuit

1.1.1. A brief history of wetsuit

Diving has become more and more widespread all over the world, and the demand for diving suits by diving enthusiasts has gradually increased. It is an important equipment of diving operation, widely used in military and civil diving. Diving has a history of more than 2000 years. It is used for salvage, repair, and underwater exploration and engineering with or without professional tools, it was popular in military applications during World War II.

V. Mark made the first diving suit in the 1910s. It is developed for the U.S. Navy and is mainly used in deep-sea and salvage works to provide maximum body protection [48]. DuPont scientists invented Neoprene in 1930 [53]. The real starting point of the diving suit is after the Second World War. In 1952, American physicist H. Bradner created a prototype wetsuit, and J.S. Foster modeled an early design of the Bradner wetsuit in 1953 (Figure 1.1a) [120]. In the same year, Jack O'Neill created the first wetsuit vest with neoprene instead of foam rubber, which he sold in surf shops. (Figure 1.1b). Moreover, Bob & Bill Meistrell formed their Body Glove Company and commercialized diving suits.

In the 1950s, the diving suit was made of sponge rubber and untreated foam strip. The users used talcum powder to prevent rash, because the diving suit had no lining, and glue and the heat-sealing tape made the seams of the diving suit hard and uncomfortable. These early wetsuits were of poor quality and not durable [61]. Later, nylon material was used in the inner layer of the diving suit, reducing skin friction. In the 1960s, the wetsuits had an outer lining and a nylon inner lining. In the 1970s, wetsuits crafts became the focus of development, bringing better seam bonding technology.



Figure 1.1 – Earliest wetsuit: a – Jack O’Neil wetsuit vest; b – J.S. Foster modeling an early design of the Bradner wetsuit [120]

From the end of the 20th century to the beginning of the 21st century, with the wide application of new technologies and materials in diving equipment, diving equipment is lighter and more economical. Diving activities began to change from professional operation to mass consumption leisure sports and gradually become a new fashion sports mode.

The development of the diving suit is similar to the swimsuit. The swimsuit has become a kind of special garment in the 19th century. In the early 1910s, a one-piece short swimsuit emerged [24]. Then, the swimsuit covers more and more areas of the human body, and it is tight and ergonomic. In addition to the full-length diving suit, other styles are similar to the appearance of the swimwear, but the materials are obviously different. The evolution history of the Olympic swimming suit is as shown in Figure.1.2.



Figure 1.2 – The history of development of the Olympic suit [74]

1.1.2.The current situation of the wetsuit markets

Active diving has a good effect on the recovery of exercise injury, improvement of cardiopulmonary function and inhibition of cancer cell proliferation [122]. Due to the increased hydraulic pressure, the contact and extrusion on the body surface can make the human capillary expand and improve the circulation function of subcutaneous blood vessels. The water environment has a significant effect on sports injuries of joints, bones, and muscles. Therefore, the rehabilitation of sports injuries is combined with diving in the field of sports medicine; breathing high compressed air or oxygen underwater can improve the heart and lung function of the human body when correct diving; and the balanced hydraulic pressure on the human body can promote blood circulation [102, 110].

According to different purposes, diving activities can be divided into three categories: leisure/sports diving, professional diving, and military diving.

1) Leisure/sports diving

Leisure and sports diving began 50 years ago in Europe, the United States, and other countries. According to statistics, more than 60 million people in the United States have diving certificates, accounting for 2/5 of the world's diving activities; Europe and Australia also account for 2/5. Leisure and sports diving in Europe and America have formed a mature industrial scale, which is the main consumer market of diving equipment at present. The worldwide diving sites are mainly located in Europe, Egypt, Australia, Southeast Asia, South Pacific, Caribbean; Russian diving sites are mainly located in Barents Sea (Баренцевоморе), White Sea (Белое море), Baikal (Байкал); Chinese diving sites are mainly located in Hainan Province, Taiwan, Xisha Islands, East China Sea, etc.

Based on a report from the “Zhongqian Company (China) Prospectus 2016”. The global market value of wetsuits, equipment products, and services is approximately 2.625 trillion Rubles. Among them, the Chinese domestic market is about 36.7 billion Rubles. With the development of diving tourism and scenic spots in China, the diving tourism income has nearly reached 2.5 billion rubles in 2015

and maintained an annual growth rate of 30%, the market space is huge. According to the statistics of the Chinese Underwater Association(CUA) in 2019, more than 8 million people took part in diving activities in some coastal cities of China and maintained an average annual growth rate of 30%. So far, China has 1300 registered diving clubs according to the annual survey of the China Dive Community. At present, more than 60% of Chinese diving enthusiasts are female under 30 years old, 58% of purchasers of diving goods are female, and 83% of whom have bachelor's degree or above, their professional fields concentrated on high-pressure and high salary industries such as culture, finance, business, consulting, etc [45].

A recent report from the Diving Equipment and Marketing Association (DEMA), the cumulative worldwide divers are more than 30 million [44]. Moreover, the world's largest scuba diving training organization PADI has issued more than 27 million diver certifications around the world [64], to 2019, the annual growth rate of the Chinese diving certificate amount is about 40%, which is 8 times the global average growth rate. From the "Scuba Diving Participation Report 2019" published by the Sports and Fitness Industry Association (SFIA), there are 3 million participants in the US, and 24.5% are about 25...34 years old, 32% dive more than 8 times per year [66].

2) Professional diving

The professional fields of the diving industry include the traditional salvage activities of sunken ships or objects, as well as the extended application fields, such as the submarine mineral resources exploitation, life or emergency rescue, obstacle removal, bridge, and tunnel construction, sea products breeding and fishing, and scientific experiments, etc., the service scope covers all rivers, lakes, and seas.

According to the statistics and analysis of the China Diving & Salvage Contractors Association in 2015, it is estimated that by 2020, there will be no less than 3 million people engaged in professional diving worldwide, including fishery, industry, salvage, search and rescue, marine archaeology and exploration, etc., of

which China accounts for more than 5%.

3) Military diving

In the military field, the diving suit is necessary equipment for underwater frogman, submarine force, and deep-water salvage force.

1.1.3.Modern wetsuit design style

Diving activities often occur in cold water. Even in warm climates, underwater divers will wear wetsuits to keep warm. For example, a diver can only survive for about 3.5 hours at -10 m without wearing diving suit, and a diver wearing diving suit can survive for about 24 hours in water at the same temperature [47]. The depth limit is ruled by the certification authority, the depth of entry-level diving ISO 24801/24802 shall not exceed -18m or -20m, higher-level divers shall not exceed -30, -40, -50, or -60 m, depending on the certification level and agency.

The basic requirements of diving suits are warm and to protect the human body from hypothermia and injury [76]. Depending on function and purpose, diving suits can be divided into wet, dry, and semi-dry, as shown in Figure 1.3.

Dry diving suit is completely isolated from water, and mainly relies on the air layer. It is mainly used in professional deep water and sewage environment. The operation is more complicated and the price is high. The professional quality demand of the diver is higher.

Semi-dry diving suit is sealed through the rubber hoop of the neck, wrist and ankle to keep the body dry and warm, with the same basic characteristics as the dry diving suit, seals radically reduce the amount of water that can enter the suit. Only feet, hands, and heads directly exposed to the water or wearing wet headgear, gloves and other measures to keep warm, mainly used in diving tourism, fishing, underwater construction and so on [65].

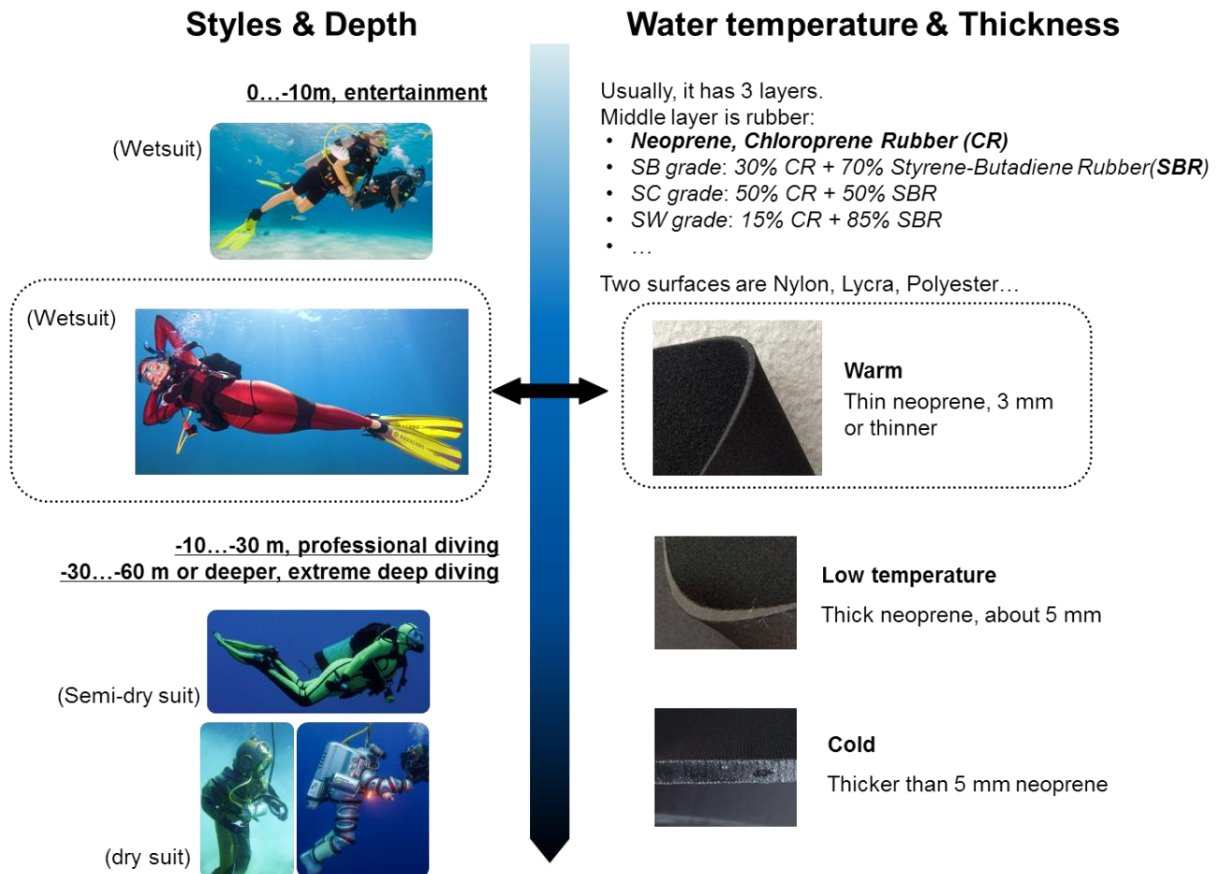


Figure 1.3 – Diving suit introduction

Wetsuits are the most frequently used in water recreation activities (such as diving, surfing, etc.), also known as free diving suits, and can be equipped with scuba (self-contained underwater breathing apparatus); wetsuits mainly work through insulation, when the body gets into the water, the neoprene allows a small amount of water to penetrate the suit and a layer of water, the body heat warms up this water layer to near body temperature. Because this layer cannot escape, it creates a barrier between the skin and the cold water surrounding the body. Wetsuits are light and flexible, comfortable to wear, low in price, high in work efficiency, suitable for diving activities during leisure sports, it is different from dry suit and semi-dry suit, it allows water to enter. Figure 1.4 shows the various kinds of wetsuit and their corresponding suitable temperatures.

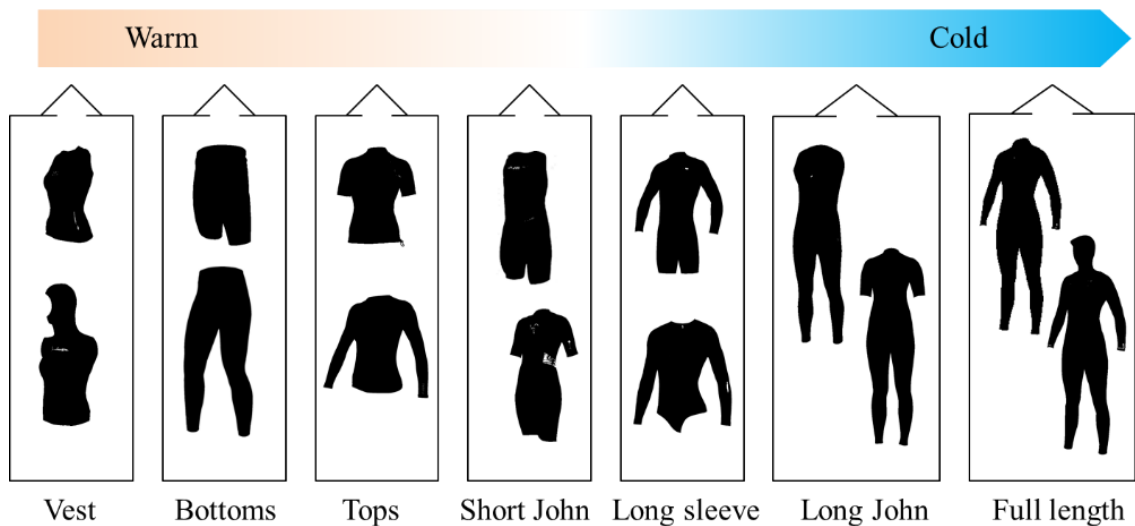


Figure 1.4 – Wetsuit types

The detailed explanation is as follows:

Vest, bottom, tops are spring wetsuits, usually for short time and warm, shallow water.

Short John / long sleeve are wetsuits with short-legs that extends from your torso down to your thigh. The shorty wetsuit is to keep the body at a comfortable temperature, during the summer sailing season.

Long John covers the torso and legs; it offers less restriction on arm movement and it is suitable for an active sailor at a warmer temperature.

Full length (long type) is a one-piece wetsuit with long arms and legs usually has a zip in the front or back with a long tether so you can pull it up and down.

As users continue to grow, higher demands are proposed on the functionality, comfort, and aesthetics of wetsuits. Not only high requirements for material, but also higher requirements for the structure and style. A correct shape ensures optimal thermal conditions. A suit that is too loose will allow too much water to circulate over the diver's skin. A suit that is too tight is very uncomfortable and can impair circulation. It depends on the inflowing water and clothing thickness to keep warm between the suit and the diver's skin, the less seawater circulation between them, the better the warm effect. So, the suit must fit the diver's body shape adequately [142]. For this reason, many divers choose to have wetsuits custom-tailored to optimize the thermal conditions [78].

The flow of water between the skin and clothing mainly depends on diving suit pattern structure, material insulation performance, and special craft. The wetsuit can be classified according to material, thickness, sport type, appearance, and style, as well as zipper opening position.

The styles and structures of wetsuits. In order to meet the needs of professional divers, the back of the diving suit is longer than the front part [37]. And water flow is the main resistance in swimming, tight design reduces the resistance in swimming. The raglan sleeve increased shoulder motion range, and the cutting seams of the sleeve are designed according to the human body size and the athlete's swimming activity. The person's arms incline forward when swimming, so sleeves are often designed to tilt forward.

Based on the characteristics of the diving suit materials, it is suitable to use cutting seams instead of darts to eliminate the extra ease [23], as shown in Figure 1.5. In a good quality wetsuit, seams are always kept away from highly flexible areas, and should not go through the shoulders or underarms, because they will affect paddling areas. More seams mean a better fitting wetsuit, but reduce flexibility and increase friction, the seams can be glued to prevent water from entering; the fewer seams means the less chance of water entering the suit, but less fit [50]. The design basis of the structural cutting seams can be roughly divided into the following two cases:

1) For protection. As shown in Figure 1.5. One is using different materials, or coating crafts to protect the vulnerable parts, mostly human elbows and knees, shoulders, and crotch (Figure 1.5a). The other is using different colors. Bright and eye-catching colors can be easily found and searched in case of danger. Australian scientists take advantage of the characteristics of shark color blindness and adopt a mixed design of hidden colors so that sharks can easily mix it with the color of seawater, which can play an "invisible" effect [51], such as the arena's SAMS (Shark Attack Mitigation Systems) wetsuit (Figure 1.5b).

2) For comfort and fit based on dynamic ergonomic design [69]. For example, the elbow joint and knee joint are the easiest to be constraint by materials in

movement, the seams meet the needs of human activities; besides, using high intensity and best elastic material in the easy deformation areas [41].



Figure 1.5– Protection design: a – different materials and coating craft on knee; b – color design of the arena’s SAMS wetsuit [59]

1.1.4. Wetsuit technology

The construction of the wetsuits plays an important role in thermal protection and restricting water circulation around the body. Water can enter the wetsuits in different ways, especially go through the zips and seams. Different manufacturers may use different methods, for example, blind stitching, gluing, taping, and liquid seams to reduce the amount of water [58].

The wetsuit has high technological requirements, and its main manufacturing process can be roughly divided into four stages. First, cut the pieces according to the pattern; second, stitch and glue pieces; then seal seams; finally, overlock the neckline, cuff and so on.

The stitching process is complex including overlock, flatlock, and blind stitch, as shown in Figure 1.6 [111].

Overlock stitch/seam – the simplest way of stitching, and the least effective of keeping water out. It is not used for high-end wetsuits, and would only be found on summer wetsuits or cheaper wetsuits. The two edges of the panels are rolled together and then stitched to hold them together. This method reduces the flexibility of the seam and also leaves a bulge on the inside of the wetsuit, which

can be uncomfortable and result in chafing.

Flatlock stitch/seam – the most basic and least expensive seam in the wetsuit (Figure 1.6a), flatlock stitching involves laying one panel edge over the other, then stitching through the neoprene, such as type of 4-needle 6-thread. The drawback to a flatlock seam is that the process involved creates many holes, and is prone to high water penetration. This makes it more suited to summer or warmer water surfing [60, 108].

Blindstitch/seam – the edges of the panels are placed end on end and glued together. They are then stitched on the inside, but the stitching does not go all the way through to the outside of the panels. Result: watertight, flexible seams. This is the ideal seam for cold water temperatures and is the one found on higher quality, more expensive wetsuits. If you are a cold-water surfer, do yourself a favor and pay extra for blind stitching (Figure 1.6 b). Also called GBS (Glued and Blind Stitched) [46].

Sealing seams– the sealant is attached to the inner seam or the surface so that the two panels can quickly bond together. Therefore, sealing seams have better durability and washing durability [118,124]. Combined with different sewing thread processes, there are several methods to increase the warmth of a wetsuit and to increase the strength of a wetsuit's seams.

- Glued seams, for entry-level to mid-level wetsuits, the panels are glued together before stitching, increasing the strength of the seam and creating a waterproof seal;

- Spot Taped Seams, it used to help prevent leaks or tears at the intersections and stress points of your wetsuit;

- Fully Taped Seams, it can be applied over the interior or exterior of the seams. These are typically super stretchy and add extra durability and comfort;

- liquid taped, the ultimate seam seal. Special liquid rubber is applied internally, externally or both [160], which makes it 100% waterproof, only be found in the high-end wetsuits, this liquid rubber can be applied;

The most efficient way is blind stitching and gluing with liquid taping, it

creates a flat seam which increases the comfort of the wetsuit [63].

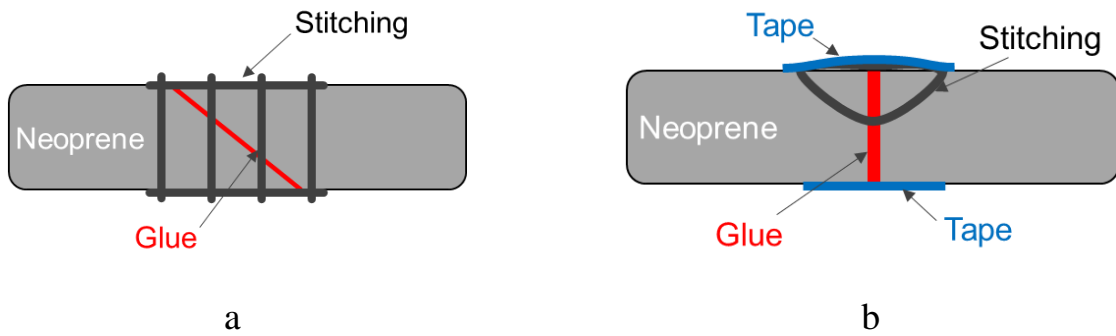


Figure 1.6 – The methods of wetsuit stitching: a – flatlock with glue; b – blind stitch with glue/tape

Generally, a layer of elastic, wear-resistant material or three-dimensional foaming rubber is usually coated on the elbow and knee surfaces.



Figure 1.7 – Zip locations: a–front zip; b – front upper zip; c – front upper zip, O’Neill Double super seal neck, wide adjustability, and a secure lock down, fully adjustable and watertight; d – back upper zip, O’Neill exclusive F.U.Z.E. (Front Upper Zip Entry) system offers a fresh alternative, closure keeps you dry and allows unrestricted flexibility [43,50]

Wetsuit zipper. In order to reduce the water seepage from the zipper and keep warm, the waterproof zipper can be selected, but the price is twice that of the general wetsuit zipper. In addition, a Velcro plane with another material at the back of zipper is made to reduce water penetration (Figure 1.7).

1.2. Current wetsuit material

1.2.1. Brief classification of wetsuit material

The material of the wetsuit needs to mention neoprene. Dr. Arnold M. Collins [61] isolated chloroprene, a liquid that polymerized to produce a solid material that resembled rubber. This product was the first synthetic rubber and is known today as Neoprene [54]. Today's wetsuit material is a combination of multiple-layer materials, as shown in Figure 1.8.

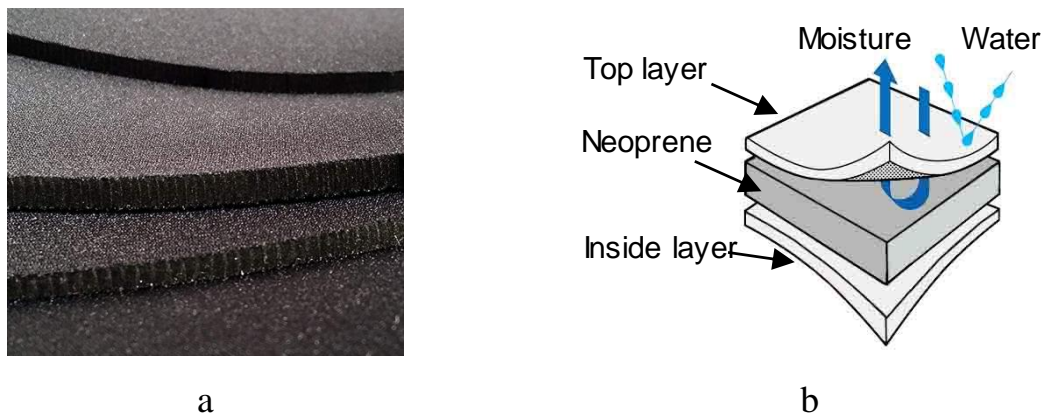


Figure 1.8 – Wetsuit material: a – different thickness materials; b – the combination of multiple-layer

The special wetsuit has three layers materials: the outside/inside are elastic weft knitted material, the middle is foam rubber (Figure 1.8) [67], the commonly used rubber is neoprene, it will reduce heat preservation because it is compressed and thinned when diving deeper [161]. At present, there are various types of wetsuit made from different materials (Nylon, Lycra, Nylon-jersey, mercerized cloth, etc.) in market, the most commonly used outside/inside materials are Lycra and nylon, but the price of Lycra is much higher than nylon. The names of

commonly used foam rubbers are abbreviated as “CR”, “SCR”, and “SBR”.

Chloroprene-rubber (CR) is a kind of synthetic rubber that is also known by the trade name Neoprene, with good performance of soft hand, thermal protection, and elasticity, which is the main material for making high-level diving suits.

Styrene-butadiene rubber (SBR) is suitable for low-level diving suit.

Styrene-chloroprene rubber (SCR) is mixed in proportion by CR and SBR with good flexibility, and the elasticity and comfort are different according to CR proportion, and it's the most frequent material used in the market [84].

Figure 1.9 shows the relationship between water temperature and wetsuit thickness. The recommended thickness is affected by the individual's physical temperature difference.

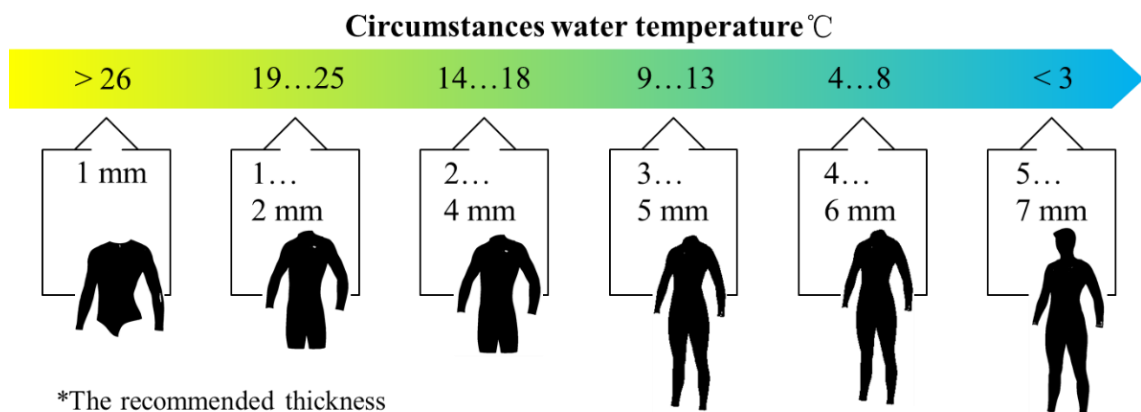


Figure 1.9 – The relationship between water temperature and wetsuit thickness

The industry produces several wetsuits types for different environments. Wetsuit thickness is common 0.5...7.0 mm. For scuba diving, in general, 5...7 mm thickness is for cold water temperatures, thinner than 5 mm is usually for warm water temperatures, and some thin “dive skin” (about 0.5mm) is for above 28°C [56].

The contemporary high-level wetsuit always has different thicknesses for different body parts, different goals and environments [55]. This is why there are often different numbers in the description. The wetsuit neoprene is usually thinner on the arms and legs, to ensure that the movement of the surfer's limbs is not overly restricted while surfing. The numbers will be separated with either “/” or

“0”, with each number corresponding to different thicknesses. The larger number, usually the first number (the number on the left), gives the thickness of the torso. The second (and sometimes third) number gives the thickness of the neoprene on the limbs. For example, “6/5/4 mm full wetsuit”, is a wetsuit that would be used in very cold water. It has a thickness of 6mm on the torso, 5mm on the arms, and 4mm on the legs. A wetsuit with 6 mm neoprene all over would be very restricting and hard to paddle and surf [57]. Besides, the knees and elbows are the most active parts with thin thickness, but these parts are easily worn out, so the coating craft is generally added to the surface.

It is a compromise between staying warm and comfortable in the surf and flexibility, the thicker the neoprene is, the less flexible but warmer it is [37]. The flexibility of the wetsuits and the ability to maintain the heat are directly related to the neoprene properties and wetsuit construction.

As the diving depth increases, the traditional foamed rubber materials will become thinner and reduce their warmth, comfort, and flexibility. To solve the shortcomings of traditional materials, many foreign diving companies began to study the application of new materials in diving suits. The emergence of new materials can significantly improve comfort, heat preservation, and protection to the human body.

The achievements obtained include the laminated composite wetsuit materials produced by the Malden Mills company and the new wetsuit materials (the outer layer is synthetic elastic fiber, and the inner layer is long plush material) in the United States, etc. [36]. In 2002, the temperature-adjustable diving suit adopted the "smart skin" technology, its working principle is that the hydrogel expands after absorbing water, and then reduces the penetration rate of the inner foam material layer to control the water flow in the diving suit and make divers keep appropriate skin temperature in various diving environments [134].

In recent years, titanium-containing wetsuits appearing in the market are very popular, because it doubles the heat material protection with the same thickness. China has also developed some non-compressed foam materials, W. Zhen [141]

applied it to the foam rubber, which significantly improve its thermal insulation performance.

1.2.2. The relationship between material properties and clothing structure

The contemporary wetsuit materials not only focus on its basic features, but also the complex relationship of elongation, pressure, and comfort.

Strain and ease between body and garment depend not only on body measurements and garment construction but also on the mechanical and structural properties of selected material [2]. As for the material KES mechanical properties (material composition, elasticity, and thickness, etc.), many scholars researched material physical parameters and elongation properties before. Z. Cheng et al. [14] analyzed various knitted materials properties through KES, which is used to study the relationship between the elastic properties and the tight clothing pattern design.

For compression clothing, the material elongation and the body dynamic posture will affect clothing pressure. Clothing ease can be designed through the material comfortable pressure range. D. Xu [155] established the basic type of swimsuit according to the anthropometric data, and then modified the swimsuit according to the material characteristics and sewing characteristics. M. Huang et al [70] analyzed the mathematical principle of the tight torso prototype and obtained the tight prototype for high elastic material based on pressure comfort. Z. Cheng [176] designed ease on different girths through analyzing the pressure of different lower torso parts and various materials elasticity.

So, further research on girth deformation by “material, postures, and hydraulic pressure” instead of traditional pressure sensitivity is demanded. We need to find the crucial parameters that most influence the compression pressure and ease, establish the relationship equation between material elongation, soft tissue deformation, pressure, and the maximum material ability to compress.

To sum up, research on the basic pattern of wetsuit and the simple and feasible pattern design method are few at present. Therefore, it is necessary to

establish an overall tight-fitting (wetsuit) pattern design method based on anthropometric data, structure, and material factors.

1.3.Compression pressure and wearing comfort

1.3.1.The classification of compression clothing

Clothing pressure is one of the most important factors that affect clothing comfort, and it is also an important index to evaluate clothing comfort. Clothing pressure is the vertical direction force applied to the human body by clothing. According to force performance, clothing pressure can be divided into three categories: weight, bound, and friction pressure [88]. The character of these three kinds of pressure and the impact on the human body are not the same.

- Weight pressure is caused by clothing weight.
- Bound pressure is caused by the over-tightening of clothing.
- Friction/face pressure refers to the pressure of the human body and the clothing dynamic contact due to the lack of clothing ease and big material friction resistance. In 2000, C. Dongsheng [10] proposed face pressure often occurs in the elbow, knee, hip, and back. The pressure is closely related to the clothing movement function performance.

Figure 1.10 shows that the current study of female compression clothing focuses on the following types. The wetsuit is strong tight-fitting.

At present, most international studies on compression clothing are mainly about the physiological performance of human body, functional analysis of compression clothing for different styles and materials, or short-term subjective and objective physiological tests carried out by sports and health institutions. The experimental samples are mostly purchased products or simple modified products, and the average total number of test samples (human body and material samples) is relatively small (less than 30).

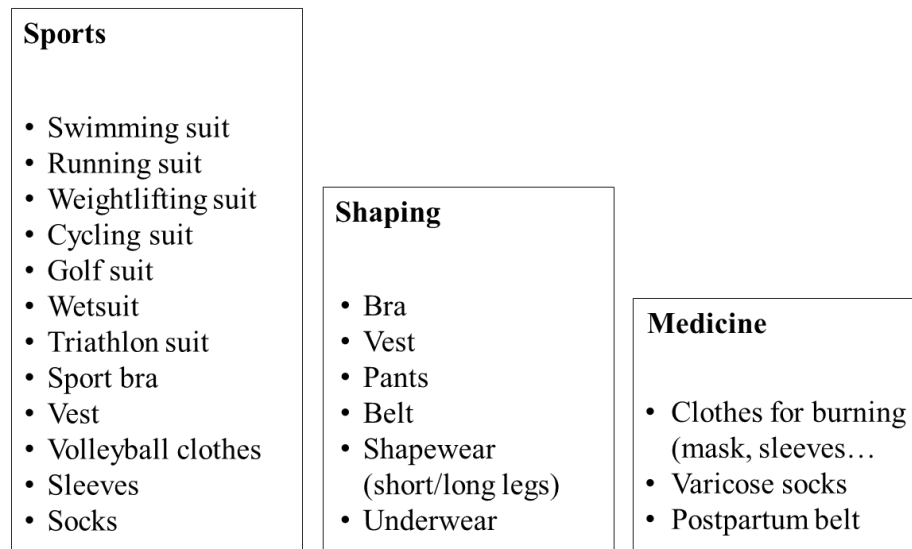


Figure 1.10– Application and research on female clothing pressure

In 1991, M.J. Berry [8] explored the effect of compression clothing on exercise or recovery hematocrit consumption, heart rate, and venous blood samples. F. Brown, K. Goto, and other scholars summarized the effect of compression clothing on sports performance by testing the exercise or recovery process of more than ten men wearing compression clothing, and obtained that compression clothing has a positive impact on athletic performance [9, 34, 95, 99]. K. Kevork [75] explored the relationship between clothing pressure and arm shape, skin, and soft tissue. M. Naebe [255] and K. Monji [101] studied materials heat-moisture properties and established a relationship between pressure and thickness.

In studies of China, Y. Yan et al. [157, 164] analyzed the dynamic performance of women wearing different pressure sports underwear through clothing pressure and heart rate test. D. Chen et al. [167] analyzed the relationship between clothing size and human neck through the results of clothing pressure and blood flow. Y. Wang et al. [138, 139] recorded the comfort range of the nine human body parts through the designed retractable compression belt.

1.3.2. Pressure measurement methods

The research of clothing pressure test technology and its application is of

great significance to optimize the structure design, enhance the added value of clothing, and improve the fit and health of clothing.

Flexiforce pressure sensor is very suitable for clothing pressure test system which consists of two layers of polyester film, and each layer of the film are coated with silver conductor and special pressure-sensitive semiconductor materials which is 0.127 mm thick and can be bent lightly and the shape can be changed according to demand. It's a wireless ELF system that is helpful to carry out sportswear dynamic pressure research.

In 2008, there is a Mju-c clothing pressure test system developed by D. Cheng [11] in order to make the pressure air bag better fit the soft body. The disadvantage of this testing system is that it can only carry out point measurement and cannot predict the local pressure distribution.

Table 1.3 shows several current common pressure test instruments.

Table 1.3 – common pressure test instruments [168]

Type	Advantage	Disadvantage
Fluid (AMI-TECHNO U-tube)	<ul style="list-style-type: none"> - Cheap, convenient and intuitive - High environmental requirements 	<ul style="list-style-type: none"> - It is easy to produce large errors - Measurements in dynamic mode cannot be performed - Unable to measure large curvatures part.
Resistance (Flexiforce)	<ul style="list-style-type: none"> - High precision and stable - The dynamic test can be carried out, portable 	<ul style="list-style-type: none"> - Must connect the reading system - Difficult to measure very soft and small curvatures part.
Barometric (AMI air-bag)	<ul style="list-style-type: none"> - Easy to operate - It can be applied to many kinds of human body parts. 	<ul style="list-style-type: none"> - Difficult to measure dynamic pressure - Small measurement area - Not portable.

AMI-3037 series air bag (Figure 1.11) contact pressure tester and pressure measuring system developed by AMI company in Japan. Stick the thin air bag (standard size 20 mm, probe with different sizes and shapes) on the test part,

compress air enters into the pressure indicator through a 0.1 mm thin tube, and the output signal reflects the pressure difference between the inside and the atmosphere. It can work under the pressure 0.1kpa or even less, and it is widely used in textile and clothing research institutes, sports colleges, medical universities, and other scientific research institutions, providing more scientific instruments for the research of ergonomics, clothing hygiene and so on.

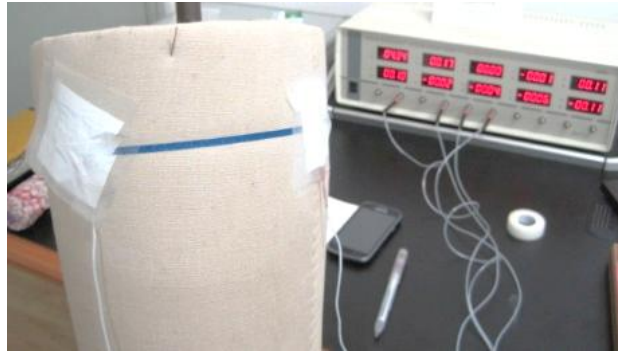


Figure 1.11 – AMI-3037 air bag contact pressure tester and pressure measuring system (Donghua University Laboratory, Shanghai, China)

X. Yuan et al. [161] used the Martin tools and AMI-3037S-5 type clothing contact pressure test instrument to study the compression comfort of tight pants by subjective and objective evaluation methods. In the objective test, the left of the human body is selected as the research object, and five points that have the greatest impact on the contact pressure of the tights are determined through the pre-test.

1.3.3. Clothing pressure distribution on the human body

Two main factors influence the pressure distribution of clothing: the human body and clothing. As the human body is a complicated system, pressure distribution on the human body is closely related to the below factors [85]:

- The shape and curvature of human body, the elastic modulus of skin, and soft tissue have a great influence on the clothing pressure distribution.
- Body parts, the shape and size of the skeleton, muscle thickness, compression ability, and elastic modulus are different; these factors will have a

certain effect on the pressure distribution.

- When the body posture changes, the skin will produce different degrees of deformation.

Different body parts have different pressure tolerance due to different hardness, shape, and nerve sensitivity.

The males' and females' distribution of muscles and soft tissue are different. Female soft tissue is mostly distributed in the breast, buttocks, and abdomen.

In early 1970, M.J. Denton [25] concludes that under the same binding conditions, the greater the curvature of the body surface, the greater the pressure. Due to different curvatures, the pressure on both sides of the human torso is greater than that on the front and back.

When wearing sports protective equipment, people's subjective pressure feeling is not constant because of different movement states. In general, the body's feeling of clothing pressure will become weak and the pressure comfort has gradually increased with time increasing during movement, this is also called pressure adaptation phenomenon. According to the dynamic functional demands, the pressure distribution is different. Take the swimsuit as an example to illustrate. Adidas swimming sports suits in accordance with the athlete's body structure provide gradient pressure [87]. Z. Xiaoxu, D. Xu et al. [153, 166] studied and proved the static pressure test of a female one-piece swimming suit in 2012, and found that in a static vertical state, the various parts pressure distribution and the range of the pressure comfort from top to bottom gradually decreased.

1.3.4. Clothing comfortable pressure

In the systematic study of wearing pressure comfort, the clothing types involved should be divided, and the effect of each required function should be tested to determine the reasonable pressure. Clothing with moderate pressure can protect human body and improve sports ergonomics [151]. If the pressure is too high, it may directly damage human health, such as affecting the normal progress

of the respiratory system; if the pressure is too low, it cannot achieve the fitting effect [26].

Each part of human body has its comfort pressure range and the maximum pressure limit, so the size of clothing pressure directly affects the sports function and wearing comfort of sports protective equipment. It is mainly affected by many factors such as the curvature of the body surface [169], body fat percentage [137], different postures [109], different external environments [150], the extensibility and features of the materials and ease, etc. Besides, human body parts have different pressure tolerance due to different soft hardness, shapes, and neural sensitivity. Therefore, further comprehensive human body data measurement is needed to establish a database for different human bodies or parts. M.J. Denton and J. Pratt [119] conclude under normal circumstances, the clothing pressure that makes the body feel comfortable is between 1.96 and 3.92 kPa. When the clothing pressure value exceeds 5.88...9.80 kPa, the blood flow is difficult. When the clothing pressure is more than 9.80 kPa, the human body cannot bear it. Z. Wenbin [165] in "Garment Ergonomics Science" lists some clothing styles of the comfort pressure range, the comfortable pressure range of swimming suit is 0.98...1.96 kPa; tight clothing is less than 1.96 kPa; corset for 2.94...4.90 kPa. H. Makabe [97] has studied a variety of shape pants pressure comfort. They found that the waist, thigh, and front thigh are easy to cause discomfort. Z. Guo [38] finds shapewear pressure has effects on human heart rate and respiratory rate when pressure is between 4.0...6.6 kPa, then lower core temperature is dropped, finger pulse and respiration rate.

Furthermore, the nerve conduction mechanism of the human body pressure response has not been fully revealed, it is necessary to establish pressure sensitivity distribution. Female body parts can withstand the clothing pressure from strong to weak in order: shoulders, chest, back, side, abdomen, hip [90, 156, 170]. The human body's comfortable clothing pressure is about 0.49...2.60 kPa in general movements [97, 70, 154]. In violent movement, the comfortable pressure of each part changes, its trend is higher than the general movement, generally larger than

the usual about 1.96kPa [133, 77].

1.4. Anthropometric measurement

1.4.1. Modern systems of dimensional features

Well-fitted clothes should provide good morphology and comfortable subjective feeling. Fit plays an important role in clothes design, which significantly affects appearance and comfort [80].

The body characteristics which indicate the torso morphology is changing. Many professionals have proposed many ideas and approaches to sizing systems based on different sorts of situations before improving the wearers' satisfaction. The developing sizing systems now are consisting of the collections of traditional or new measurements such as three-dimensional ones obtained by 3D body scanners. This direction is to improve clothes fit for different groups of customers.

S.P. Ashdown [19] made the comparison of garment sizing systems and compared the general body measurements taken from bodies and shoulder areas of the Korean and the U.S. elderly female to supply basic data for the apparel design in detail. She has done an investigation about the structure of three multidimensional optimized sizing systems generated from the anthropometric data of ASTM D5585-94 [3]. W.SYbilska et al. [129] used the Wanke typology in bone measurements and mathematical calculations to define the types of young women as “V(Y), A, H, I” silhouettes. M.L. Staples and D.B. Delury [126] analyzed the body measurements for a representative number of the U.S. females (over 10,000) and proposed the sizing system for female garments. H.Enjaket al. [42] established the sizing system for girls' clothing (aged 13...20 years) in Croatia based on the anthropometric data using the data mining technique. The girls were classified into three clusters as possible representatives of basic torso body types with a larger number of torso measurements according to the heights. This field of research, especially about the development of a new sizing system, focused on special persons or ages with the 3D body scanners.

According to the latest census [49], the total population of China is near 1.3

billion, which almost accounts for 18 % of the world total population. Accordingly, the original Chinese sizing systems also need more theoretical and practical explorations to delete some existing problems related to the clothes fitting and generated by the acceleration, obesity, fitness, lifestyle changing, and other reasons.

The sizing system is closely connected with garment size standards. Different countries use several approaches to classify the bodies through main body measurements such as height H, bust girth BG, waist girth WG, hip girth HG. The Japanese female classification standard [73] divides all bodies into four categories “Y, A, AB, B” according to the difference between HG and BG when one remains unchanged. Heights are divided into four categories from 142...166 cm by adding 8 cm as the grade. There is a standard body type A with a stable BG for each height. The difference between HG and BG is the basis to classify the body types with the grading value is 4 cm in this way, cm: Y (-3...-8), A (-3...13), AB (1...16), and B (7...17). The Chinese female body classification [31] is based on the difference between BG and WG at one height grade, and all bodies are segmented into four categories as Y (24...19), A (18...14), B (13...9), and C (8...4).

The method of the female torso classification in Germany [20] resembles the Japanese methods. The height is divided into three categories: 160 cm, 168 cm, and 176 cm, then match three heights with all bust girths, and regard the body with moderate hip girth as the standard size.

The contemporary approaches of female body classification mentioned above reflect the traditional measurements which don't consider all features of pattern block making as the necessity. The use of BG, WG, and HG has a long history in pattern drafting [33]. But nowadays the full girth is divided into several parts with scanning software. J.Su et al. [128] analyzed the neck girth by dividing one into parts - the front and the back - and measured ones between the anthropometrical landmarks. In our opinion, the bodies' shapes and constitution could be characterized more exactly in this way.

Traditionally, all pattern prototypes are created by a set of drafting

instructions and construction formulas based on key measurements. Such as the Japanese Buka prototype, the body is divided into two pieces that the front and the back are extremely approximate [152]. The Chinese method of pattern making imported from Japan and based on a similar calculation (1.1)

$$(BG/2 + E_{BG}) / 2 = W_{BGF} = W_{BGB}, (1.1)$$

wherein BG is the bust girth; E_{BG} is the ease allowance of BG according to the clothes style; W_{BGF} is the width of the front part on the bust level; W_{BGB} is the width of the back part on the bust level.

Traditional methods based on full girths (BG, WG, and HG) will be limited in the coming time of customization that needs individualized pattern prototypes. Traditional measurements often lead to misfit especially for a female with non-typical morphological features. Traditional methods may just satisfy the fit demand for the standard torso and cannot satisfy the fit for all torsos. The equality of front and back does not reflect the real torso morphology, because some females have the big breast and narrow back, or small breast and thick back. Sometimes the difference between two parts reaches 4 cm or more [112]. Therefore, the pattern block drafting by Japanese or Chinese methods cannot guarantee a quiet fit for these torso appearances.

To describe and formulate the features of female torsos, a set of new body measurements relating to the bust, waist, and hip girths as a base might be developed. It is necessary to distinguish the wearers' soft tissue, muscle development, and other morphological characteristics of different anthropometrical levels and influence on the elements of a pattern (line configuration, curve parameters, etc.).

1.4.2. Influence of dynamic postures on the change in dimensional features

By watching the diving video and trying on the existing wetsuits in the market, as well as the analysis of a large number of diving movements found in the survey,

the postures of divers underwater are mainly lying prone and face down (swimming posture). For female wetsuits, the movement of the upper torso and upper limbs needs to be studied [7,29]. Besides, the representative diving postures should be considered with pressure comfort test, underwater experimental evaluation as well as pattern analysis to optimize the pattern of the wetsuit.

For wetsuit or compression suits, the skin deformation is more reflected in body girths. Besides, the divers work with different postures under a large range of hydraulic pressure [148], the soft tissue will be compressed, and the value of compression should be taken into consideration. A measurement change of body in dynamic positions is a complex issue that cannot be considered only from the aspect of basic anthropometric measurement, but also the specific body morphology parameters [113]. But most researches do not consider body measurements in specific dynamic conditions [104], which are changing under the influence of laying prone posture and underwater environment. It is necessary to fully study and analyze the movement of the human body.

X. Gao [30] measured more than two hundred young women aged 18-35 by using Martin measuring instrument and 3D human body scanning equipment and selected 10 yoga representative movements to study the skin deformation in yoga state by body surface tracing. Based on the deformation rules of the human skin and the material properties, two kinds of optimally fit yoga pants patterns are obtained by dividing and stretching the parts of trousers corresponding to the greatest stretch of the human body. T.A.Shimana et al. [30] made model construction research with a special swimming posture. I.A. Senitsky et al. [171] made local modeling and modification for the female soft tissue part based on the compression deformation characteristics when standing statically; C. Loercher [94] proposed a method to measure the measurements change in 10 postures (squat, step, bend, raise hands horizontally, etc.).

As shown in Figure 1.12, M.M. Naglic et al. used 3D scanner Vitus Smart to measure male and female dynamic postures in one static and five dynamic positions.

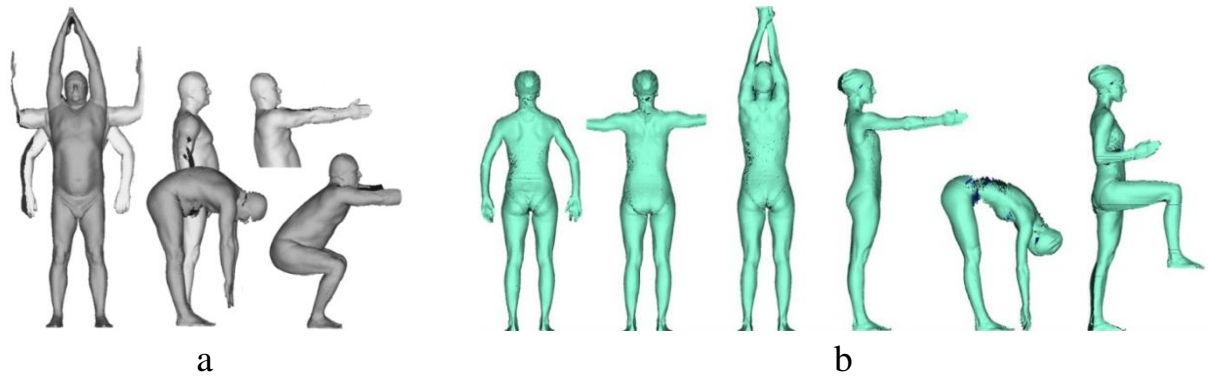


Figure 1.12 – Scanned dynamic postures: a – male [104]; b – female [105]

Thickness change of female body soft tissue (fat) under different dynamic postures needs to be analyzed emphatically. M. Ernst [28] studied the compression deformation of soft tissue in the sagittal plane of the female 3D model with much fat content; besides, female's chest size changes greatly, which also needs to be analyzed emphatically. C.E. Coltman et al. [21] measured female breast volume change when standing with hands up and lying prone. For example, Y. Zhang [136] selected six representative golf postures, measured thirty-eight human body parts, and analyzed the relationship between the material elongation, the body skin deformation rate, and ease. G.E. Van et al. [131] scanned a swimming posture to compare the try-on effects.

So, it needs to study the soft tissue deformation range of different body parts based on basic diving postures and hydraulic pressure, the body sizes change in static and dynamic position can be obtained.

1.5. Construction of a modern wetsuit drawing

At present, less research is about the design and comfort evaluation of long wetsuits. Only a few scholars from South Korea, Japan, and the United States make research related to wetsuit design, as usual, devoted to one aspect (pattern design, or material, or simulation, etc.). The construction of a female wetsuit was derived by applying the 3D → 2D method, which involves the construction of a

garment model by drawing and creating pattern lines directly on the surface of a digital body and separation of discrete 3D surfaces as well as transformation into 2D cutting parts [116].

H.J. Khur [71, 105] made an investigation of the wearing condition and the size system for wetsuits of different brands. M.M. Naglic et al. studied wetsuit patterns obtained directly from the female body (Figure 1.13 a). J.H. Choi [16, 17, 18] made the study about pattern development, production, and consumer satisfaction of male wetsuit in their 30's, and he also used a standard approach to make the pattern blocks with standing postures (Figure 1.13 b).

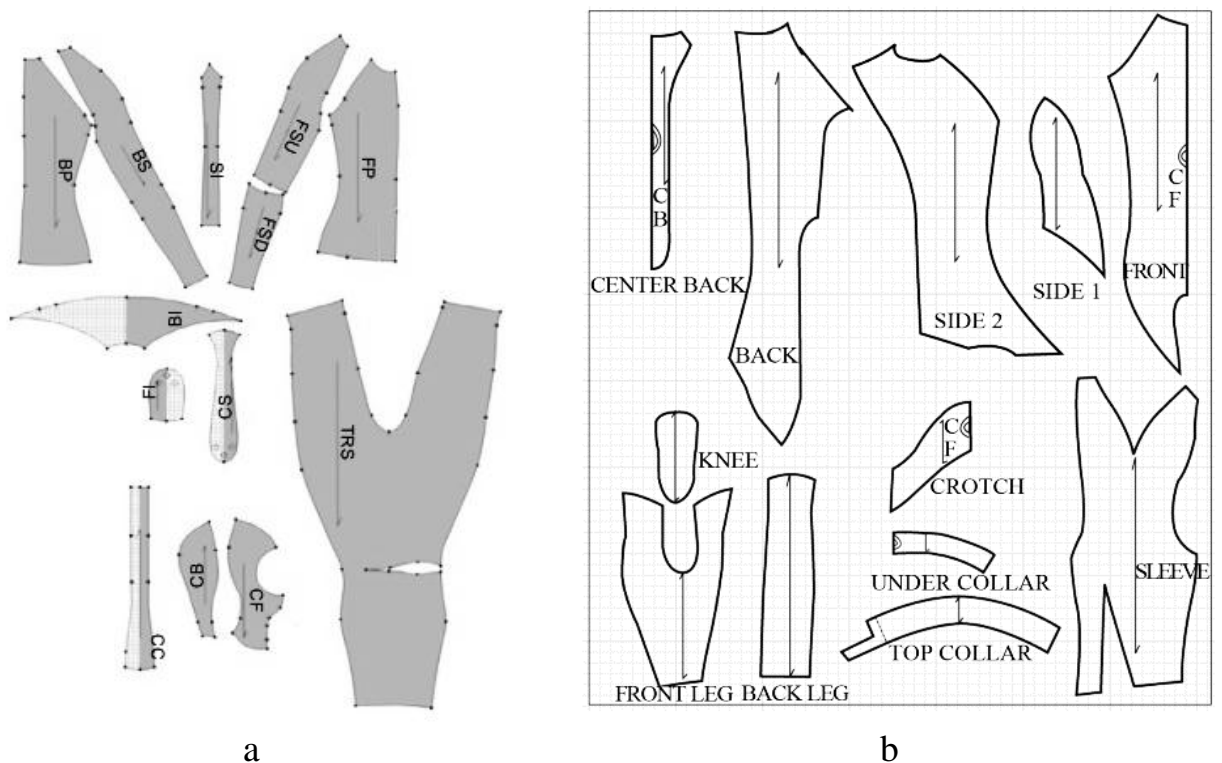


Figure 1.13 – Wetsuit patterns: a – the pattern derived from 3D to 2D [105]; b – a pattern for the standard body type of Korean men [16]

Through the research and analysis, at present, the methods of wetsuit pattern design mainly rely on 2D and 3D technologies, one method: only use computer 2D pattern making with several basic data (bust, waist, hip, height), the other method: the wetsuit patterns are derived on customized parametric body models from 3D to 2D, and then make corrections to get the final pattern. It is usually based on

"individual-customed" experiments.

These two methods can be found in the existing research data. However, in China's wetsuit factories, they mainly use the "modification" method to make the wetsuit pattern - only rely on a set of finished patterns, constantly modify according to different human bodies or small design changes and finally get the new pattern based on experience.

The existing process needs to be further strengthened:

1. The existing pattern designs have many cutting lines, and the existence and location of these lines are not strictly reasoned.

2. The drawing is not based on the analysis of a large amount of information about the morphology of the human body.

3. Little attention is paid to the elasticity and thickness of materials in the construction of drawings, their physiological effects on the human body, the rationale for the impact of structural increases on comfort, pressure, and compliance with the human body;

4. There is no algorithm for using indicators in the drawing.

To explore the factors that need to be improved in wetsuit design, we conducted a study of the structures of more than 300 wetsuits from different manufacturers (Figure 1.14). The main attention was paid to the analysis of structural lines and the feasibility of the design. Lines of internal seams are usually located in the area of the shoulder girdle, on the sleeve, on the outside of the leg, in the knee area. The zipper is located at the back.

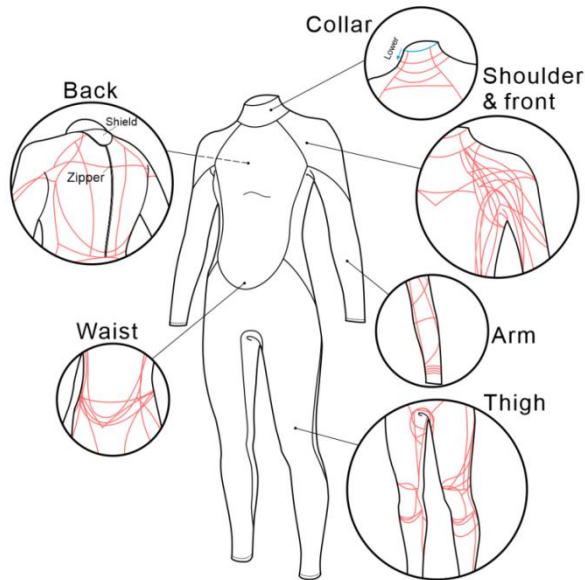


Figure 1.14 – Wetsuit division line options

We surveyed 1000 women with experience diving in 3 Chinese diving clubs (network group), of the feedback on the quality of the fit of wetsuits bought in a store or borrowed from clubs was negative.

Figure 1.15 illustrates the ranking of areas that cause discomfort underwater: shoulder part (25.5%), waist (15.7%), upper arms (15.4%). The people interviewed wished to improve the design of the wetsuit or adjust it according to their body morphology or customize it for their body morphologies.

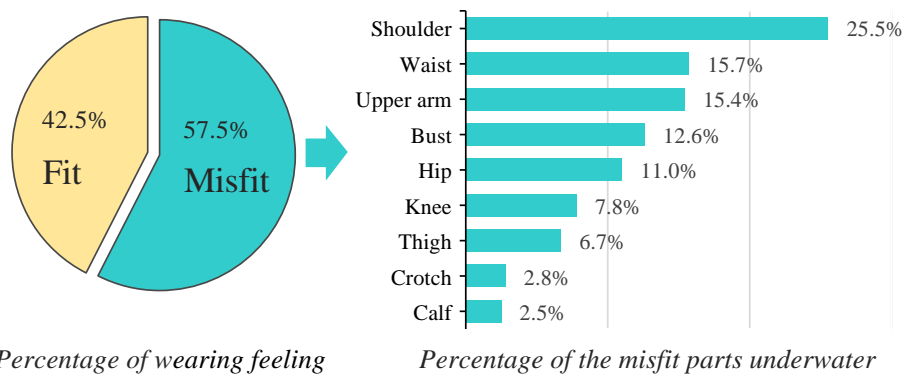


Figure 1.15 – Rating of problem areas when swimming underwater

The lack of theoretical knowledge has led to many practical problems in diving suits. Some customers cannot find the appropriate wetsuit according to their sizes, and feel discomfort during diving; and the problems about absence of body

database, grading of pattern blocks under manufacture production, and the application of material properties also exist in many wetsuit factories.

1.6. Application of 3D technology in clothing design

1.6.1. Application of scanned body and avatar

The 3D body scanner is necessary for wetsuit design and evaluation [35]. Body scanners have been applied in some researches to get accurate measurements, generate scanatars, get cross-sections, and analyze key parts such as the crotch and bust [22]. 3D scanning technology can also be used for obtaining dynamic anthropometry data, which is especially important when developing clothing for special purposes with high demands on functionality and fit [32].

For example, most original human models are automatically created by static 3D scanning [135], and then processed and optimized by complex calculation methods [100,132]. Some researchers studied the human lower part skin deformation by analyzing some swimming and dynamic postures through the scanned human or avatar to design compression sportswear, as shown in Figure 1.16 [98, 107, 123, 130].

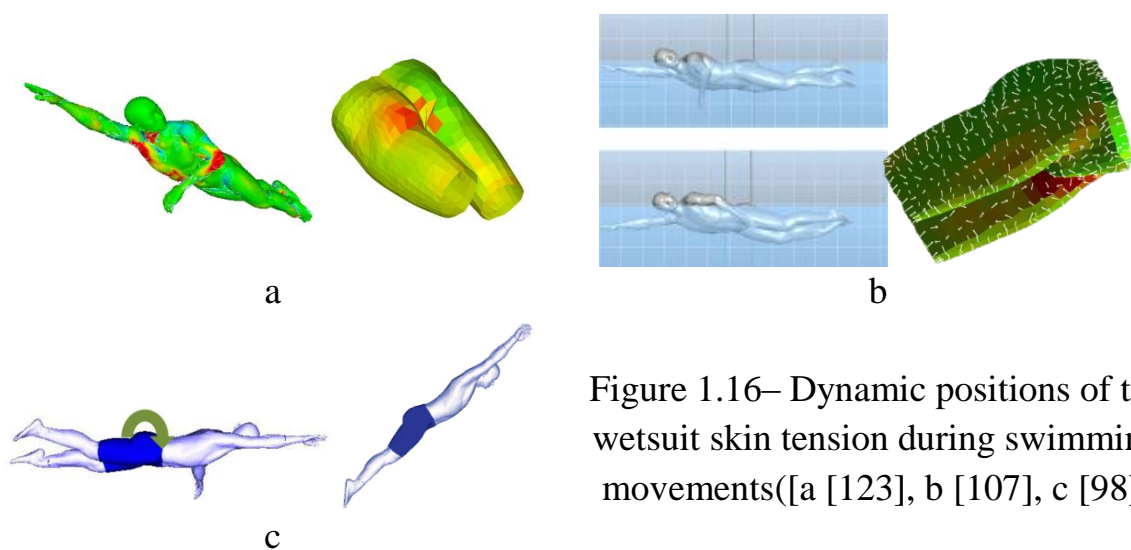


Figure 1.16– Dynamic positions of the wetsuit skin tension during swimming movements([a [123], b [107], c [98])

In the study areas of virtual design, at present, it is not only limited to the

analysis of the original scanned human models, but also the analysis of deformed and regenerated human models [27]. Some scholars [15, 23, 83] established the correlation between them and provided the method to express the morphology characteristics of the human body after analyzing the changed multiple body parts. H.Han [40] used a 3D scanning model to extract the sagittal plane and cross-sectional contour of human body, and T.Mah [96] developed 3D human body construction based on body feature points. Z.Cheng et al. [13,] proposed a modifiable deformation method for a digital human model to design the compression garments with the help of a 3D body scanner. M.Avādanei [4] simulated dynamic diving postures. Z.Wang [140] presented the method of 3D human data acquisition based on 3D scanning and non-contact fit evaluation of clothing based on the distribution features of residual space between the clothing and the human body. J.Zhang et al. [163] used the 3D images, horizontal cross-sections taken from scanned bodies and jackets to produce an upper clothing model for 3D and 2D patterns using ease allowances. Y. Liu [93] collected for 275 subjects using a 3D scanner and 108 measurement values were extracted by reverse engineering software Polyworks.

Because most subjects wear underwear during scanning, the body details of the human model built by a scanner or other methods are not accurate, which leads to the model cannot be completely the same as the original structure characteristics of the human body. The surface morphology and dynamic/static postures of the human model will directly affect the virtual performance of the compression clothing [162]. Besides, the study of parameterized body adjustment based on individual measurements also revealed some shortcomings in the adjustment, especially in body posture, spine tilt, and shoulder rotation, which are particularly important for specific tight clothing applications [115]. According to personal measurement and analysis of clothing structure, it is best to use a scanned human body model to obtain an accurate body shape. The computer 3D prototype will be added to the simulation process [114]. Similar methods have been used in many other studies [121, 127].

1.6.2.3D compression clothing design

At present, there are many software that can be used in 3D clothing virtual design, the mainstream of which are 3ds max, Maya, CLO, OptiTex, Vidya, MarvelousDesigner, and so on. 2D pattern design software is more diverse, such as AutoCAD, CLO and Opitex, Assyst, Lectra, Gerber AccuMark, Chinese Richpeace, BUYI ET, Modasoft, and so on.

In recent years, the international application of simulation technology in the field of clothing research is mainly about the inelastic loose clothing, which focused on one single research direction, and simple design and displays the wearing performance with the help of software; the simulated clothing research are mainly inelastic fabrics (cotton, hemp, silk, etc.) [12]. Many simulation studies do not pay attention to the characteristics of clothing material properties [117]. The related virtual pattern design and tight clothing research are female compression bra, female tight pants, etc. [1, 92, 91].

M.Li [86]used Visual C++ language and OpenGL graphic interface, the interactive design of tight prototype and bra cup basic layout is realized, and the algorithm and technical route to realize the digital design of 3D chest modeling are explored.M.Hu et al. [68]established a fit female torso prototype without ease by analyzing the structural characteristics between the waist and the chest and the plane expansion shape of the three-dimensional model.M.Avădanei [4] performed a simple3D virtual try on of wetsuit with 3dmax software.

J. Kanika [72]design of motorcycle rider clothing sketched directly on the avatar (Figure 1.17 a). H.J. Lee [81, 82]designed compression pants with Yuka CAD program and Rapidform XOR program for leg structural features (Figure 1.17 b).

Y.L. Lin [89]proposed an innovative method of clothing fit evaluation for virtual try on using a 3D digital human model and the information of clothing fit obtained in this study which together can be applied to the development of clothing products in the apparel industry. K.W. Yeung [158]studied the virtual design and

evaluation of female compressed bra and analyzed the relationship between clothing deformation, clothing pressure, and female breast deformation.

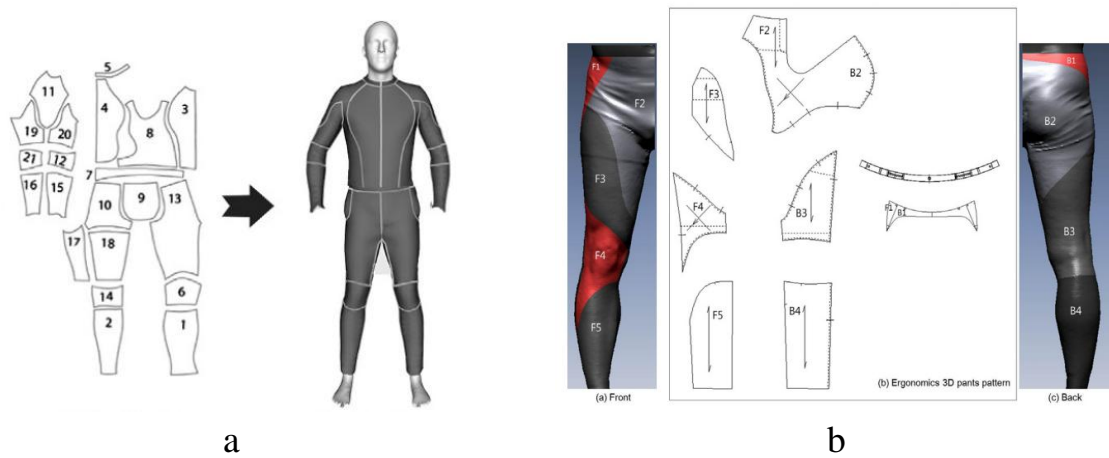


Figure 1.17 –3D design of a motorcyclist suit (a) [72] and compression pants (b) [81]

Figure 1.18 shows some existing 3D structural design studies on wetsuits. For the 3D simulation of wetsuit pattern design. M.M. Naglic [105, 106] scanned bodies on the land in six postures, such as raising hands and squatting, and designed a virtual diving suit with software Optitex (Figure 1.18 a). T.H. Staal [169] used CLO software to test the final fitting effect and material strain of male wetsuit, but did not propose an optimization scheme and a specific comfort evaluation scheme for the pattern (Figure 1.18 b).

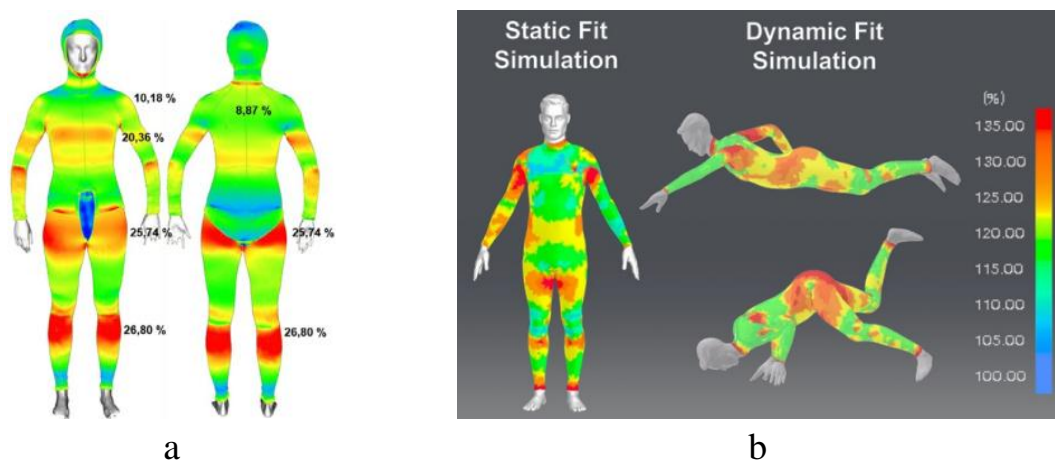


Figure 1.18 – Virtual wetsuit testing: a – digital deformation [105]; b –map of the material strain [125]

The purpose and directions of the dissertation research

Nowadays, there are some scientific and practical problems in the current wetsuits, it is mainly reflected in the lack of theoretical knowledge research. Many researchers believe that material performance is the most important factor that influences wearing comfort of wetsuits. However, reasonable garment pattern design can also improve wear comfort and aesthetics significantly, the size and pattern of the diving suit should be completely adapted to the measures and shape of the diver's body.

This research focuses on one type of wetsuit – the long wetsuit, 5m diving, for outdoor activities. The purpose of this research is to develop a scientific approach for wetsuit design through body scanning data, textile material properties, and pattern design. A wetsuit should maintain good physical condition during dynamic dives, provide comfortable soft tissue deformation under the influence of typical diving postures and hydraulic pressure.

To achieve the goal, it is necessary to solve the following tasks:

1. To study the modern design of female wetsuit, to summarize all available information, options for constructive solutions, an anthropometric database, to conduct artistic and constructive assessments and analysis.
2. Develop a new grouping of female torsos that reflects the characteristics and morphology of the body through the distribution of girths between the front and back and use the results to build drawings of the wetsuit.
3. To study the ranges of deformation of soft tissues of various parts of the body, taking into account the basic dynamic postures for diving and the hydraulic pressure of water.
4. Study the relationship between material elongation, soft tissue compression, and body dimensional change to determine the minimum structural ease for 8 body types.
5. Develop an algorithm for designing a female wetsuit in a virtual environment and test the rationality of the design in terms of a virtual pressure

assessment.

6. Make wetsuits in the factory based on virtual results to test the practicality of the new female wetsuit design process and establish evaluation criteria.

7. Test the developed recommendations by manufacturing and testing wetsuits.

Chapter 2. ANTHROPOMETRICAL DATABASE

The results obtained in this chapter are published in 3 works [143, 144, 173].

2.1. Grouping torsos of female bodies

2.1.1. The ratio of the front and back half-girths of the body

The grouping of the torso is based on existing and new body measurements after 3D scanning. The VITUS Smart XXL 3D body scanner (Human Solutions, Germany, standard DIN EN ISO 20685) and the program for reading and visualizing scanned bodies (scanatars) by Anthroscan 2014.

96 Chinese female subjects volunteered to participate in this test from Wuhan Textile University (China). Their ages were from 18...27, the heights (Anthroscan 2014 "Measure inspector" ID is 0010) are from 147.3...173.6 cm, and BG (4510) are from 73.0...105.1 cm. Girls in the age were particularly selected, because the age survey of diving clubs shows youth participation with great consumption power in diving recreational activities is increasing quickly.

Table 2.1 shows the distribution of body types (normal body shape) chosen following the Chinese standard [31, 52].

Table 2.1 – Bodies types involved in the experiment

Torso type	Difference δ between BG and WG, cm	Proportion, %
Y	$19 \leq \delta \leq 24$	21.9
A	$14 \leq \delta < 19$	50.0
B	$9 \leq \delta < 14$	20.8
C	$4 \leq \delta < 9$	7.3

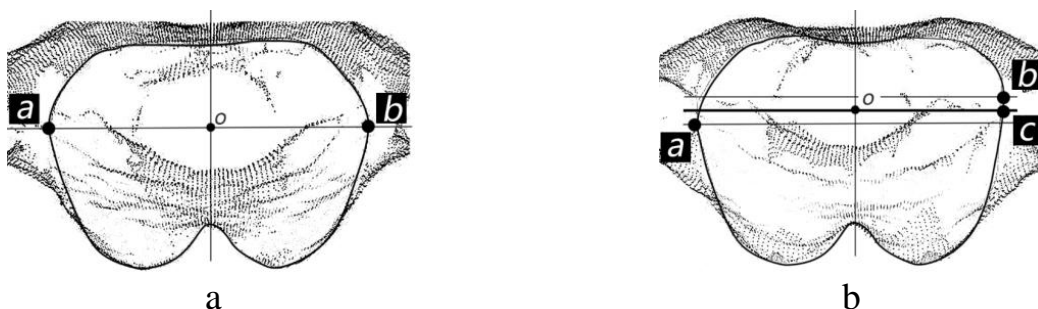
2.1.2. Cross-sections of the female torso

The software Anthroscan 2014 is used to read, visualize, reconstruct and measure the data clouds of a scanned body. The girls wore light-colored underwear and kept the natural standing posture during the scanning. Slices of BG, WG, and HG were cut out from scanning bodies and transformed into cross-sections as the curves taken from BL, WL, and HL levels.

As known that the proportional distribution of bodies' horizontal girth in front and back is determined by vertical guild lines, which are different due to different body shapes. In order to describe and formulate quantitatively the relationship between features and pattern elements, we generated the horizontal cross-sections from the main levels. To analyze shapes of all girths, we divided ones into two segments – the front and the back: BG_F (front segment of bust girth), BG_B (back segment of bust girth), WG_F (front segment of waist girth), WG_B (back segment of waist girth), HG_F (front segment of hip girth), and HG_B (back segment of hip girth). The mentioned segments above were considered as the new torso measurements.

To divide the main cross-section of BG between BG_F and BG_B for a clearer understanding of torso characteristics, we used the method as Figure 2.1 shows.

We determined positions of “a”, “b” points as the most prominent landmarks of the left and right sides of the cross-section according to the below method. Firstly, a vertical line and move it to touch left side of cross-sections. Thus, marking point “a”. Point “b” was found in the same way on the right.



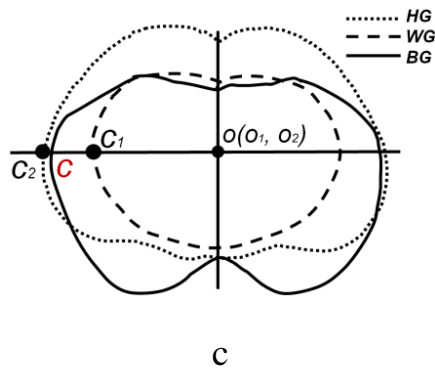


Figure 2.1 – Definition of landmarks “*a*” and “*b*” for the division of BG into BG_F and BG_B: *a* – sections of a symmetrical bust; *b* – section of an asymmetrical bust; *c* – alignment of the girths of the bust, waist and hips with a common sagittal line and the midpoint “*o*” (*o*₁ - point at waist level, *o*₂ - point at hip level)

After founding “*a*” and “*b*”, two situations occurred:

1) Both points “*a*” and “*b*” belonged to the same horizontal line, as shown in Figure 2.1a. In this case, points “*a*” and “*b*” were connected by a horizontal line through the section of the bust. The midpoint of segment *ab* (point “*o*” of intersection with the midsagittal plane) was designated as the center of the cross section and its point was used to analyze the waist and hip cross sections in the following steps.

2) Both prominent points were not in one horizontal line, for example, as shown in Figure 2.1b. This situation took place if the left and right woman breasts were not absolutely the same or a torso had an asymmetrical constitution. We draw two horizontal lines in *a* and *b*, divided the distances between lines *a* and *b*, draw new (adjusted) horizontal line *c* and marked midpoint *o*.

According to midpoint *o* located on bust cross-section, similar points were found in the form of a projection to the anthropometric levels of the waist and hips located below and divided them into two parts. Figure 2.1 c shows combined cross sections: first, three vertical central lines of sections of bust, waist, and hips were combined; then three lines *c*, *c*₁, *c*₂ were combined. After that, the length of the front and back parts of the sections BG, WG, and HG was measured.

2.1.3. New grouping of bodies by shape and torso

To solve the misfit problem of female wetsuit, a new grouping of the torso has been established. Through analysis of BG_F, BG_B, WG_F, WG_B, HG_F, HG_B, and their

average values, we found that the differences at BG are the biggest in any case. Accordingly, BG represents torso morphology much more apparent than other measurements. For this reason, we have chosen the proportion between BG_F and BG_B as the base to develop a torso grouping.

Traditional groups Y, A, B and C were increased by two times by separating each group into two subtypes: Y – Y1 and Y2, A – A1 and A2, B – B1 and B2, C – C1 and C2. Group I includes four subtypes Y1, A1, B1, and C1 when the bust front segment (BG_F) is bigger than the bust back (BG_B) segment. Group II includes four subtypes Y2, A2, B2, and C2 with an opposite situation.

$$\delta = BG - WG \quad (2.1)$$

$$G_I = \{Y1, A1, B1, C1\} \quad (2.2)$$

$$G_{II} = \{Y2, A2, B2, C2\} \quad (2.3)$$

where δ is the basis for determining the body type group, Y ($19 \leq \delta \leq 24$ cm), A ($14 \leq \delta < 19$ cm), B ($9 \leq \delta < 14$ cm), and C ($4 \leq \delta < 9$ cm); Group I is $BG_F > BG_B$; Group II is $BG_F < BG_B$.

Table 2.2 shows the average girths of front and back segments of each subtype. Figure 2.2 shows examples of A1, A2 subtypes of female bodies.

Table 2.2 – Average front and back segments of 8 subtypes

Body segment	Segment girths of subtypes, cm							
	Y1	Y2	A1	A2	B1	B2	C1	C2
BG_F	44.9	42.4	44.0	41.1	46.4	42.3	47.0	41.3
BG_B	41.5	46.0	40.2	43.6	39.9	45.2	37.9	42.8
WG_F	33.8	32.5	35.6	34.6	38.3	38.1	43.7	42.3
WG_B	32.3	32.7	32.2	33.3	36.1	37.5	39.8	39.5
HG_F	42.8	42.6	43.3	43.4	44.6	44.1	44.1	45.9
HG_B	43.8	47.6	48.3	48.2	50.4	49.6	48.4	48.7

The large differences of $(BG_F - BG_B)$ are subtypes of Group I, and the positive difference from large to small is $C1 > B1 > A1 > Y1$; the proportions of WG_F and

WG_B are almost similar, and the large difference of HG_B minus HG_F is subtypes of Group I.

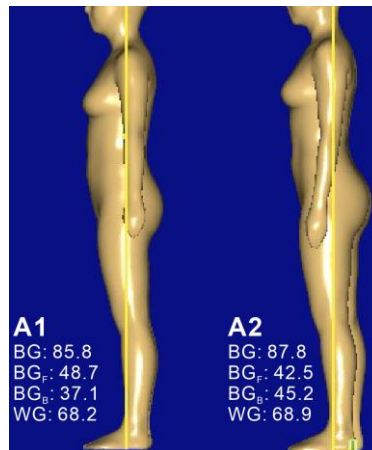
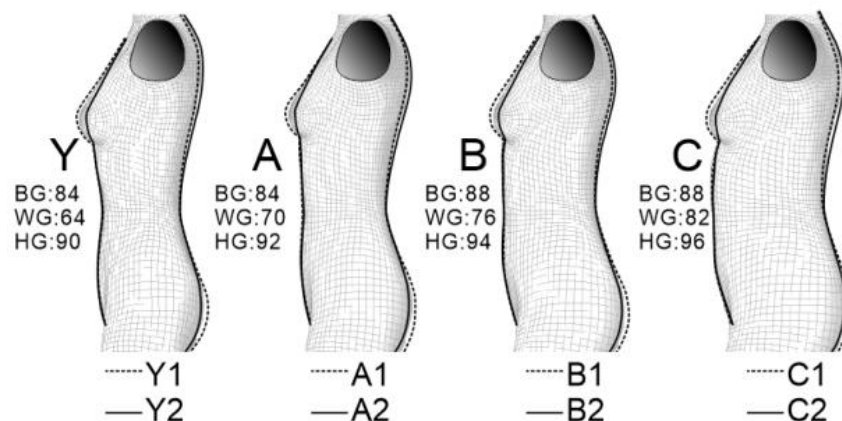


Figure 2.2 – Profile of standard torsos A1 and A2

2.1.4. Improved mannequins of typical bodies

CorelDraw software is used to redraw all cross-sections and to find the average cross-sections by using a mathematical analysis method.

Figure 2.3 shows the sagittal planes of standard types and the corresponding subtypes (Y1 and Y2, A1 and A2, B1 and B2, C1 and C2) are aligned based on waistline. Through comparison, it can be seen that the BG_F of group I has a significant large volume, and the HG_B volume is relatively large. Group I emphasize more physiological characteristics of women – volume differences in sexual features.



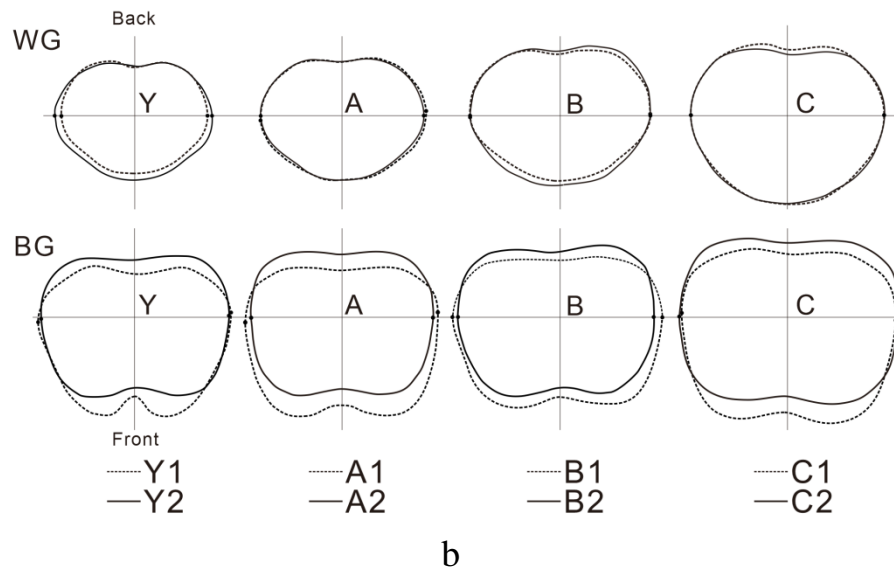


Figure 2.3 –Outline of standard torsos: a – sagittal planes of standard torsos (Y, A, B, C) and subtypes; b–cross-sections of the bust and waist

Based on collected results, the type A (A1 – 37.5%, A2 – 12.5%) accounted for the highest proportion, followed by the types Y (Y1 – 10.4%, Y2 – 11.5%), B (B1 – 14.6%, B2 – 6.3%) and C (C1 – 4.2%, C2 – 3.1%).

Subtype B is shown as an example in Figure 2.4. Typical mannequin B was converted to the first ($BG_F > BG_B$) and second ($BG_F < BG_B$) subtypes by increasing or decreasing the half-circumferences of the bust, waist, and hips according to the previously obtained average sectional shapes. Figure 2.4 shows mannequins B, B1 and B2 made of plastic and transformed by a knitted belt worn at bust, waist, and hips.



Figure 2.4 –Mannequins B (traditional), B1 and B2 altered to new torso types

The measurement results are given in Appendix A.

2.2. Changing the dimensional features of the human body

2.2.1. Body measurements in static

In order to study how the body measurements change during diving, Body measurements of diving dynamic postures on the floor and underwater were measured. All data are obtained through non-contact scanning (on the floor) and contact manual measurement (on the floor and underwater). All measurements are following standard ISO 7250, and 22 measurements of which were selected by Anthroscan 2014. Therefore, the total number of measurements was 42.

Figure 2.5 shows the scheme of measurements with its ID and the postures of the tester. Table 2.3 shows the main body measurements after scanning for generating a digital replica. These simplified representative features can express dynamic measurements which are changed in virtual reality and which can be used to complete replication of a human body.

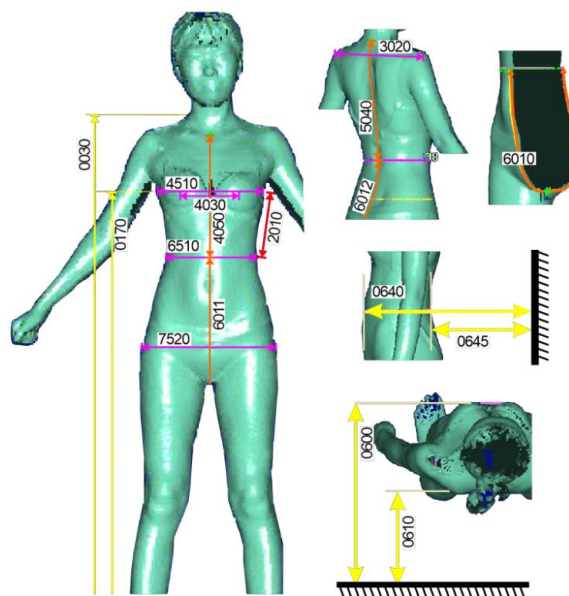


Figure 2.5 – Scheme of body measurement by Anthroscan

To prove that 96 female subjects are enough for this exploration, two body measurements have been analyzed – height and bust girth. Figure 2.6 shows the $Q-Q$ plots of a bust girth and a height. The Shapiro-Wilk ($S-W$) test and the diagnostic tool of $Q-Q$ plot were used to test the normality of data.

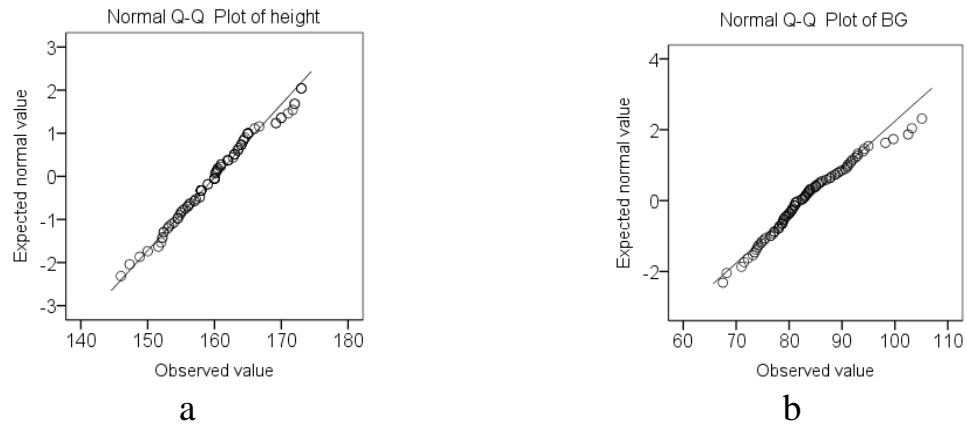


Figure 2.6– Probability distributions of $Q-Q$ plots: a – height; b – BG

As shown in Figure 2.6, $Q-Q$ plots of bust girth and height proved that both measurements obey normal distribution. The Cronbach's α is 0.974 by SPSS, which means that all data have good scores of reliability analysis of internal consistency. The same conclusions have been made about other measurements. So, 96 bodies are enough. Distribution diagrams are given in Appendix A.

Table 2.3 – Main body measurements from 3D body scanner

Category	No.	ID	Measurements interpretation	Symbols	Average, S.D., cm
Distance	1	0510	Distance 7CV (BNP) to vertical	-	27.0 ± 1.8
	2	0515	Distance neck front (FNP) to vertical	-	36.6 ± 2.0
	3	0550	Distance waist to vertical	-	44.2 ± 3.0
	4	0530	Distance waist back to vertical	-	26.1 ± 2.9
	5	0600	Distance bust to vertical	-	46.3 ± 3.1
	6	0610	Distance back in bust height to vertical	-	23.1 ± 2.4
Width	7	3020	Cross shoulder width	W_{SP}	41.6 ± 4.1
	8	4030	Bust points (BP) width	-	17.2 ± 1.8
	9	4010	Across/bust front width	W_{BF}	32.7 ± 4.4
	10	5020	Across back width	W_{BB}	33.1 ± 2.9
Girth	11	4510	Bust girth	BG	83.9 ± 4.7
	12	6510	Waist girth	WG	69.5 ± 7.5
	13	7520	Buttock/hip girth	HG	90.5 ± 5.3
	14	9510/	Thigh	TG	51.2 ± 3.3

		9511			
Height	15	0030	Neck (7CV/BNP) height	-	136.9 ± 8.0
	16	0170	Bust (BP) height	-	115.7 ± 7.8
Length	17	2010/ 2020	Side upper torso length	SL	19.0 ± 2.1
	18	4050	Neck front (FNP) to waist	FNP-WL	31.1 ± 3.3
	19	5040	Neck to waist centre back	BNP-WL	36.1 ± 3.2
	20	6011	Crotch length, front	-	36.1 ± 3.2
	21	6012	Crotch length, back	-	38.0 ± 2.7
	22	6010	Crotch length	L _{Cr}	74.1 ± 5.7

*“verticals” is the wall of the scanner located behind the torso.

To clarify the shape of the torso during compression and its visualization, a triangle was drawn through the BP points (as the most characteristic ones) and the middle point of the back. When the bust is compressed, it is seen that the points of the bust are shifted to the sides with varying degrees. The distance between the points increases, as shown in Figure 2.7.

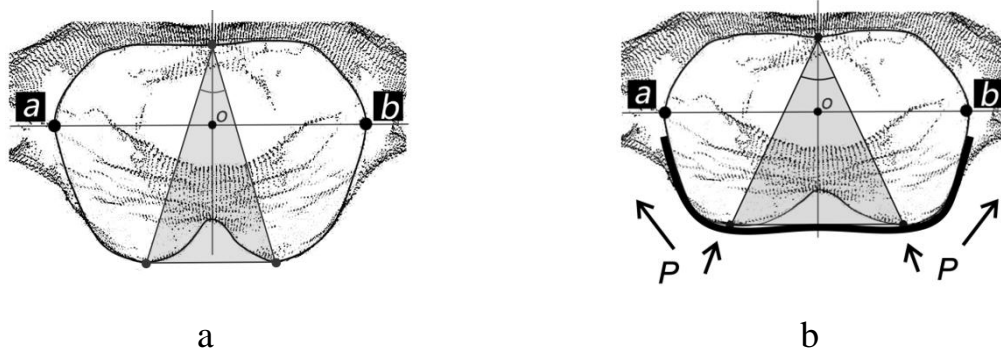


Figure 2.7–Change in the cross section of the girth of the bust in statics: a – the initial shape of the section; b – section shape after compression

2.2.2. Body measurements change in dynamic

The experiment includes the following postures (the abbreviations P1, P2, P3, P4, P5, and P6; P1, P2 are standing, P3, P4 are breaststroke positions when sliding and slowing down (lying on a floor); and P5, P6 are when swimming underwater[62], as shown in Figure 2.8. The testers in postures P1 and P2 were scanned by 3D scanner. The testers in postures P3, P4, P5, and P6 were measured

manually. Each measurement is measured six times to get the average value, and the testees hold breath for 2...3 seconds during each measurement.

Four postures are constructed under the next conditions:

- standing on a floor with hands down (P1) and hands up (P2);
- lie prone on a floor with face down – the arms stretch forward, the legs straight backward (P3); the arms stretch forward, and the feet draw up towards the hip, calf 90° with the body (P4);
- P5 and P6 were the same as P3 and P4, but all measurements were made underwater through manual tape.

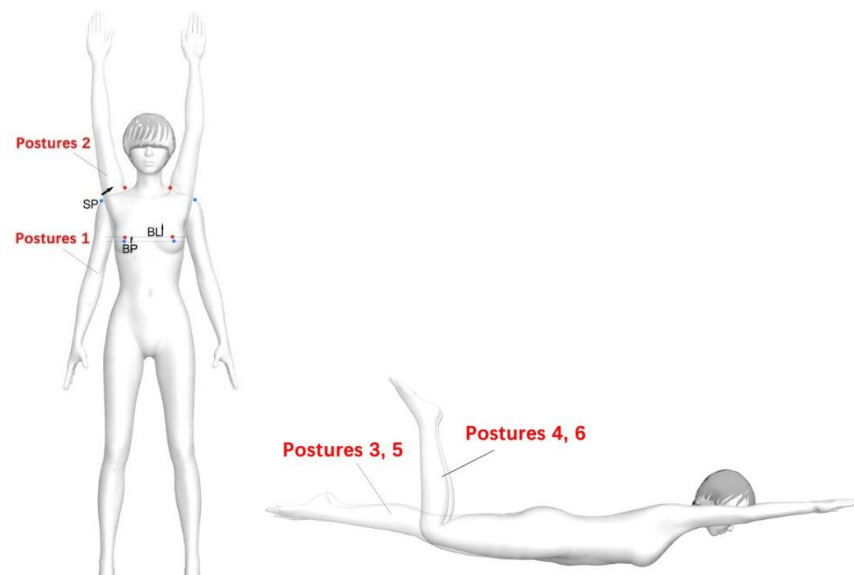


Figure 2.8 – Dynamic postures

To figure out how each posture influences body measurements, the average differences (DIF) between the same body measurements in standing and lying prone postures were compared; $DIF(m-n)_i$ is the difference between i -measurements of Posture m and Posture n , e.g., $DIF(P2-P1)_i$. The differences $DIF(P2-P1)$, $DIF(P3-P1)$, $DIF(P4-P1)$, $DIF(P5-P1)$, and $DIF(P6-P1)$ were calculated.

- $DIF(2-1)_i$ – the difference between i body measurements P2 and P1;
- $DIF(3-1)_i$ – the difference between P3 and P1;
- $DIF(4-1)_i$ – the difference between P4 and P1;

- $DIF(5-1)_i$ – the difference between P5 and P1;
- $DIF(6-1)_i$ – the difference between P6 and P1.

Take body type A as an example. Figure 2.9 shows the differences between P1 and P_i of BG, WG, HG, and SL for body type A, the bodies were extracted from 3D scanatars and were overlapped in point CR through real experiments.

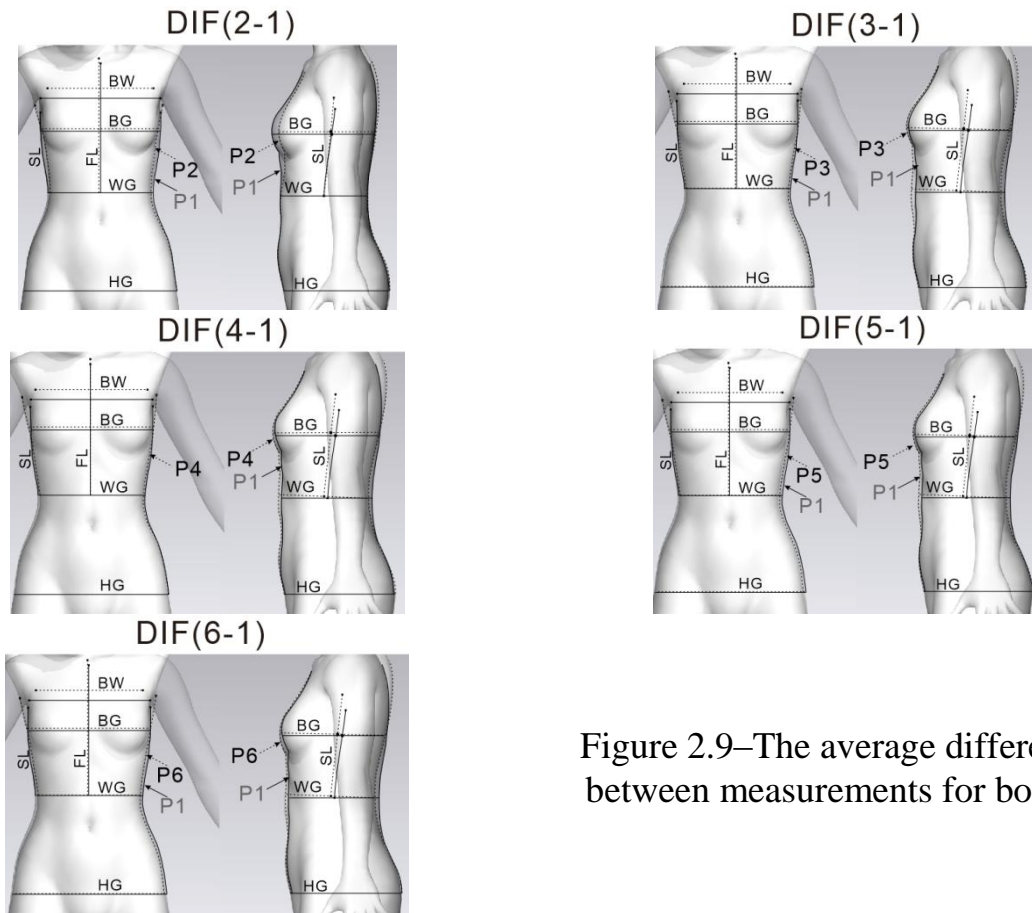


Figure 2.9–The average differences between measurements for body A

As shown in Figure 2.9, the profile of P1 is presented in solid line, through comparison, the bust line moves upward when hands up; the torso tilts backward and the abdomen bulges forward when lying. Two kinds of differences were named as ΔG_{DIF} or ΔL_{DIF} : ΔG represents the changing of girths, ΔL_{DIF} represents the changing of lengths. ΔG_{DIF} and ΔL_{DIF} are not equal to design ease (E) value, it is only the dynamic measurement change of the human body. Table 2.4 shows the differences between the front and back segments of girths. Table 2.5 shows the differences ΔL_{DIF} between the body lengths.

Table 2.4 – The maximum ΔG_{DIF}

Subtypes	ΔG_{DIF} of full girths, front and back segments, %								
	BG	BG _F	BG _B	WG	WG _F	WG _B	HG	HG _F	HG _B
Y1	1.9	-11.2	19.4	-0.8	-4.4	1.5	-1.5	-1.8	-6.9
Y2	2.0	-11.3	16.2	-0.9	-2.3	-1.7	-1.7	-1.4	-5.2
A1	3.3	-14.8	17.9	-2.8	-3.8	-1.5	-2.6	1.3	-7.7
A2	3.0	-15.5	18.5	-3.1	-4.8	-0.6	-2.2	1.5	-5.5
B1	3.1	-12.0	18.7	-2.4	-4.1	1.4	-2.7	1.1	-6.7
B2	4.0	-15.3	19.0	-2.5	-3.3	-1.7	-1.3	0.8	-5.7
C1	3.5	-12.5	19.2	-2.2	-4.9	2.3	-2.6	-2.4	-5.9
C2	3.7	-11.7	17.9	-2.3	-7.3	5.3	-2.0	3.6	-7.4
Avg., S.D.	$3.1 \pm$ 0.8	-13.0 ± 1.8	$18.4 \pm$ 1.0	$-2.1 \pm$ 0.8	$-4.4 \pm$ 1.5	$0.6 \pm$ 2.5	$-2.1 \pm$ 0.5	$0.3 \pm$ 2.0	$-6.4 \pm$ 0.9

Table 2.5 – The maximum ΔL_{DIF}

Subtypes	ΔL_{DIF} of measurements, %						
	SL	FNP-WL	BNP-WL	W _{BF}	W _{BB}	W _{SP}	L _{Cr}
Y1	22.9	10.5	-18.0	-31.3	31.2	-38.2	0.7
Y2	23.5	13.3	-14.2	-30.1	30.2	-32.0	0.5
A1	30.4	11.4	-15.3	-29.2	31.5	-43.8	-1.3
A2	24.3	9.9	-11.7	-30.8	32.7	-41.4	1.3
B1	28.1	10.3	-13.5	-32.0	30.1	-43.6	0.4
B2	30.8	10.1	-17.5	-35.5	35.3	-40.5	1.5
C1	36.8	12.6	-22.5	-39.1	30.8	-45.0	4.4
C2	32.3	6.4	-11.2	-33.6	34.1	-41.2	2.3
Avg., S.D.	$28.6 \pm$ 4.9	$10.6 \pm$ 2.1	$-15.5 \pm$ 3.7	$-32.7 \pm$ 3.3	$32.0 \pm$ 1.9	$-40.7 \pm$ 4.1	$1.2 \pm$ 1.7

If clothing is designed with zero ease (E), If clothing constructs with zero ease, a dynamic changing of body girths will make a clothing misfit and affect dynamic fit underwater. Therefore, it is necessary to design a pattern block with negative eases (E), considering that the dimensions of the body parts will be smaller in the

dynamic state. For example, if the BG_B value increases more than the BG_F value decreases, then overall BG increases. Therefore, the suit will fit snugly on the bust, and there is no need to increase the absolute value of the negative ease at the BG level; WG decreases significantly in dynamics, and the absolute value of the negative ease at the WG level must be increased so that the clothes fit the body.

Table 2.5 shows the dynamic difference between body key lengths. Some measurements have changed obviously in dynamic. For example, the back measurements of BNP-WL and W_{SP} significantly decreased when raising hands, and the measurements of the corresponding parts of the wetsuit need to be appropriately decreased based on the material properties, otherwise, the material will accumulate on the back and shoulder.

That is to say, the decreasing values in Table 2.4 and Table 2.5 can be used to analyze and calculate negative ease to keep the wetsuit fit.

To establish the digital replicas, a simulation of important torso parts is conducted. Figure 2.10 shows two kinds of differences which take place at the bust part:

1) under the influence of material compression in static. Figure 5.8a shows two cross-sections: first, BP without compression; second, BP' under compression. Generally, BP moves to BP' in two-dimensional;

2) under the influence of dynamic postures. Figure 2.10b and c show the bust cross-sections of two positions: P1 (hands down) and P2 (hands up). After hands up, the BG cross-section becomes smaller, and the position of bust line becomes higher. Generally, BP moves to BP'' in three-dimensional.

In the developed approach, the cross-section consists of two segments – front and back. It can be observed that the main change takes place in front segment. The female breast shape under compression has been modified in 3ds Max through editing the “mesh” with coordinates, as shown in Figure 2.10. The coordinates of the center point "o" is (0, 0), the coordinates of the initial position at BP are (7.235, -15.148) as shown in Figure 2.10 a (unit: cm), the new coordinates of the compressed position at BP' is (8.709, -13.566), and then according to the

calculation of the coordinates, BP moves $\Delta x = 1.474$ cm and $\Delta y = 1.582$ cm to the new position of BP'.

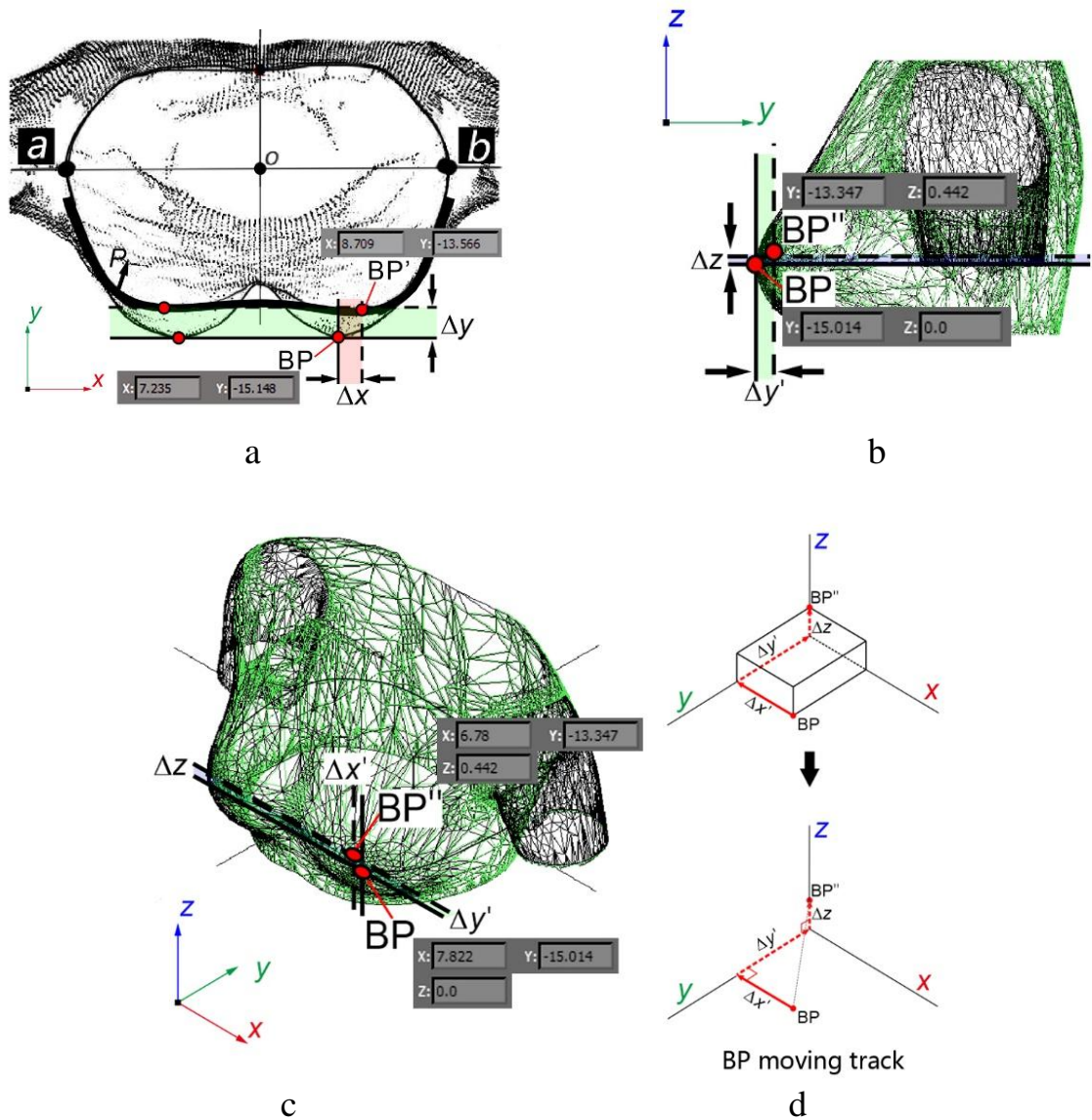


Figure 2.10 – Digital replica mesh of the female body: a – bust cross-sections before and after static compression; b, c – cross-section of bust girth before and after changing the position of the hands in dynamics; d – polygonal mesh editing scheme

Figure 2.10 b and c show the torso of two postures: P1 in black mesh, P2 in green mesh. Figure 2.10 b shows how the position of BP changed (Δz and $\Delta y'$) in the side view when raising hands, Figure 2.10c shows the same change in three-dimensional view. According to the coordinate calculation, the initial BP (7.822, -15.014, 0.000) moved to the new position of BP'' (6.780, -13.347, 0.442)

when $\Delta x' = -1.042$ cm, $\Delta y' = 1.667$ cm, and $\Delta z = 0.442$ cm. Moreover, the parallelepiped in red line illustrates the moving track of BP in three-dimensional space ($\Delta x'$, $\Delta y'$, and Δz).

For more accurate construction and control of the deformed avatar, it is necessary to simultaneously control several points. Figure 2.11 shows the cross sections of the scanatars of real bodies in the sagittal planes for positions P1 and P2 combined at the CR point. The anthropometrical points: FNP – upper sternal point, FWP – anterior waist point, BWP back waist point and BNP – bases of the back of the neck were used to determine the lengths of sections 4050 (from FNP to waist) and 5040 (from BNP to waist) respectively.

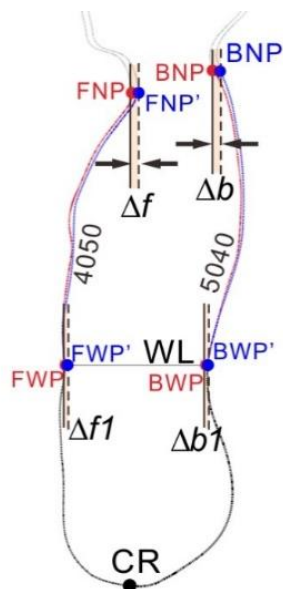


Figure 2.11 – Section in the sagittal plane in the position of the upper body tilt forward

As shown in Figure 2.11, the front centre line in red – from FNP to FWP (FNP-WL = 4050) and the back centre line in red – from BNP to BWP (BNP-WL = 5040) of the torso are in initial positions. Besides, the points and lines in blue illustrate the changing of the upper torso tilts backward after raising hands. Based on measurement data (in Table 2.3), the dynamic change of digital replica can be controlled by adjusting the four key points (FNP, BNP, FWP, and BWP) and the

length of measurements 4050, 5040. The methods of controlling the deformed replica after raising hands are as follows:

1) the front length 4050 increases a little (avg. is 10.6%), and FNP moves to FNP' in Δf , FWP moves to FWP' in Δf_l ;

2) the back length 5040 decreases a little (avg. is -15.5%), and BNP moves to BNP' in Δb , BWP moves to BWP' in Δb_l .

Conclusion of chapter 2

This chapter presents the measurements needed to make drawings of wetsuit parts.

1. For each of the existing types of bodies Y, A, B, C, two new subtypes have been developed that differ in the shape of the torso, namely, the ratio of dimensional features of the front and back parts of the bust girth.

2. Measurements and statistical analysis of changes in dimensional characteristics of 96 female bodies were carried out during swimming and in a standing position. The change in body size in typical dynamic postures during diving has been studied, and the difference between them in statics and dynamics has been established. Their values are determined, which are necessary when calculating the wetsuit increments for each of the subtypes of bodies.

3. The deformed digital replicas of the female body are constructed in the virtual system to test wetsuit design and the material strain and compression ability are identified. The digital replicas based on real data transformation are feasible and practical, and the process of establishing digital replicas with 3D body scanning technology is valid and accurate.

Chapter 3 STUDY OF COMPRESSION OF MATERIALS

The results obtained in this chapter are published in 2 works [145, 172].

3.1.The material compression on female body girths

This chapter is to study the pressure influence on body girth and to describe the compressible range of human soft tissue within the tolerable range of human body. Because of the difficulty and cost of the experiment, it is impossible to measure the human body in a real hydraulic environment. In this experiment, the controllable "strip" is selected to "squeeze" the key parts of the human body to simulate the hydraulic pressure.

Wide strips are used to stretch around the body girth to simulate hydraulic pressure, to study the compression range and limit value of body parts within the acceptable pressure. So, no matter how much pressure is exerted on the human body underwater, the tolerable compressible range of the human body has been determined above water. This is the key point of this experiment, which provides a reference for ease design.

Four commonly used wetsuit materials were selected for the basic properties test, as shown in Table 3.1.

Table 3.1 – Experimental wetsuit materials

No.	Face/wrong side layers	Middle layer	Level
M1	Nylon/Nylon	100% CR	High-end
M2	Polyester/Polyester	SCR (30% CR + 70% SBR)	Middle-end
M3	Polyester/Polyester	SBR	Low-end
M4	Nylon/Nylon	SCR (30% CR + 70% SBR)	Middle-end

*CR is chloroprene-rubber; SCR is styrene-chloroprene rubber; SBR is styrene-butadiene rubber

The outer layer of wetsuit neoprene is bonded with knitted material, so the physical properties of neoprene will be affected by the performance of the outer layer.

In order to study the influence of wetsuit material properties on compression performance, the experiment that simulates the compression pressure influence on the soft tissue is conducted, and the changing (decrease) of the body girths ΔG , material pressure P and relative material elongation E were measured.

To simulate the effect of hydraulic pressure on the soft tissues of the body girth, the change (decrease) of body girths ΔG and the material elongation were measured. To create compression effect, a strip of material 10 cm wide was used to tighten the measured body girths. 16 volunteers participated in the pressure test, including three volunteers of A1, five volunteers of A2 and 3 volunteers of B1, one volunteer of each of the other body types.

Figure 3.1 shows the scheme of the deformation of body girth, the equipment AMI-3037-10 for measuring pressure using pneumatic sensors and the method of attaching the sensors to the surface of the body.

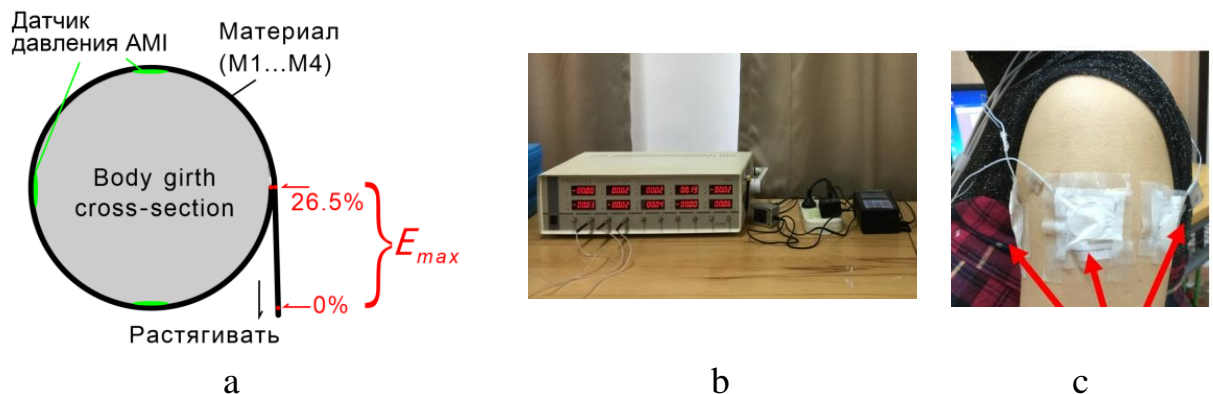


Figure 3.1– The pressure tests: a – test schematic diagram; b – AMI-3037-10 system; c – sensors

Gradually stretching the material in the uniaxial direction, they stopped when the maximum pressure on the soft tissue became critical, and recorded the data (Figure 3.2). Seven constructive girths of the body were chosen for measurements: shoulder, forearm, bust, waist, thigh, buttocks and calf. Pneumatic pressure sensors

were placed in front, on the sides, and behind on each of the girths of the body. Changes in girths were noted on a strip of material.

The wetsuit strips were stretched around the seven body girths respectively in ware (across the looped columns of the knitted material) and course (along the looped columns of the knitted material) directions respectively until to maximum elongation E_{\max} within maximum acceptable pressure P_{\max} . The maximum allowable pressure was determined from published literature about ≤ 3.11 kPa [11, 70, 79, 90, 109, 139, 154, 156, 157, 159, 166, 169].

Table 3.2 – Recommendations of other researchers about P_{\max} , kPa

P_{\max} on key body part	Clothing Types			Avg.
	Shaping	Sports	Medical	
Arm	-	2.6	3.49	≤ 3.11
Bust	3.75	3.27	4.66	
Waist	4.52	2.35	5.33	
Hip	2.68	2.68	-	
Thigh	2.22	2.1	2	
Calf	2.34	2.4	2.67	
Avg.	3.1	2.57	3.63	

The corresponding maximum body girth deformation is recorded (Figure 3.2), and the corresponding maximum acceptable pressure P_{\max} for each testee is calculated and recorded.

Figure 3.3 shows the most easily compressed and deformed part is the waist girth ($\Delta G_{\max} = -14.8\%$), and the most difficult part is the calf ($\Delta G_{\max} = -7.8\%$). If the waist girth decreased by $\Delta G_{\max} = -14.8\%$, it can be assumed that the waist can be maximum compressed the value of -14.8% by hydraulic pressure underwater (also the limit value that humans can tolerate).

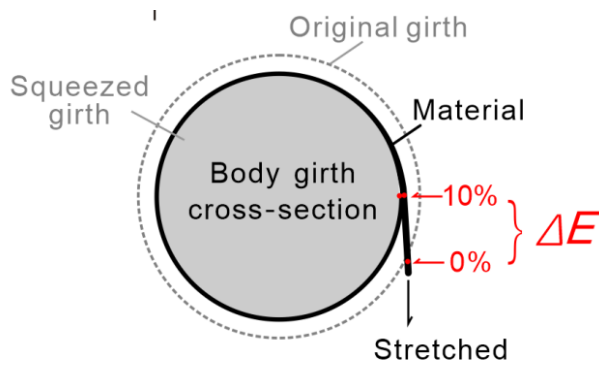


Figure 3.2– Scheme for measuring the deformation of the girth of the body during elongation of materials

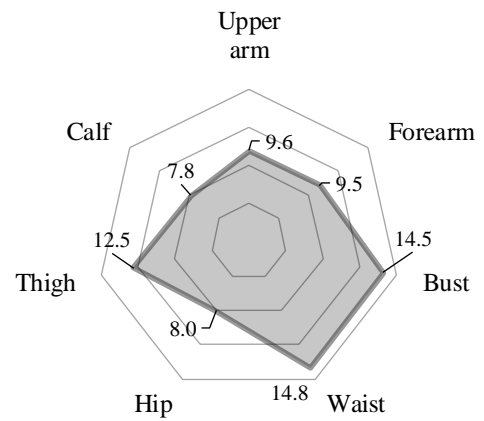


Figure 3.3 – Values of maximum deformations of body girths ΔG_{\max} , -%

Figures 3.4a and b show the Q-Q plots normal graphs of measured material pressure and elongation on the body. The normal distribution is within the 95% confidence interval.

Figure 3.5 and Table 3.3 show the measured average maximum material M1...M4 elongation E_{\max} on seven body girths (Appendix B, Table B.1). The 4 materials in 2 directions were tested for P_{\max} and E_{\max} on 7 body parts, with a total of 56(4*2*7) sets of average data.

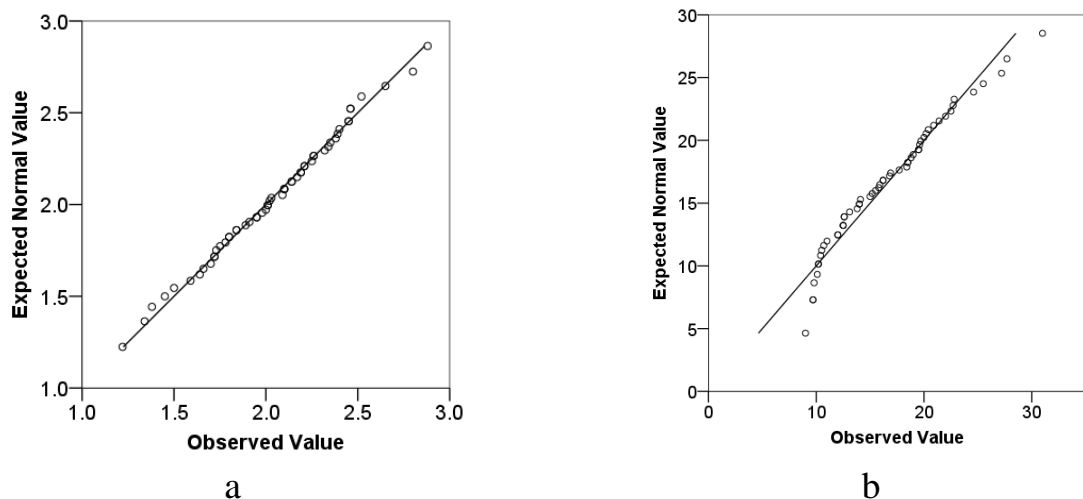


Figure 3.4 – Q-Q plots: a – measured pressure P_{\max} ; b – measured elongation E_{\max}

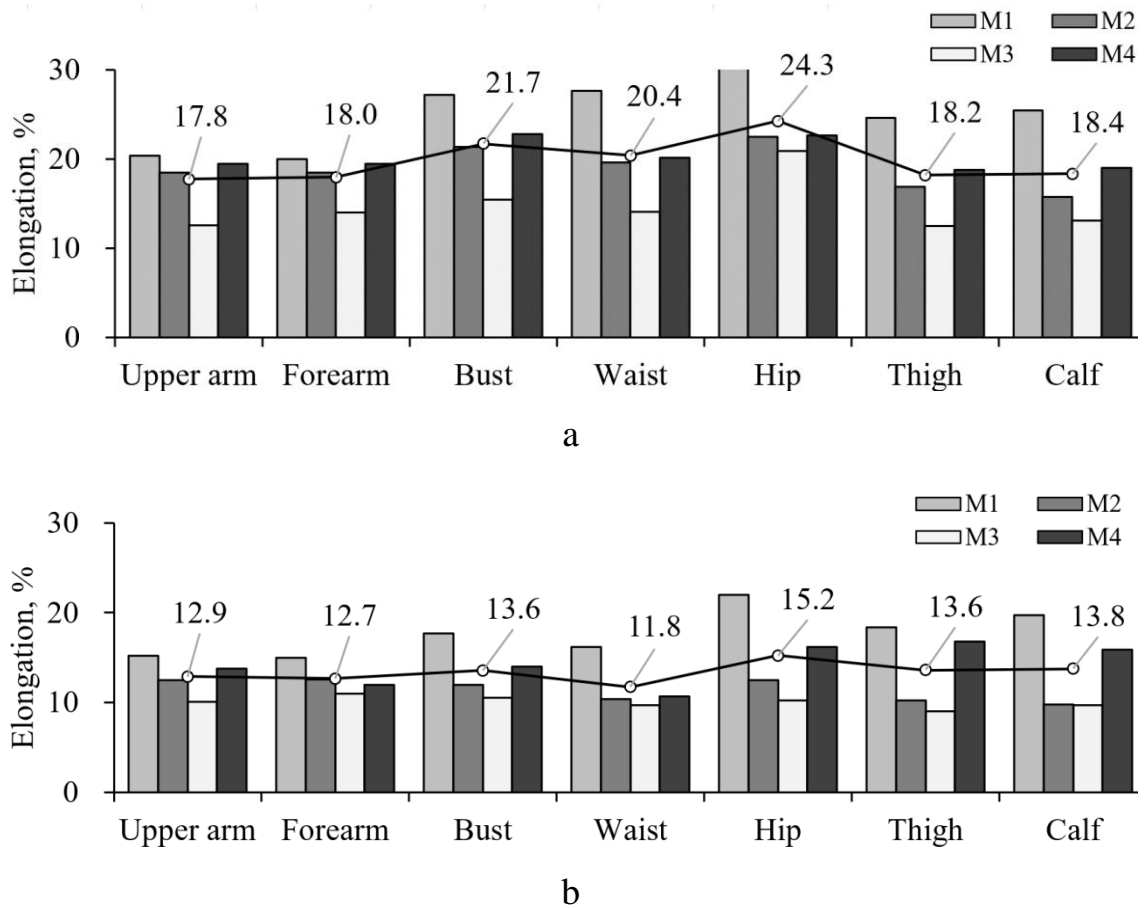


Figure 3.5 – Maximum ease values E_{\max} on seven body girths, %: a – measured under the material course; b – measured under the material wale

The average E_{\max} measured in material course is 19.8%; in material wale is 13.4%. The average maximum E_{\max} between course and ware is 16.6%.

Table 3.3 – The average E_{\max} of materials M1...M4, %

Body girth	E_{\max} values for materials				Avg.
	M1	M2	M3	M4	
Upper arm	17.8	15.5	11.4	16.7	15.3
Forearm	17.5	15.6	12.5	15.8	15.3
Bust	22.5	16.7	13.0	18.4	17.6
Waist	22.0	15.0	11.9	15.5	16.1
Hip	26.5	17.5	15.6	19.5	19.8
Thigh	21.5	13.6	10.8	17.8	15.9
Calf	22.6	12.8	11.4	17.5	16.1
Avg.	21.5	15.2	12.4	17.3	16.6

Table 3.3 shows the material can stretch to the maximum value at hip ($M1 = 26.5\%$), which means the hip can tolerate relatively larger tensile material deformation. For example, if the material stretches to the $E_{\max} = 19.8\%$ at hip and the corresponding girth value is maximum compressed by $\Delta G_{\max} = -8\%$, it means the material length at hip should be decreased by 19.8%, that is, the design ease is -19.8%.

Figure 3.6 and Table 3.4 show the measured P_{\max} on seven body girths under two materials directions (Appendix B, Table B.2).

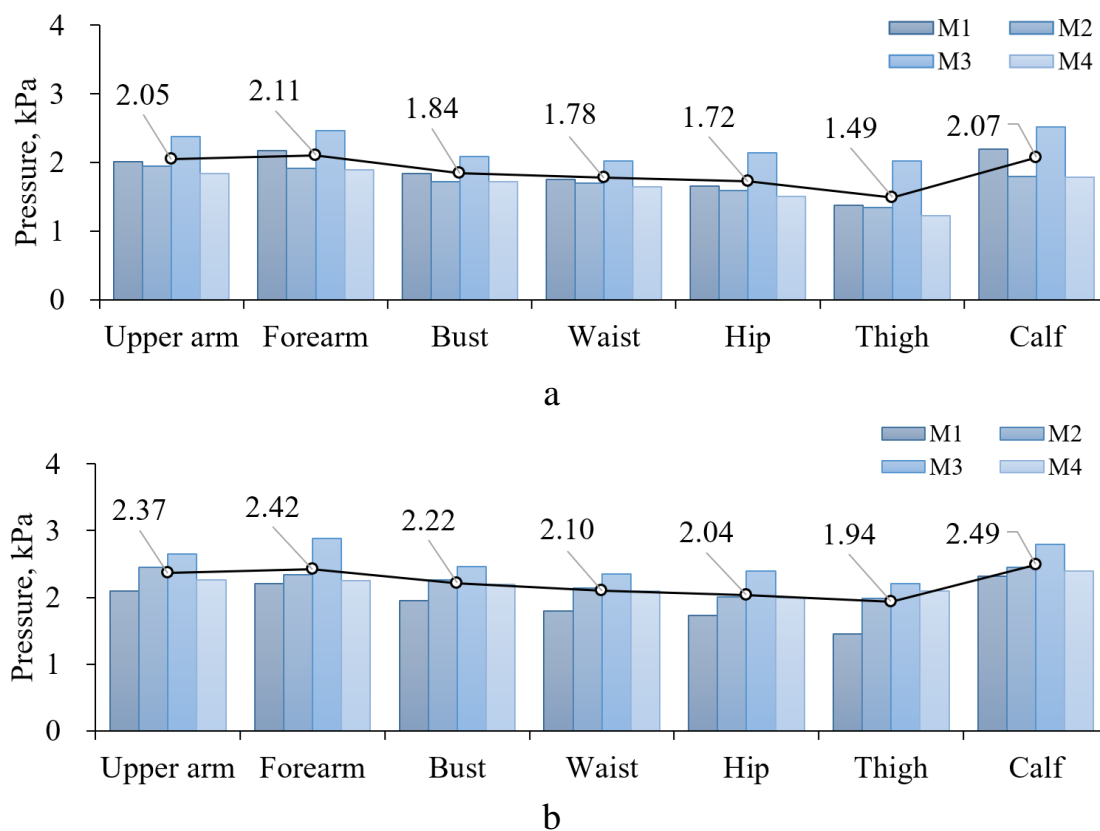


Figure 3.6 – Measurements of the average maximum P_{\max} , kPa: a – measured under the material course; b – measured under the material wale

The pressure measured under the material course is 1.87 ± 0.26 kPa; measured under the material wale is 2.22 ± 0.25 kPa. The average pressure is 2.04 ± 0.36 kPa

Table 3.4 shows the average minimum pressure measured on thigh; the average maximum measured on calf.

Table 3.4 – The maximum materials P_{\max}

Body parts	Pressure P_{\max} , kPa, on materials				Avg.
	M1	M2	M3	M4	
Upper arm	2.06	2.2	2.52	2.05	2.21 ± 0.22
Forearm	2.19	2.13	2.67	2.07	2.26 ± 0.28
Bust	1.90	1.99	2.28	1.96	2.03 ± 0.17
Waist	1.78	1.92	2.19	1.87	1.94 ± 0.18
Hip	1.70	1.80	2.27	1.75	1.88 ± 0.26
Thigh	1.42	1.66	2.12	1.66	1.71 ± 0.29
Calf	2.26	2.13	2.66	2.09	2.28 ± 0.26
Avg.	1.90 ± 0.30	1.97 ± 0.20	2.39 ± 0.23	1.92 ± 0.17	2.04 ± 0.36

All these measured pressure values are less than 2.7 kPa, which are within the acceptable range and the recommended pressure (≤ 3.11 kPa).

3.2. The relationship between body girth decrease, material elongation, and pressure

3.2.1. Compressibility of the soft tissues of the human body

To study the effect of P_{\max} on the body ΔG_{\max} , a ratio RC_b (ratio of compressive performance of the body) is proposed to analyze and parameterize the performance of seven body parts under the material compression

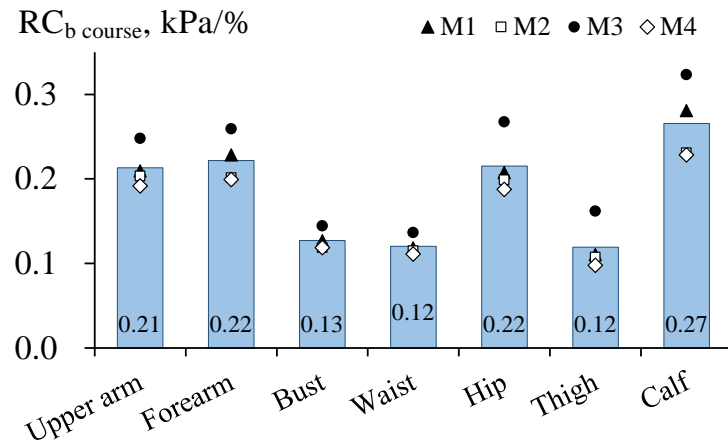
$$RC_b = |P_{\max} / \Delta G_{\max}| \quad (3.1)$$

where RC_b is ratio of compressive performance of the human body, kPa/%; P_{\max} is material pressure measured on the body, kPa; ΔG_{\max} is girth decreasing value, %.

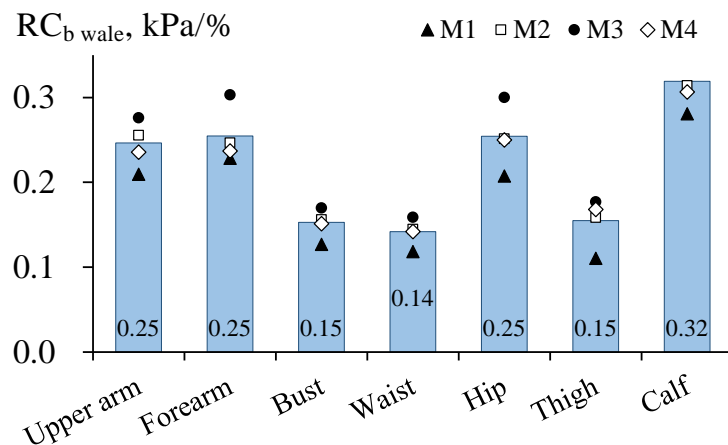
The coefficient RC_b indicates the amount of pressure that occurs under a 1% stretched material.

It can be seen from Figure 3.7 that the smallest RC_b values are obtained at the waist and hip girths, which means these parts are easily compressible and

deformable (Appendix B, Table B.3). In other areas, smaller material elongation leads to significant compressive pressure.



a



b

Figure 3.7 – The RC_b values: a – in the material course; b – in the material wale

Table 3.5 shows the relative minimum RC_b occurs at the waist, the maximum occurs at the calf. RC_b can predict the compression pressure value exerted on the female body girth. The larger the RC_b value, the stronger the compression pressure on the girth. For example, when the M2 $RC_b = 0.27$ at calf, it means the ΔG decreased per 1.0%, the predicted compression pressure will be increased by 0.27 kPa.

Table 3.5– The average materials RC_b on M1...M4, kPa/%

Body position	RC_b , kpa/%, on materials				Avg.
	M1	M2	M3	M4	
Upper arm	0.21	0.23	0.26	0.21	0.23
Forearm	0.23	0.22	0.28	0.22	0.24
Bust	0.13	0.14	0.16	0.14	0.14
Waist	0.12	0.13	0.15	0.13	0.13
Hip	0.21	0.23	0.28	0.22	0.24
Thigh	0.11	0.13	0.17	0.13	0.14
Calf	0.28	0.27	0.34	0.27	0.29
Avg.	0.19	0.19	0.24	0.19	0.20

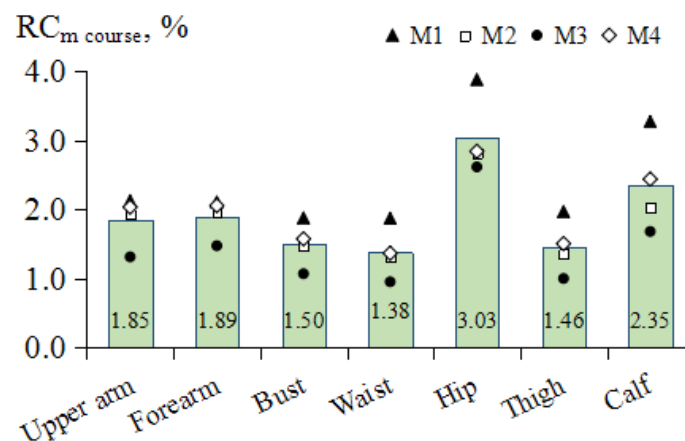
3.2.2. Tension of materials

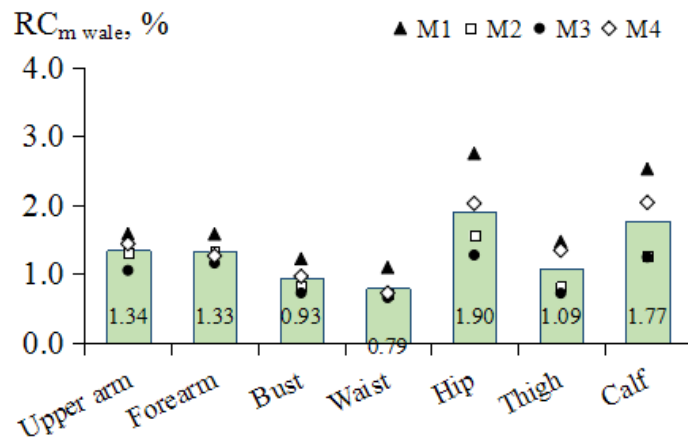
The RC_m index (material extensibility coefficient) (Appendix B, Table B.4) was proposed and calculated according to the equation (3.2) to match the ability of the soft tissues of the body to compress under the influence of material stretching, adequate to the constructive negative ease

$$RC_m = | E_{\max} / \Delta G_{\max} | \quad (3.2)$$

wherein RC_m is the material compression ratio; ΔG_{\max} is girth decreasing value, -%; E_{\max} is material elongation value, %.

Figure 3.8 shows that the RC_m values, the lowest RC_m values were obtained on waist and hip.





b

Figure 3.8 – The RC_m values: a – in the material course; b – in the material wale

Table 3.6 shows the RC_m of M1...M4 in static test of the female body.

Table 3.6– The average materials RC_m on key body parts

Body position	M1	M2	M3	M4	Avg.
Upper arm	1.85	1.61	1.18	1.73	1.60
Forearm	1.84	1.64	1.32	1.66	1.61
Bust	1.55	1.15	0.90	1.27	1.22
Waist	1.48	1.01	0.80	1.04	1.09
Hip	3.31	2.19	1.94	2.43	2.47
Thigh	1.72	1.08	0.86	1.42	1.27
Calf	2.90	1.64	1.46	2.24	2.06
Avg.	2.09	1.48	1.21	1.69	1.62

The relative maximum RC_m is M1 occurs at hip, and the measured average RC_m is 1.62. RC_m can predict the value of the materials that deformed (compressed) the female body ΔG . For example, the M2 $RC_m = 2.19$ at hip, it means the M2 needs $E = 2.19\%$ to compress the hip $\Delta G = -1.0\%$.

The RC_m can be used to calculate and find:

-from the relationship between the measured ΔG_{DIF} and material RC_m can calculate the E_{min} for pattern design; the larger the RC_m value, the larger the result

of E_{\min} value(Equation 3.3).

- the degree from easily to difficultly deformable (compressible) of the female body girth is obtained. The larger the RC_m value, the more difficulty the girth compressed.

- to justify a suitable material, taking into account the compression properties to select a suitable material: the greater the value of RC_m , the more extensible the garment material.

3.3. Structural additions

The wetsuit is designed with negative ease. In order to ensure that the wetsuit can still fit underwater, the wetsuit should be as close as possible based on satisfying the movement. Therefore, it is necessary to design a reasonable ease range from E_{\min} to E_{\max} , which can not only satisfy the wearing comfort but also satisfy the dynamic size change of human body for keeping tight fit.

The steps of E_{\min} calculation are as shown in Figure 3.9.

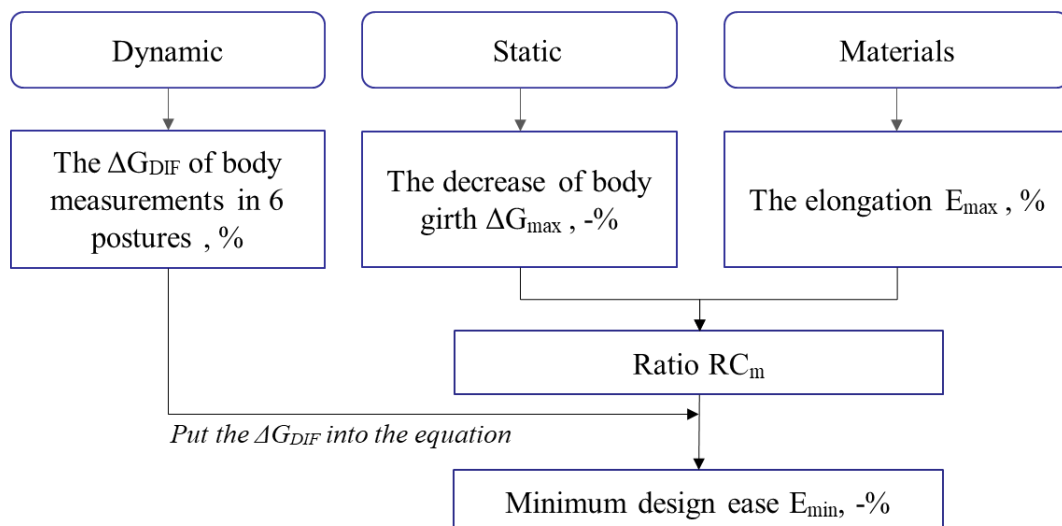


Figure 3.9 – The steps of the minimum design ease E_{\min} calculation

The relationship between the measured ΔG_{DIF} and material RC_m can be calculated as the minimum ease value E_{\min} for pattern design.

$$E_{\min} = RC_m \cdot \Delta G_{\text{DIF}} = (E_{\max} \cdot \Delta G_{\text{DIF}}) / \Delta G_{\max}, \quad (3.3)$$

wherein E_{\min} is the minimum ease value, %; RC_m is the compression ratio of materials; ΔG_{DIF} is the girth decreasing value in dynamic postures P1...P6, %

For example, if waist girth $\Delta G_{\text{DIF}} = -3.8\%$, take the material M1 average $RC_m = 1.48$ (Table 3.5) at waist, the E_{\min} can be calculated is $1.48 \cdot (-3.8) = -5.6\%$.

Combining the average RC_m at main body parts (in Table 3.5) with ΔG_{DIF} (in Table 2.4, Chapter 2), the E_{\min} of the main body girths of 8 body types are calculated by Equation (3.3) (Appendix B, Table B.5...10). The calculated material E_{\min} of M1...M4 for 8 body types are shown in Table 3.6. E.g., to calculate the E_{\min} in WG, multiply the ΔG_{DIF} by the RC_m in WG.

Figure 3.10 shows the E_{\min} is during $-32.9...3.1\%$, they are mostly negative values.

Table 3.7 – E_{\min} of M1...M4 for 8 body types

Body girth	Negative value of E_{\min} , -%								Avg.
	Y1	Y2	A1	A2	B1	B2	C1	C2	
BG _F	13.6	13.8	18.0	18.9	14.6	18.6	15.2	14.2	15.9 ± 2.2
WG	0.9	1.0	3.1	3.4	2.6	2.7	2.4	2.5	2.3 ± 0.9
WG _F	4.9	2.6	4.2	5.4	4.6	3.7	5.5	8.1	4.9 ± 1.6
HG	4.6	5.3	8.0	6.8	8.3	4.0	8.0	6.2	6.4 ± 1.7
HG _B	21.3	16.1	23.8	17.0	20.7	17.6	18.2	22.9	19.7 ± 2.9
Thigh	1.9	1.8	1.6	2.4	0.7	2.2	3.3	3.1	2.1 ± 0.8
Calf	4.8	4.0	4.3	4.0	5.0	2.5	7.3	5.3	4.7 ± 1.4
	Positive value of E_{\min} , %								
Upper arm	0.5	1.4	2.3	1.8	1.6	1.1	1.2	1.8	1.5 ± 0.5
Forearm	0.9	1.4	2.1	2.1	2.1	1.8	2.5	2.1	1.9 ± 0.5

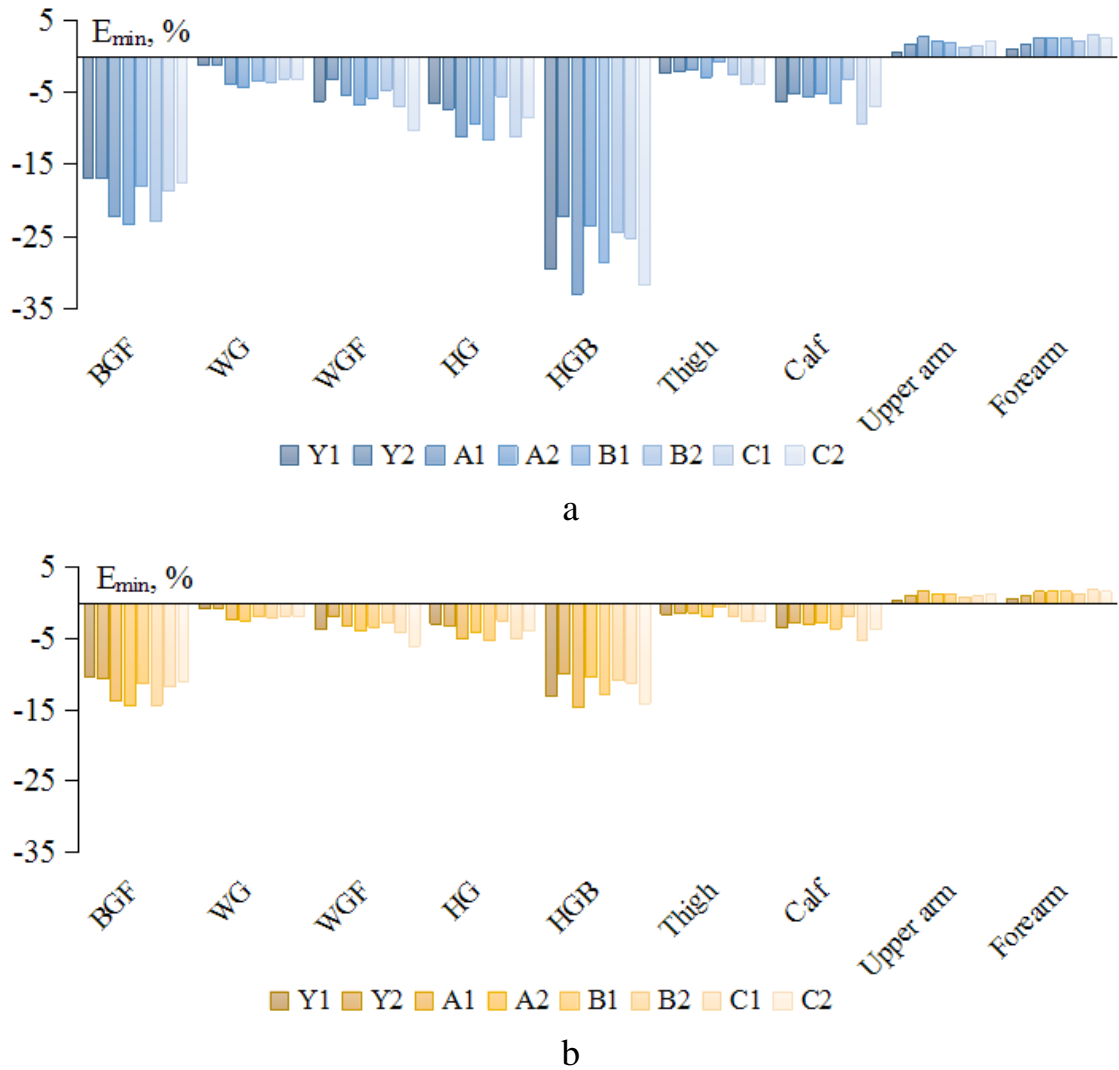


Figure 3.10 – The E_{min} values, %: a – in the material course; b – in the material wale

Thus, for the first time, constructive additions are differentiated depending on the completeness of the body. The found values of E_{min} for the girths of the body will be used in the design of the wetsuit by coordinating them with the dynamic change in the dimensional features of the body.

Conclusion of chapter 3

The pressure values of wetsuit materials on the body were measured. A statistical analysis of the pressure values exerted by various wetsuit materials on the soft tissues of the female body was carried out.

1. The average E_{\max} of body is -19.8% (course) and -13.4% (wale). Therefore, the allowable values for the decrease in girths in the design of the wetsuit were -16.6...0%.

2. The index RC_b is proposed to predict the material pressure on the female body parts and improve the procedure for choosing the appropriate wetsuit material.

3. The relative decrease values of body girths were measured from the most to the least compressible in order –*waist, bust, thigh, upper arm, forearm, hip, calf*. The average ΔG of all girths is -11.0%.

4. The RC_m is proposed to find and predict the female body ΔG under the action of a tight-fitting clothing material with relative elongation E . The index can be used to calculate the average elongation needed when the body girth is decreased per 1%.

5. The negative ease values E_{\min} for the construction of a wetsuit and the design ease E_{\min} values for 8 types are obtained to maintain the underwater tight and dynamic motions.

Chapter 4 RELATIONSHIP BETWEEN INDICATORS OF MATERIALS MECHANICAL PROPERTIES AND PRESSURE OF CLOTHES ON THE BODY

The results obtained in this chapter are published in 1 work [146].

4.1. Wetsuit materials mechanical test

The wetsuit is close to the surface of the human body by the elasticity of the material, and it will generate a large contact pressure after wearing it on land. Factors that affect the pressure characteristics of wetsuit include various physical properties of materials, and the relationship between them needs to be considered when studying pressure.

In order to further study the relationship between the material mechanical properties and the pressure values exerted on the human body, a set of instruments KES-FB1...4 (Kawabata Evaluation System-Fabric produced by KATO TECH Japan) was used in this study: Tensile & Shear Tester KES-FB1, Bending Tester KES-FB2, Compression Tester KES-FB3, Surface Tester KES-FB4.

According to the direction of the loop structure of the outer knitted fabric, the wetsuit materials are divided into wale and course. Four materials are cut into the same size samples: the size of each sample is 20×20 cm, and each material is cut into three pieces in the wale and course respectively.

Figure 4.1 shows the wetsuit materials used in the experiments. The wetsuit material consists of 3 layers, the inter layer (middle layer) is neoprene, and the inner and outer sides are knitted materials (Figure 4.1a). Four kinds of experimental materials were selected for the study, and the enlarged display of their surfaces is shown in Figure 4.1b.

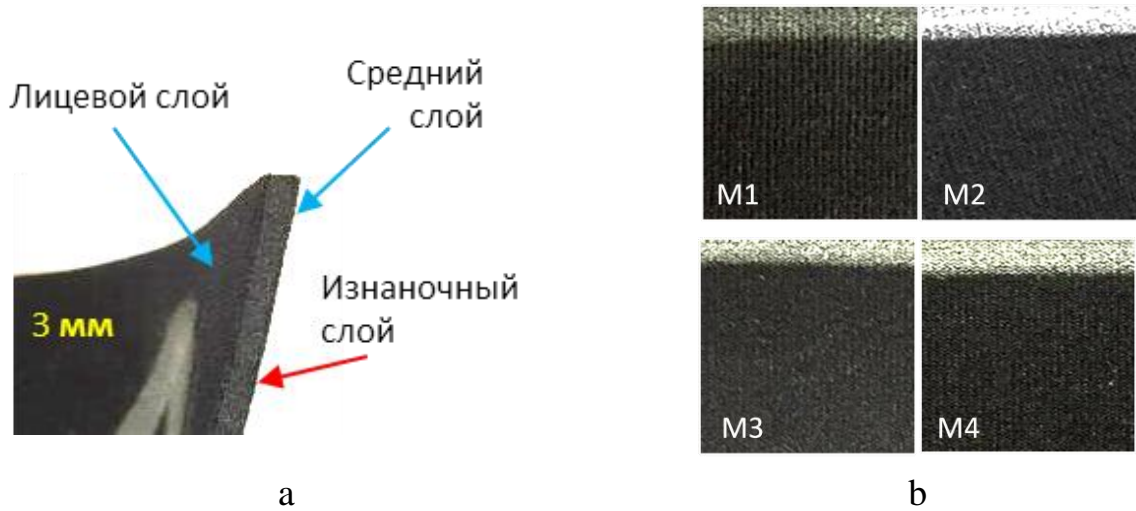


Figure 4.1 – Experimental fabric: a –structure of layers; b – Knitted structure of surface

Firstly, the tension properties of materials are tested by KES-FB1. The index of strain (elongation) is named EMT (%), as shown in Figure 4.2 and Table 4.1 (Appendix C, Figure C.1...12). The larger the value, the better the extensibility of the material.

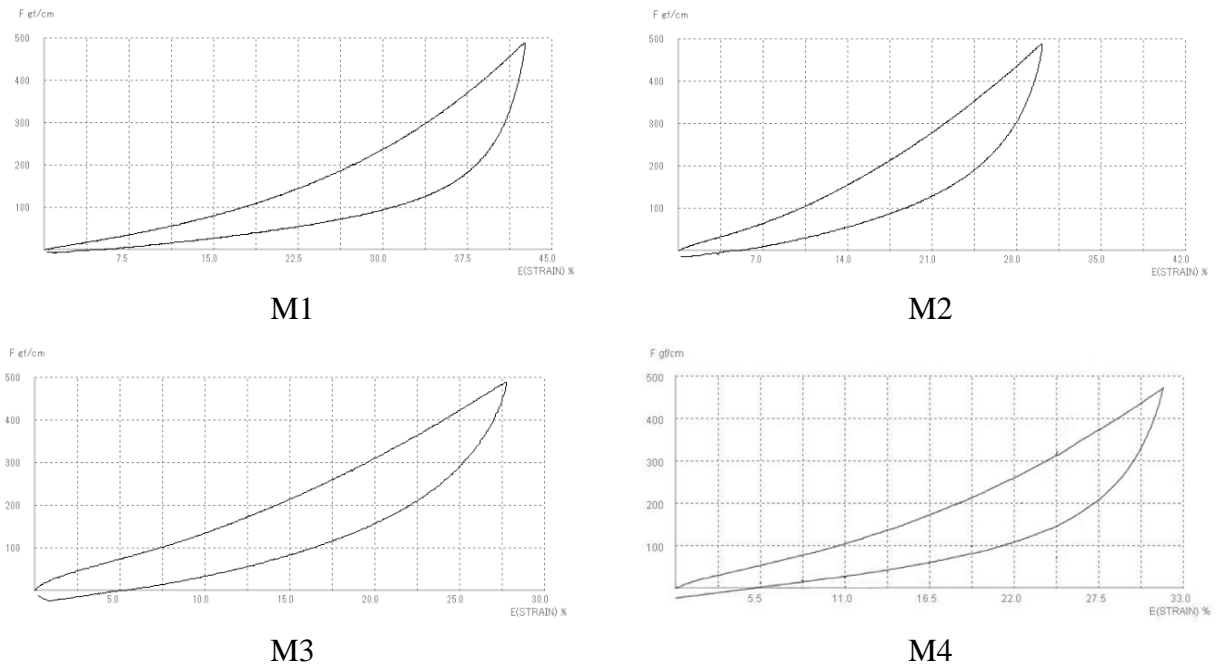


Figure 4.2 – KES tension (500 cN/cm) test M1...M4 in course

Based on test results, those materials elongations are weak in the wale, so the EMT is tested only under standard load 500 cN/cm in the course direction; and the

EMT is tested under low load 50cN/cm (high sensitivity) in two directions, as shown in Table 4.1.

Table 4.1 – Materials EMT values

Materials	Standard 500 cN/cm	High sensitivity 50 cN/cm	
	EMT _c , %	EMT _c , %	EMT _w , %
M1	42.65	22.45	18.03
M2	30.17	26.40	12.69
M3	27.80	11.64	9.32
M4	30.56	24.84	13.91

It can be found that M1 high-end materials perform better in extensibility, followed by M2. Next, other mechanical properties were also tested, some key parameters are shown in Table 4.2.

Table 4.2 – KES-FB1...4 indexes (*Low load 50 cN/cm)

Indexes	Direction	M1	M2	M3	M4
LT*	Wale	0.47	0.52	0.61	0.54
	Course	0.53	0.56	0.63	0.58
G (cN / [cm·(°)])	Wale	2.52	3.59	7.31	3.14
	Course	2.49	3.57	7.08	3.62
WT (cN.cm / cm ²)*	Wale	2.12	1.65	1.43	1.88
	Course	2.99	3.70	1.82	3.57
RT (%)*	Wale	61.79	58.79	50.35	54.79
	Course	62.88	61.89	53.85	54.06
2HG	Wale	5.28	8.75	19.20	7.85
	Course	4.15	7.35	18.90	8.13
RC (%)	-	51.52	58.00	53.64	57.43

In Table 4.2, the harder the material, the larger the value of LT (the max. LT = 1) and G. The stronger the material's resistance to deformation, the larger the value of WT. The stronger the recovery ability and the better the elasticity, the larger the value of RT, but the smaller the value of 2HG. The better the compression recovery capability of the material, the better the thickness durability and the fullness, the larger the value of RC. Therefore, the comparison of the data shows that the material elasticity and recovery compression performance of M1 is better, followed by M2.

Through the KES test and comparison, the physical quantity reflecting the characteristics of the wetsuit material can be obtained to describe the material. For example, the compressibility and stretchability of the material affect the pressure comfort of the wetsuit. When the ductility of the material is strong and the compressive properties are excellent, the general deformation of the material will cause a smaller feeling of squeezing to the human body; otherwise, it will be larger because the material appears to be "harder". Moreover, the resilience and soft thickness of the material will also have a more significant impact on the wetsuit comfort.

Then, the tension load F was used to analyze the relationship between the material and the pressure on the body.

The relationship between load F (Standard 500 cN/cm) and elongation E is shown in Figure 4.3.

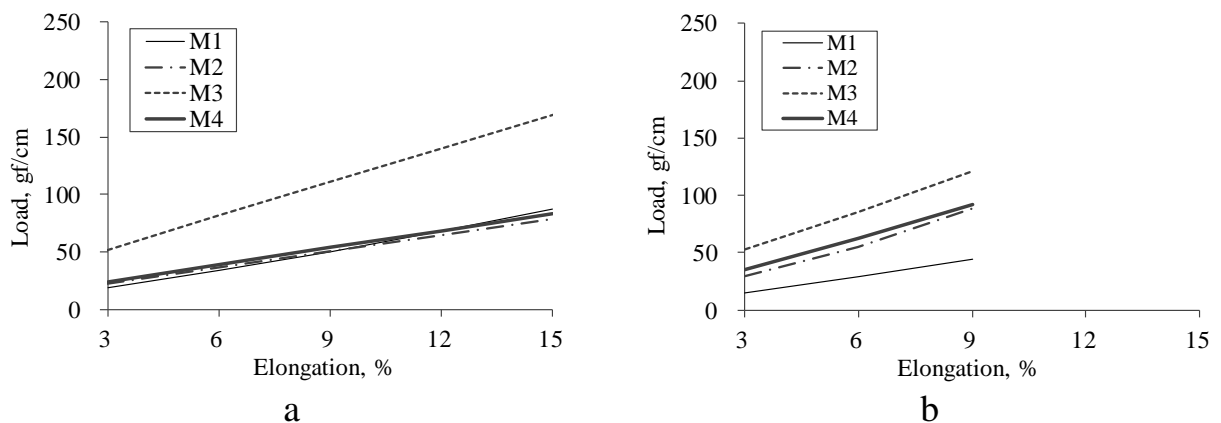


Figure 4.3 – Relations between the tension load and the elongation EMT: a – in the course; b – in the wale

In the course of the material, the average elongation is less than 14.7%, which should be connected to the maximum allowable elongation E of the material M3 measured when tightening the body girths (Chapter 3). Therefore, the integer value of EMT_c was chosen to be less than 15.0% and the load values for them were found from the graphs to analyze the properties of M1...M4. The load was for M1, M2, M4 – 78.2...86.70 cN, M3 – 168.9 cN. EMT_w must be less than 9.32% (M3).

Then, for various elongations of 3, 6, 9, 12, 15%, the force values were chosen.

4.2. Correlation analysis between KES parameters and pressure

To study the correlation between KES mechanical data and human perception (pressure value), further analysis is needed (the tension load data is in Appendix C, Table C.2 and 3), the correlation coefficients were calculated (Table 4.3). Calculations were performed for a 95% confidence interval for $n = 4$. “Bold” means $r > 0.811$ and significance $sig. < 0.05$.

Table 4.3 – Correlation coefficients between P_{max} , E_{max} and KES indexes

KES indexes	P_{max}		E_{max}	
	Course	Wale	Course	Wale
LT	0.693	0.973	-0.937	-0.834
WT	-0.988	-0.967	0.496	0.989
2HG	0.822	0.956	-0.904	-0.818
F3	0.893	0.970	-	-
F6	0.914	0.971	-	-
F9	0.930	0.968	-	-
F15	0.959	-	-	-

**LT* is tensile rigidity, *WT* is tension energy, $gf \cdot cm/cm^2$; *2HG* is elasticity for minute shear, gf/cm

It can be seen that the correlation between the maximum acceptable pressure P_{max} , elongation E_{max} and the KES parameters WT, LT, F_x under elongations 3%, 6%, 15% are higher.

4.3. Prediction model

Through SPSS analysis (AppendixC, Figure C.13...17), the function models composed of KES parameters have been established.

The pressure value provided by elastic materials is in a certain range, thus S-curve (sigmoid function), and Inverse proportional function models are used to predict the relationship between pressure and material properties.

$$y = e^x = \exp\{f(x)\} \quad (4.1)$$

$$y = k / x + \varepsilon_i \quad (4.2)$$

where y is the dependent variable of pressure, e is the natural base; x is independent variables of material properties, $i = 1, 2, 3, 4$, $x \neq 0$, $y > 0$, ε_i is the random error (random variable) term.

Then multivariable Equations (4.3)...(4.7) below are obtained, coefficients *sig.* < 0.05 and Pearson correlation coefficient R-Square > 0.930 , these selected equations have good fit.

in course

$$P_{\max} = 2.70 - 78.81 / F15_c \quad (4.3)$$

$$P_{\max} = 1.17 + 1.95 / WT_c \quad (4.4)$$

in wale

$$P_{\max} = 0.81 + 2.45 / WT_w \quad (4.5)$$

$$P_{\max} = 4.47 - 1.20 / LT_w \quad (4.6)$$

$$P_{\max} = e^{\left(1.03 - \frac{1.96}{2HG_w}\right)} \quad (4.7)$$

wherein e is the natural base approx. 2.718; WT and LT are KES parameters of material tension properties; 2HG is the KES parameter of material shear properties.

As we can see, all equations have $sig. < 0.05$ and good fit. P_{\max} is the maximum pressure value, the equations of (4.3...4.6) can derive the pressure range during $0 < P_{\max} < 4.47$ kPa, (4.7) only can derive the pressure range from $0 < P_{\max} < 2.80$ kPa.

The obtained equation can be used to predict the pressure value of wetsuit material on female body. Firstly, the KES tension properties of the material were measured. Secondly, the course F_x of the material sample was extracted, and the value of tensile force was F15 when the elongation in course reached 15%. Then, we can predict whether the pressure value to the human body is appropriate or not.

4.4. Check on prediction mathematical models

Although the equations (4.3) to (4.7) have high correlations, the error δ in the equations still needs to be determined by data inspection. The KES test data of the wetsuit material can be put into the equation for test calculation.

$$\delta = \Delta / y \cdot 100\% \quad (4.8)$$

where δ is actual relative error, %; Δ is the absolute error, predicted value \hat{P} minus measured value P_{\max} by material strips; y is measured value P .

Table 4.4 shows the P_{\max} comparison, P_{\max} is measured by material strips, \hat{P} is calculated using the five equations.

Table 4.4 – Absolute difference between calculated and measured material strips
M1...4 pressure

Equations	Material property index	Absolute difference value between theoretical and actual pressure, %				
		M1	M2	M3	M4	Avg.
(4.3)	F15 _c	-3.56	-1.40	0.03	5.76	2.68
(4.4)	WT _c	-1.88	-1.09	0.38	3.65	1.78
(4.5)	WT _w	1.47	2.78	 -0.49 	-3.25	2.00
(4.6)	LT _w	 -0.21 	-3.16	-0.79	3.09	1.82
(4.7)	2HG _w	 -0.25 	0.26	 -0.27 	 -0.11 	0.22

It can be found that the maximum absolute difference calculated by equations is -3.56...5.76%, the minimum absolute difference is 0.03%, Eq. (4.7) has the smallest absolute difference of 0.22% (0.002 kPa). Therefore, it can be judged that in the case of wetsuit material strips, all of these prediction equations are feasible and have a certain accuracy. In the subsequent prediction of the pressure value of the finished wetsuit, its rationality will be further tested.

Conclusion of chapter 4

1. The relationships between different factors are obtained in this chapter. The KES parameters are used to get multivariate equations for predicting the range of comfortable pressure.

2. The maximum elongation in KES-FB1 is between 9.32...42.65%, which was greater than the maximum elongation of 10.80...26.50% measured on the human body in the accepted range with a large difference.

3. New indexes measured on material samples (tensile forces by certain values) are proposed for compression wetsuit design in the actual “body-shell” system. The suitable conditions of the Fx for predicting the pressure equation are as follows: when the tensile strain degree (x) of material is between 3...15%, the tension F is less than 200 cN / cm and the thickness of T₀ is about 3 mm.

Chapter 5 DEVELOPMENT OF WETSUIT DESIGN

The development of a new technique for designing female wetsuit, and verification in a virtual environment and industrial environment (the results were published in 6 papers) [147, 148, 149, 150, 174, 175].

5.1. Wetsuit prototype design

5.1.1. Initial prototype of tight clothing

Currently, there is no complete and detailed methodology for constructing drawings of tight-fitting full-length clothing combining the lower and upper parts. According to the location of the main structural lines reflected in the female body, Figure 5.1 shows the scheme of their display in the design drawing based on anthropometric theoretical and practical knowledge. The layout scheme of the body is made by 9 vertical secant planes 0-8. The layout scheme of the basic grids was taken as a basis according to the method “EMKOCЭB”.

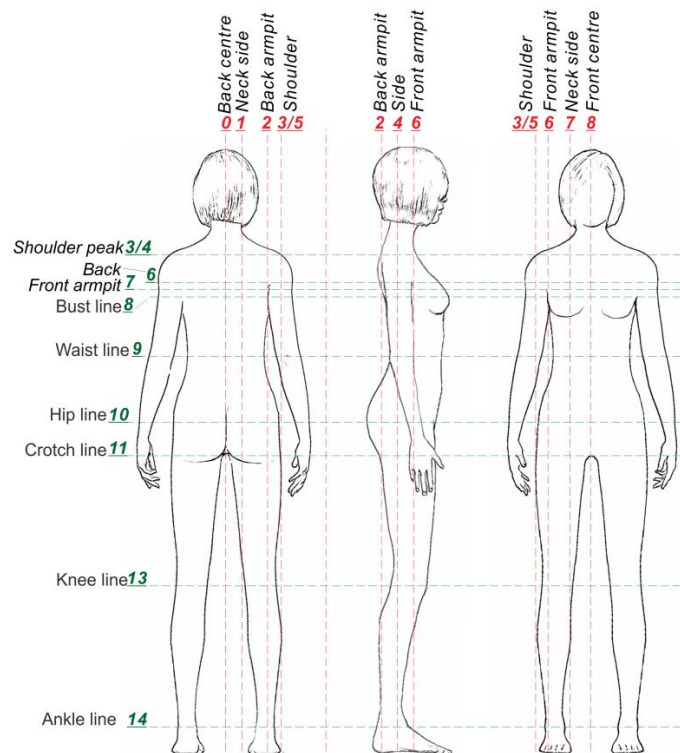


Figure 5.1 – Reference lines corresponding to the female body

The horizontal lines are marked with green numbers 0, 1, 2, 3,...n; vertical – red numbers 0, 1, 2, 3,...n. The body and the lower part are numbered continuously. The intersection points of the lines are numbered with two digits. The first digit corresponds to the horizontal number, the second – to the vertical number.

Figure. 5.2 shows the drawing method of the initial prototype of average size with zero ease.

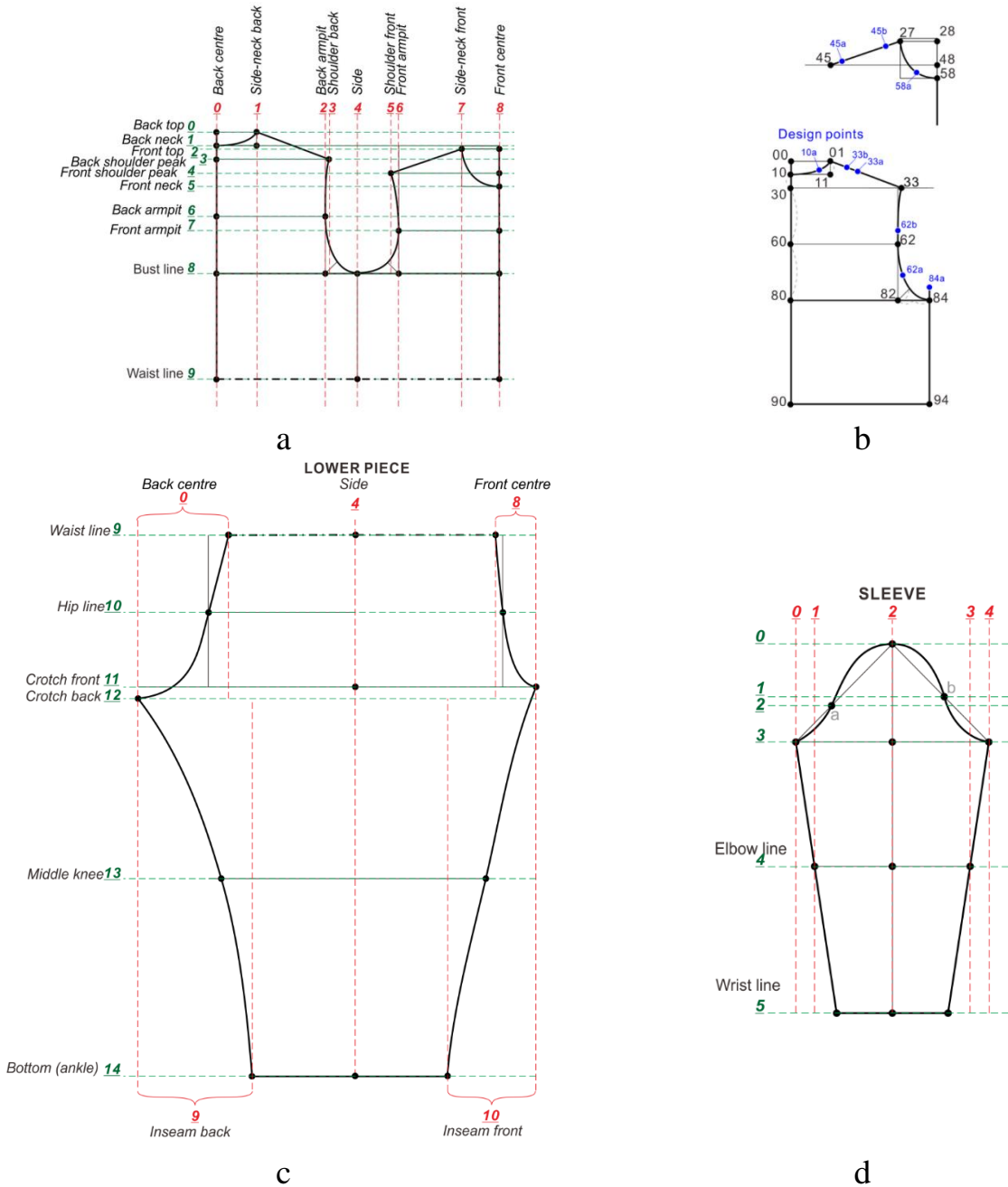


Figure 5.2 – Drawing of the prototype: a – the top with points marks; b – example of points marks; c – the lower; d – sleeve

The necessary calculations were made according to the formulas given in the books on the design of clothes[5, 39, 152] (Figure 5.3). The algorithm for constructing a drawing of the basic structure is given in Appendix D, TableD.1...6.

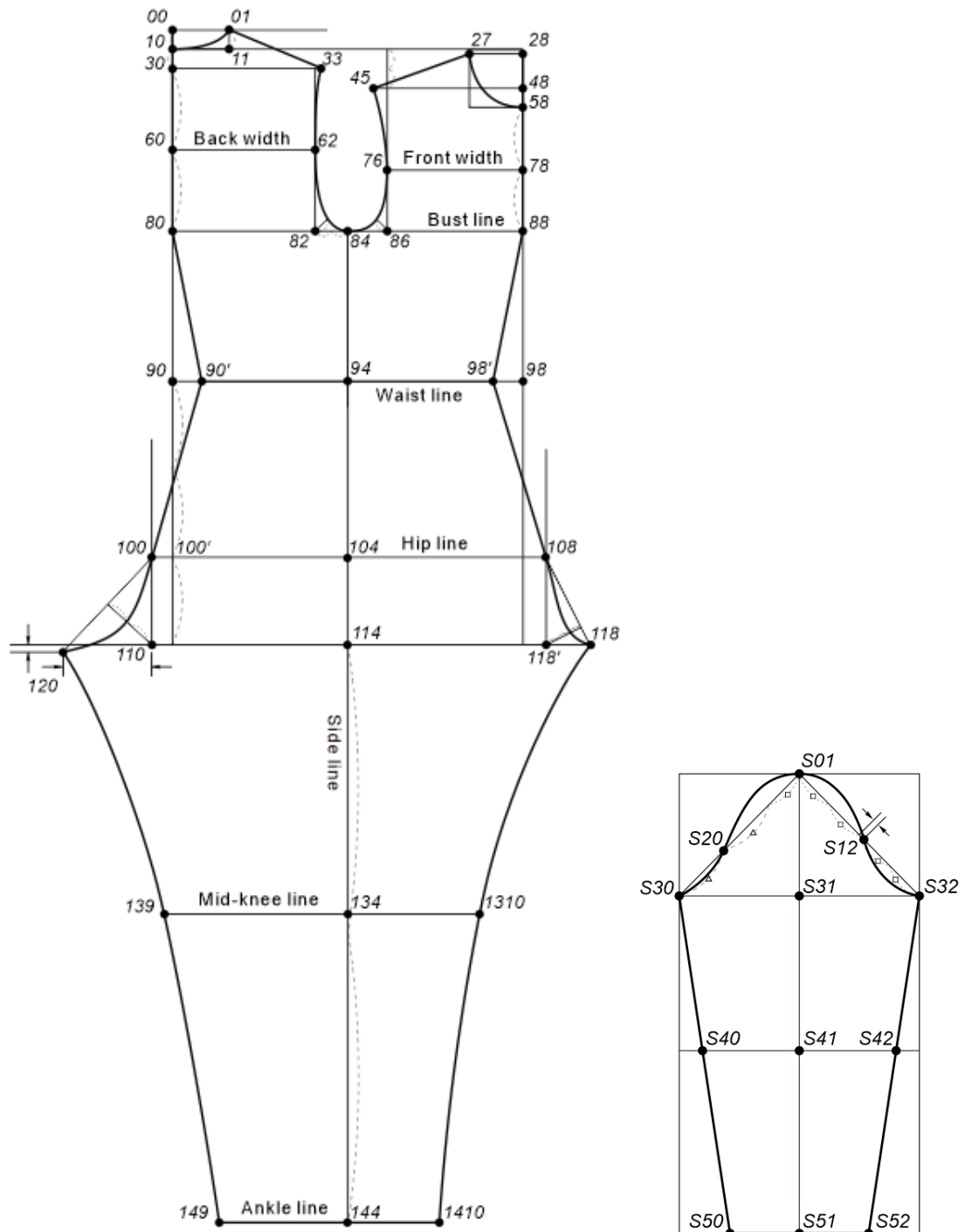


Figure 5.3 – Finished drawing of initial prototype

5.1.2. Basic wetsuit pattern

Taking M2 fabric and A1 body type as an example, the average measured anthropometric data are applied to the initial prototype to change the structure of multiple parts and modify some details, and a basic type wetsuit pattern is obtained.

Figure 5.4 shows the basic type wetsuit pattern modified (black line) based on the initial prototype. Seamless in front center, a straight line from the neckline to the crotch point, and most wetsuit openings (zipper) are usually designed on the back.

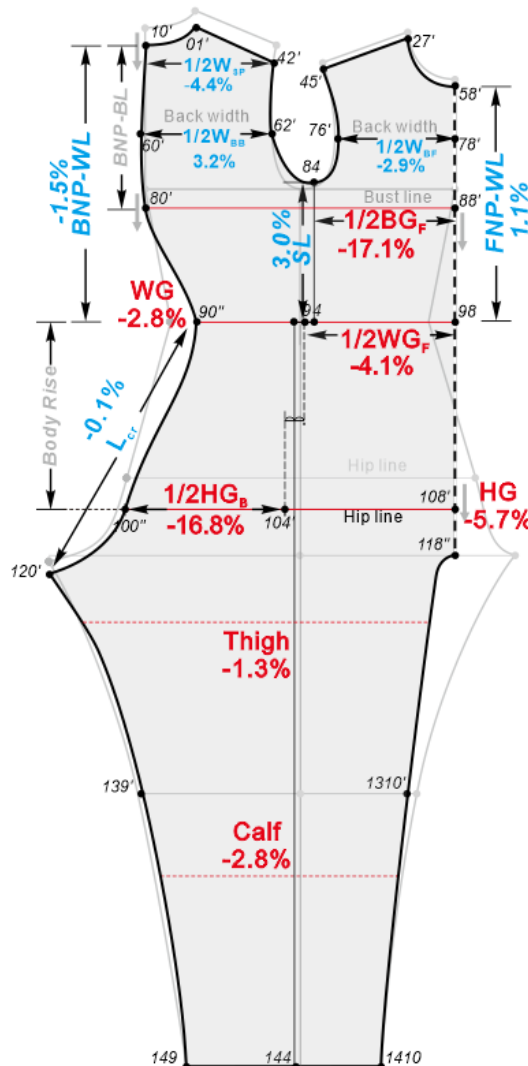


Figure 5.4 – Basic wetsuit pattern modified based on the initial prototype

The rules of basic wetsuit construction are as follows:

1) for the girth, put minimal dynamic design ease $E_{\min} = RC_m \cdot \Delta G_{\text{DIF}}$ (Table 3.6) on bust, waist, and hip girth, etc. (following the ΔG_{DIF} results in Table 2.4 and 2.5, RC_m results in Table 3.5). E.g., firstly, add the E_{\min} value (material M2) for A1 body type – WG -2.8% and HG-5.7%; then further determine the distribution size of front bust girth, front waist girth, and buttocks – BG_F -17.1%, WG_F -4.1% and HG_B -16.8%.

2) for width and length, it is necessary to adjust the structural values according to the longitudinal measurement value, shortening the length of the upper body, such as the position of BL, HL for A1 body type. Then, adjust the ΔL_{DIF} (in Table 2.5) to maintain certain movement flexibility of the wetsuit without affecting the structural characteristics. Therefore, according to the dynamic deformation of the upper torso, it is recommended to add only one-tenth of the SL (3.0%), FNP-WL (1.1%), and BNP-WL (-1.5%); one-tenth of the W_{BB} (-3.2%), W_{BF} (-2.9%), and W_{SP} (-4.4%).

3) then, the design ease E_{\max} can be applied to bust, waist, hip, and other girths in line with the horizontal material deformation and the maximum material elongation E_{\max} on seven body girths (e.g., bust \geq -16.7%, waist \geq -15.0%, and hip \geq -17.5%).

5.2. Development of digital replica

5.2.1. Simulation of important torso parts

The next step is the simulation test with the help of 3D technology. The virtual try on process of wetsuit construction with the new method is simulated in the program of CLO 3D and 3ds Max. The main steps are shown in Figure 5.5.

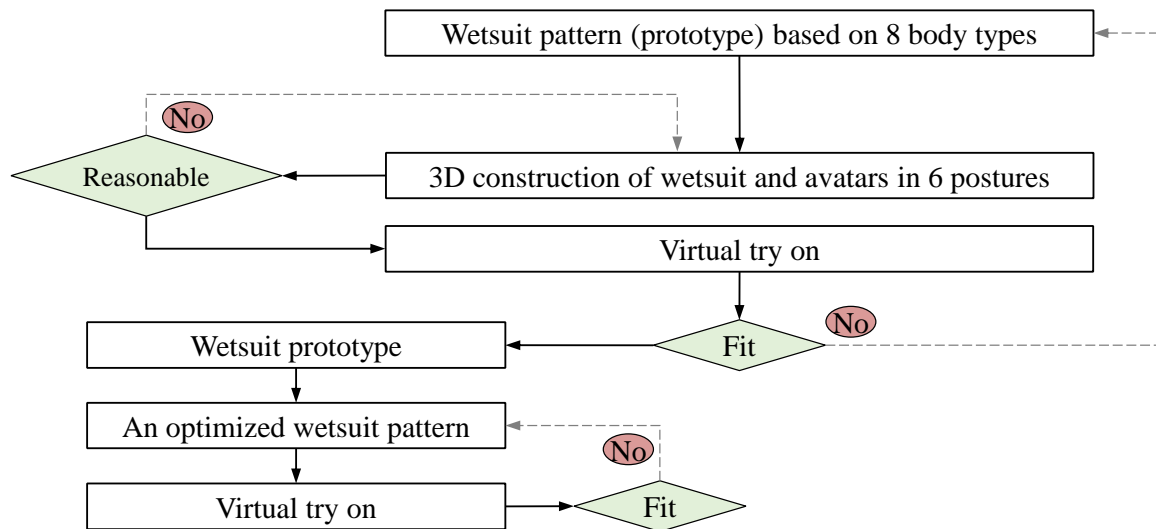


Figure 5.5 – Flowchart of the wetsuit simulation process

The methods of simulation are:

- 1) Scan the body, obtain a scanatar and identify the subtype according to Chapter 2.
- 2) Creation of digital replicas of the body and wetsuit,
 - selection of a body avatar from the CLO 3D and its modification to fit the size of the scanatar;
 - importing the body avatar into 3ds Max 2015 and creating a deformed avatar (DR) based on the shape, size and various positions of the body;
 - adjustment of those DR girths that change in the new body positions;
 - adjustment of the avatar contour in the sagittal plane in accordance with the change in the tilt angle of the torso during movement.
- 3) Changing the dimensions of the scanatar and building a 2D wetsuit design in accordance with the dynamic measurements of the body.
- 4) Conducting a virtual fitting of the wetsuit based on the study of fit, compression pressure and material stretch.

5.2.2. Simulation of the initial and basic wetsuit patterns

We use the ET CAD (BUYI Technology, China) 2D software and CLO 5.0 3D software to construct virtual initial “prototype” and “basic wetsuit pattern”, firstly test the rationality, and then compare the difference between the structures.

To evaluate a wetsuit in virtual reality, the next steps should be done:

- 1) an import of 2D pattern of wetsuit into CLO 5.0 software;
- 2) an application of two tools – "tack" to fix a wetsuit on digital replica of body and "sewing" to sew wetsuit pieces and try on;
- 3) a deformed DR in accordance with body type, posture, wetsuit type, and meanwhile test pressure, material strain.

M2 has been selected to conduct this experiment (the elongation under 500 cN/cm is 30.2% in course, the maximum shrinkage is about 3% in wale). Due to the particularity of wetsuit material, the properties of multi-layer material M2 cannot be directly imported in CLO, so the default value of “elastic knitted material” is selected to conduct simulation, and the thickness (main value) is set to 3 mm thickness with the following property indicators: “PhysicalProperty” – “Preset” is Knit_Jersey, “Density” is 400 g/m², “Simulation Properties” – “Shrinkage warp” is 97% and weft is 100% (initial value), “Surface” – “Skin Offset” is 0.1 mm.

Figures 5.6 and 5.7 show the try on performance of two patterns with the same material on an avatar with dimensional features of A1 type with BG 84.2 cm, WG 65.5 cm, and HG 89.8 cm to evaluate the digital replica performance and the rationality of the pattern design. The virtual pressure measurement is shown in Figure 5.8 (Appendix D, Table D.7).

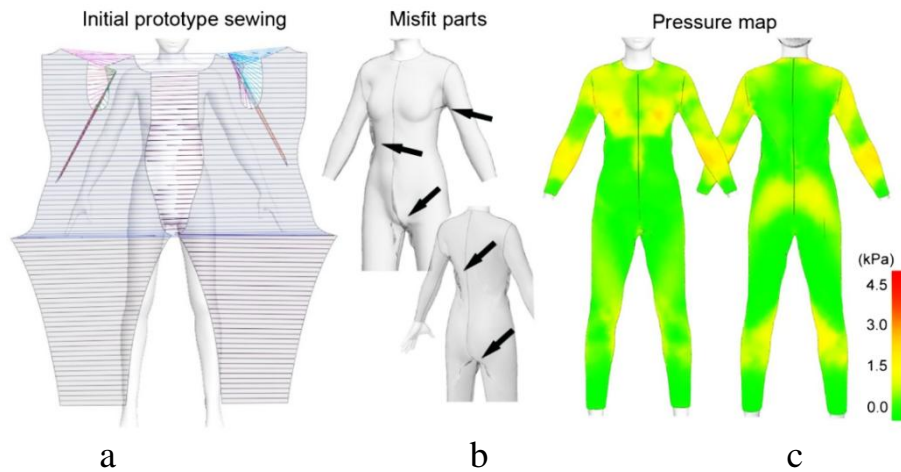


Figure 5.6 – Try on the wetsuit on the initial undeformed avatar: a – virtual sewing of the wetsuit prototype; b – areas with misfit, c – compression pressure distribution

As shown in Figure 5.6 b, the misfit parts pointed by the arrows indicate folds, the clothing is not good fit because extra ease allowances exist under the armpit, waist, back, and buttocks. It can be seen from the pressure map and measured values (Figure 5.6 c) that the pressure values in most parts of the initial prototype are very weak (the average value is less than 1.0 kPa), the pressure value of each part has a great difference, which means the prototype is not fit or not tightly in contact with the body. Therefore, it needs to be modified some details of the initial prototype according to wetsuit characteristics.

Figure 5.7 shows try on test with the basic wetsuit and a pressure distribution map.

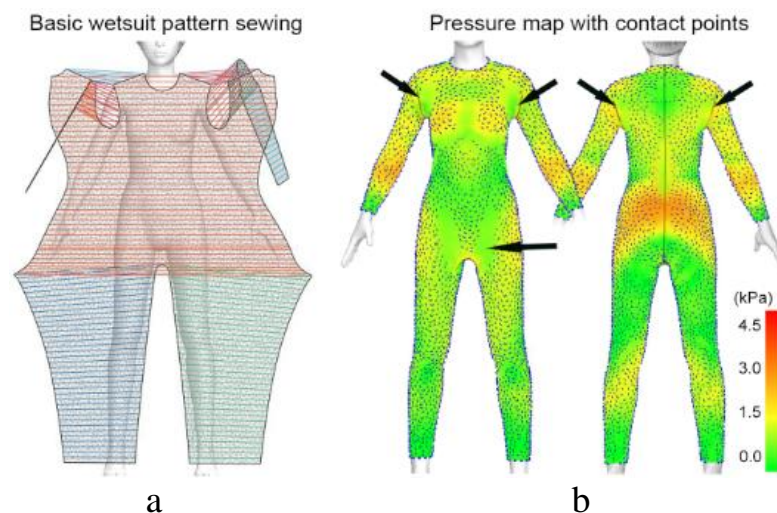


Figure 5.7 – Try on test with basic wetsuit (Fig. 5.4): a – virtual sewing of basic type wetsuit; b – try on in CLO

Figure 5.7 shows that the number of areas with folds has decreased, and the pressure is distributed more evenly over the surface of the avatar, the fit of the wetsuit is better than before.

Figure 5.8 shows the pressure values on different avatar parts of the initial prototype and basic wetsuit.

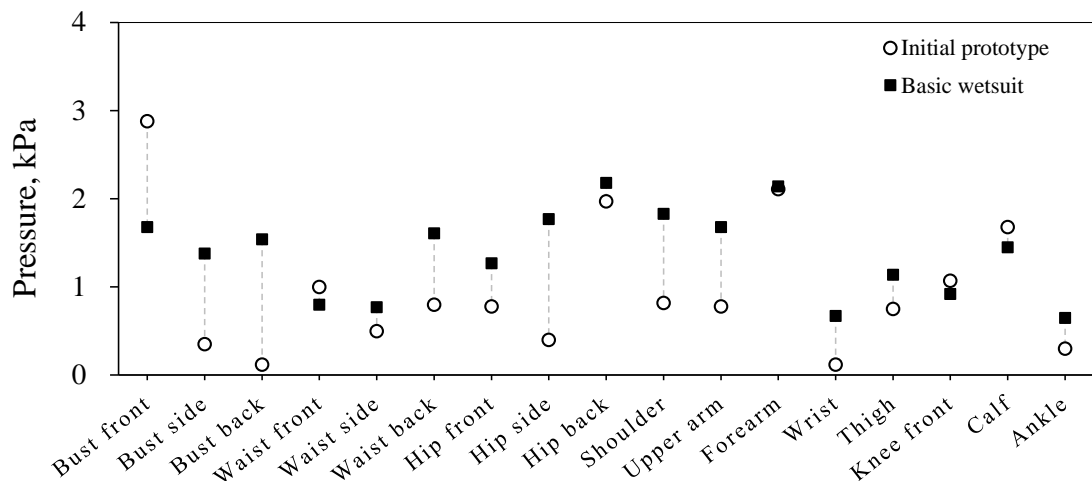


Figure 5.8 – The measured virtual pressure values on body part

After processing the results, the following compression pressure values were obtained:

Type of wetsuit	Range of pressure values, kPa	Average value, kPa	The coefficient of variation
Initial prototype	0.12...2.88	0.97	0.77
Basic design	0.65...2.18	1.38	0.49

The overall pressure values increased, and the pressure value of each part has little difference. The “pressure dots” generated by CLO on the wetsuit can be seen as the marks of contact between the wetsuit and the skin. Due to the body surface features and shortcomings of the basic wetsuit structure, the armpit, back waist, and front groin are not tightly in contact with the body. Therefore, the basic wetsuit structure should be further improved.

5.3. Optimization of the designed wetsuit

To substantiate the location and configuration of the cutting lines, the following approaches are used to optimization design: 1) the location of the lines was chosen in accordance with the human body morphology, 2) the location and curvature of the cutting lines were changed according to the pressure and material deformation in virtual system, 3) try to use fewer cutting lines to design optimal performance and complete this preliminary design process in the virtual system.

The “step by step design” method was applied in a fixed range of acceptable compression pressure values to find and test the “best” location of cutting lines that meet dynamic and static changes in the “avatar-wetsuit” system. The steps are explained below:

- step 1: raglan line,
- step 2: side line,
- step 3: cutting lines of two-seam sleeve instead of one-seam one,
- step 4: additional crotch part,
- step 5: other cutting lines.

5.3.1. Optimization and verification of the sleeve construction

The raglan sleeve is usually applied in wetsuit design, it simplifies a complex structure under armpit, and reduces sewing difficulties as well as a risk of breakage during diving.

Step 1: The main representative points were selected, such as shoulder point (SP), bust point (BP), and side point (landmarks a and b, in chapter 2). These anthropometric points are easy to find on the avatar. The below criteria for choosing the raglan line configuration we used: 1) the minimum relative difference in clothing pressure values in virtual system of two body postures: in static standing position and dynamic raising arms, displaying virtual pressure maps in real time; 2) fit degree.

The most suitable solution for the raglan line was determined by the virtual pressure difference of the wetsuit ΔP between hands up and down.

The relative difference between hands up and down is

$$\Delta P = 100 (P_u - P_d) / P_d, \tag{5.1}$$

where ΔP is relative difference, %; P_u is the pressure value when hands up, kPa; P_d is the pressure value when hands down, kPa.

Figure 5.9a shows the position of raglan seams based on the location of female neck muscle and chest fat.

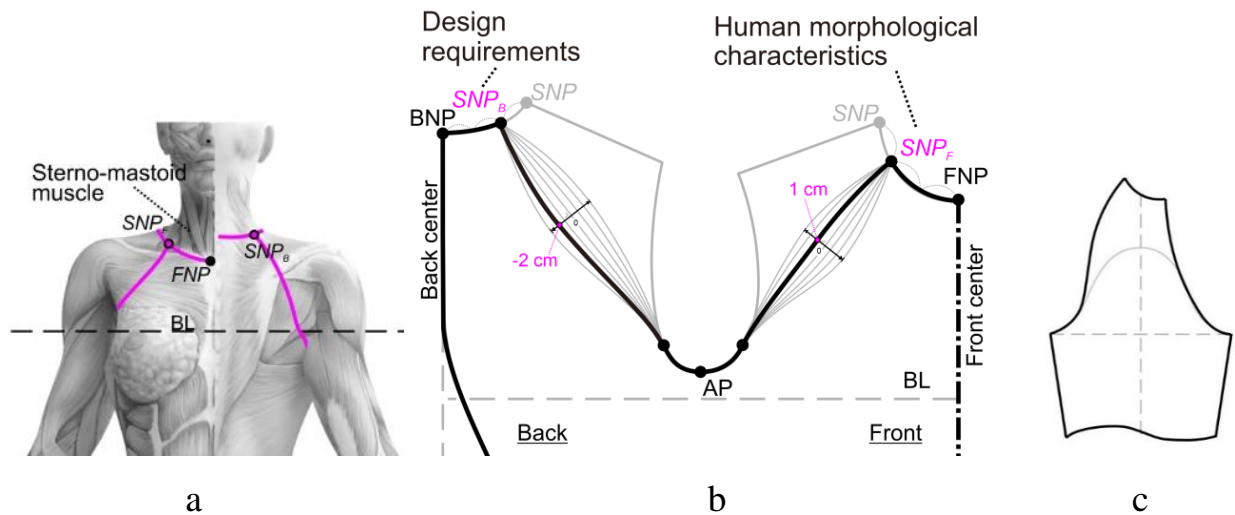


Figure 5.9 – Raglan line design schemes: a – the position of the raglan line on the body in front (left) and behind (right); b – diagram of the drawing of the best sleeve; c – variants of the studied configurations of raglan lines

Different configurations of lines are within the range (-3...3 cm). The front torso is taken as an example to illustrate how the straight line (marked as "initial line" 0) from SNP_F to armpit transform into different convex curves which were marked as 1, 2, and 3 one by one. The opposite concave curves were marked as -1, -2, and -3 one by one. Therefore, there were designed seven lines on the front and back. To sum up, the total number of connections between front and back sleeves is $C_7^1 * C_7^1 = 49$ with different arc-change configuration from -3 to 3 cm.

Table. 5.1 shows the line configuration options.

Table 5.1–Configuration design number

Deflection of the raglan line in the back, cm	Configuration design number of the virtual suit for deflection of the raglan line in the front, cm						
	-3	-2	-1	0	1	2	3
-3	#1	#8	#15	#22	#29	#36	#43
-2	#2	#9	#16	#23	#30	#37	#44
-1	#3	#10	#17	#24	#31	#38	#45
0	#4	#11	#18	#25	#32	#39	#46
1	#5	#12	#19	#26	#33	#40	#47
2	#6	#13	#20	#27	#34	#41	#48
3	#7	#14	#21	#28	#35	#42	#49

Then the best configuration of the sleeve was chosen through comparing the corresponding pressure values or material deformation values in virtual reality.

Figure 5.10 shows the sum of absolute values of the differences ΔP of the three measured parts for P1 and P2.

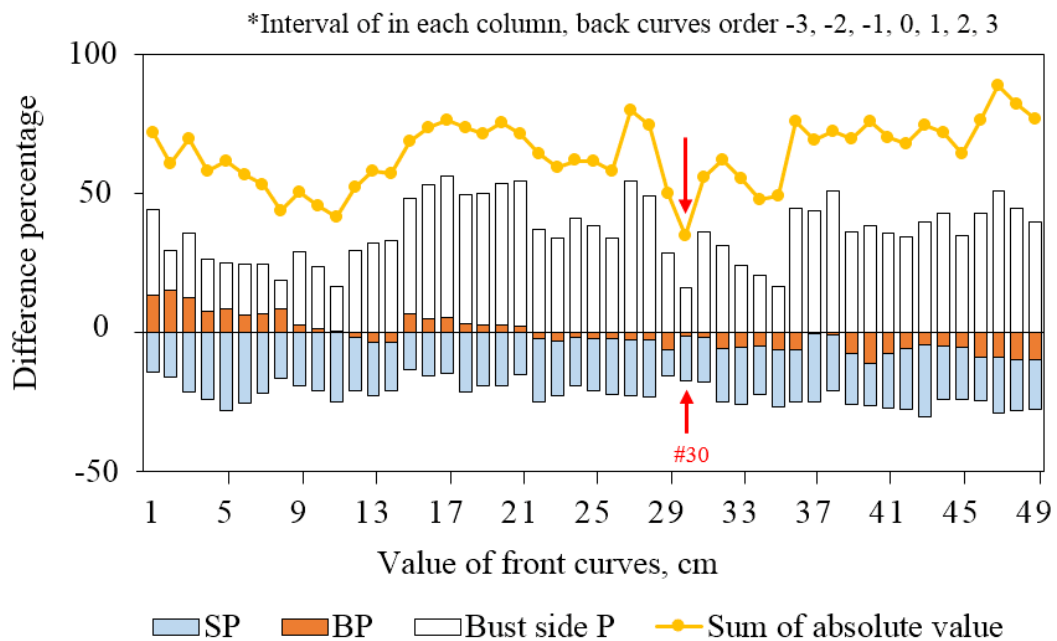


Figure 5.10 – The pressure differences of 49 sleeve designs

If the absolute value is the smallest in all designs, it means the corresponding ΔP in dynamic will be the smallest, and the structure line helps to maximize

improve the dynamic fit on the shoulders. Then the design can be proved to be the best.

The significant differences of these designs focus on the side part. It can be directly observed that the sum of the absolute values of design #30 (deflection in front 1 cm and back -2 cm), marked in the figure, is 34.7% (SP is -17.3%, BP is -1.3%, and side is 16.2%). This is the lowest value of all designs. At the same time, it is found that most ΔP of other designs is more than 50%, so it can be determined that the raglan sleeve design #30 is the best among these designs.

Based on the digital replicas, the sleeve optimization design was verified by the virtual test, and the optimized configuration of the raglan sleeve can obtain reasonable pressure in dynamic. The raglan sleeve in wetsuit design can obviously improve the fit performance of the shoulder area.

To evaluate the rationality of optimized design and digital replicas, the experiment of virtual try on based on the digital replicas was conducted. The evaluation procedure is based on three postures P1, P2, and P3.

Figure 5.11 shows the wetsuit patterns of static standing and raising arms, the original and deformed DR avatars, and the results of the virtual try on.

Figure 5.11 left shows the measurements are modified in the virtual system to achieve deformed replicas (DR) based on real static and dynamic data. In this way, the DR with P1 is modified to P2 and P3. Meanwhile, the design ease values of several body parts are calculated according to the relationship between dynamic measurements and material tensile properties.

Figure 5.11 (in middle) shows the wetsuit patterns made of M2 for the body types A1 and B1 as examples. The previously obtained data from Table 2.5 and Appendix B, Table B.6 are used, the pattern drawing method is as steps described in Figure 5.4 of subsection 5.1.2 above. The patterns with E_{\min} and E_{\max} are shown in the black line and blue dot line respectively.

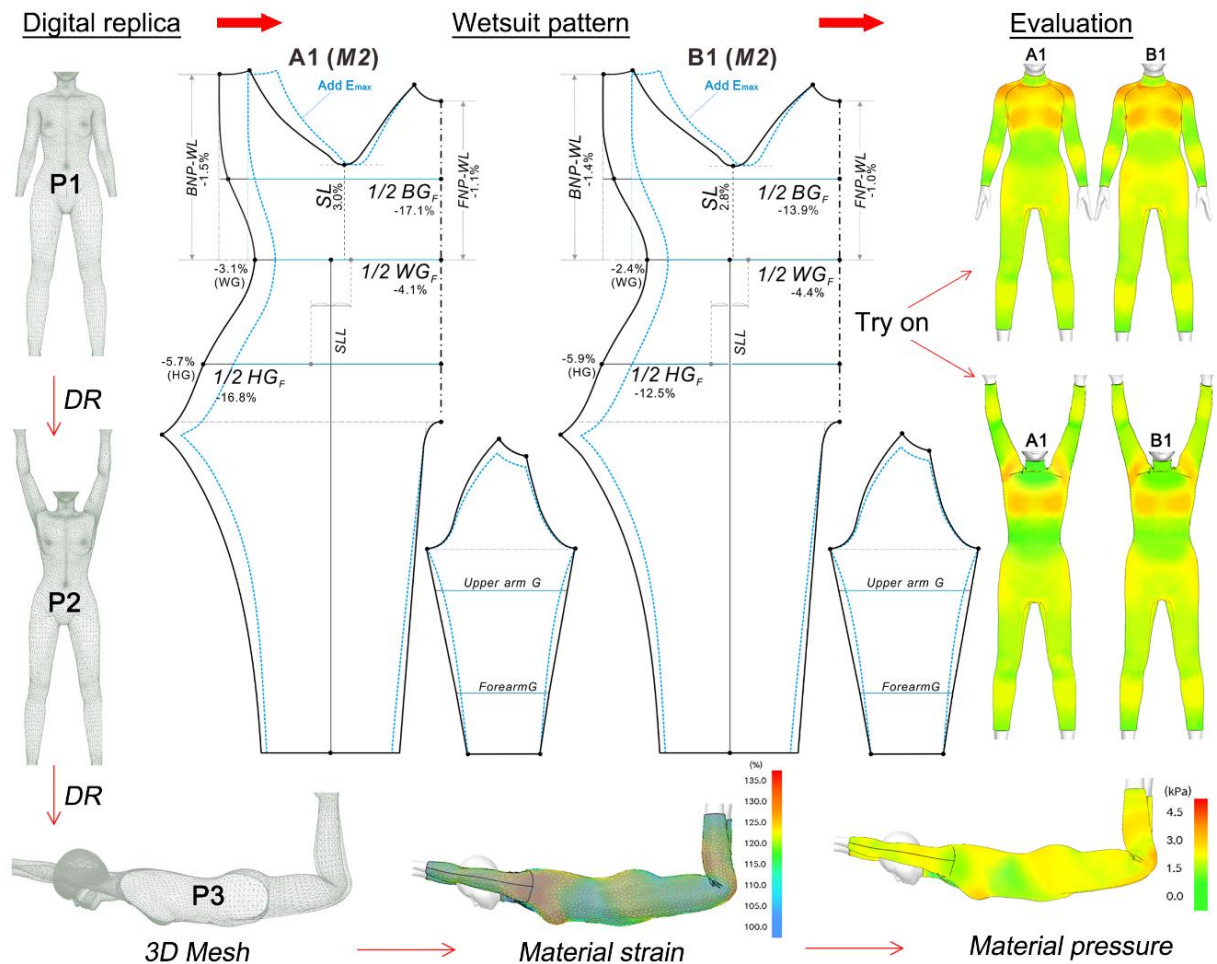


Figure 5.11 – Stages of designing virtual twins of bodies and virtual tryon in the CLO 3D program

It can be seen from the material pressure map that the optimized wetsuit for different body types has good performance – the wetsuits are very tight without folds in static and dynamic conditions, and the pressure values and distributions are reasonable (in line with the real situation). Besides, the pressure changes are relatively stable and do not change significantly in P3.

The drawing takes new measurement features, the materials properties, negative ease, and compression pressure into consideration. The experiment of virtual try on based on the digital replicas was conducted. The evaluation procedure is based on three postures P1, P2, and P3. The results of virtual verification show that the new design of wetsuit patterns has a good structure.

5.3.2. Experimental verification of other optimized designs

Step 2: Explore the possibility of improving the detail of the additional/side part to improve fit degree on the arms, waist, bust and hips and the material cutting direction (Figure 5.12).

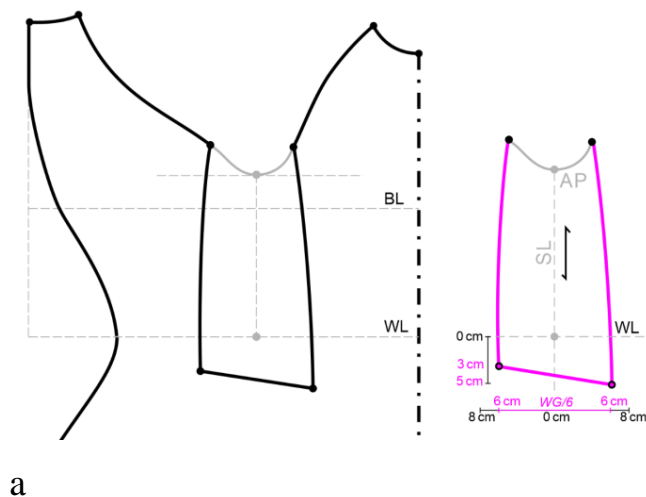


Figure 5.12 – Location and acceptable configurations of the shape of the side part of the wetsuit

To find the most suitable part shape, a horizontal line was drawn through the intersection point of the lines SL and WL, change the width, and find the best fit design. The WG of the female body in the database varies greatly (WG is 56.2...79.5 cm), so we recommend using WG as the reference to calculate the side part bottom width for easy understanding and calculation.

Figure 5.12a shows the side part bottom with the designed width 12 cm (take A1 as an example), and the side part bottom is below the WL, this width is approximately $WG/5$ for each type (for example, $WG = 63.0$ cm, side bottom width is 12.6 cm). According to the results in Appendix D, Table D.10, the best bottom points design is below WL 3 cm and 5 cm. The cutting direction of the piece is vertical.

The side part-to-sleeve connection is one design, but rarely seen in wetsuits (see Figure 1.14), which results in the destruction of the material of the garment or the seam in the armpit. Therefore, this detail needs to be further improved to

change the traditional shape of the armhole.

Figure 5.13a shows the “*h*” is the rising value, curves “*a*” and “*b*” are connected with the sleeve part. The purpose is to change the traditional shape of the armhole. According to female upper arm length (average is 30.1 cm), the recommended value “*h*” is from 1/4 to 1/2 upper arm length (7...15 cm), and extended per 2 cm for the test. The results (Appendix D, Table D.11) show that the *h* value at 15 cm has the best performance. It can be seen that the optimized side part (Figure 5.13b and c) improves fit at the armpit, reduces the sewing difficulty, and has low material deformation when raising hands.

Figure 5.14a shows the cutting lines are added in front. Due to the female physiological characteristics, the front upper bust part needs to be tightly compressed by wetsuits to reduce water accumulation. It reduces the influence of shoulder and neck movement on maintaining fit. The bust additional seam is above the BL, and can be raised along the front center line 1...5 cm. The abdomen additional seam curve is below the WL, and declines 1...8 cm along the front center line. Through the comparison of Figure 5.14b and c, it can be seen that the fitness of the upper bust and abdomen parts is obviously improved. The experimental results (Appendix D, Table D.13) show that the best design is the curves 3 cm above BL and 8 cm below WL from the perspective of appearance and objective measurement.

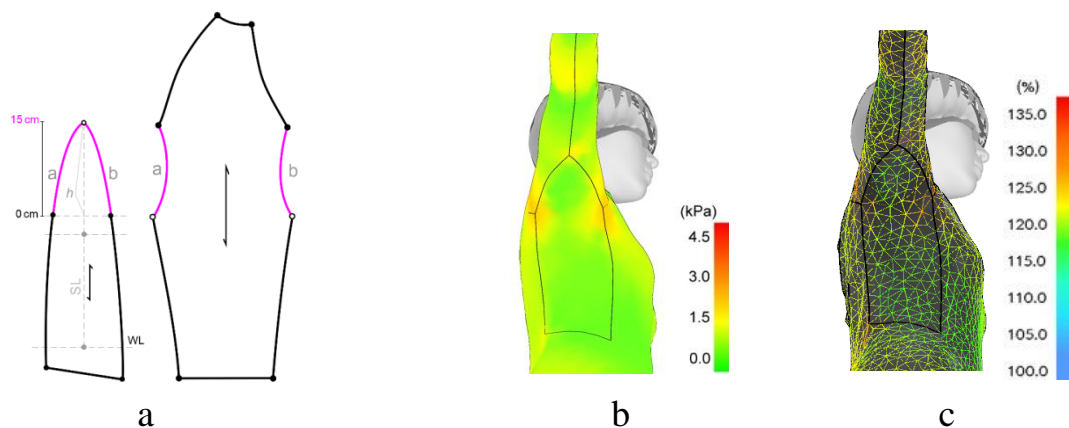


Figure 5.13 – Verification of side part configuration: a – side part optimization; b – pressure map; c – material deformation map

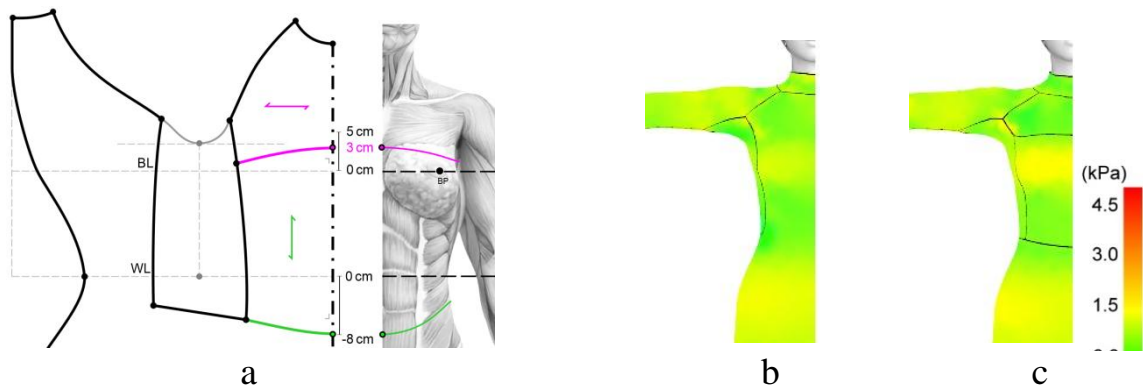


Figure 5.14 – Scheme of the drawing of the front part of the wetsuit: a – the location of the yoke and the central part in the drawing and body; b, c – virtual try on of a wetsuit without and with a yoke

Moreover, we also experimented with the two-piece sleeve design (Appendix D – Figure D.2 and Table D.12). Compared with the one-piece sleeve, the pressure value of the two-piece sleeve design is lower with general fit. In order to reduce the seams, the one-piece sleeve will be used in the design. Finally, the back waist line and the upper arm are also designed (Appendix D, Figure D.3). According to the production suggestions from the factory, the wider crotch part will better fit (not too small). It enhances sealing waterproof, sports comfort and durability (reduce the possibility of breakage) (Appendix D, Figure D.4).

The optimized design of wetsuit pattern blocks is as shown in Figure 5.15.

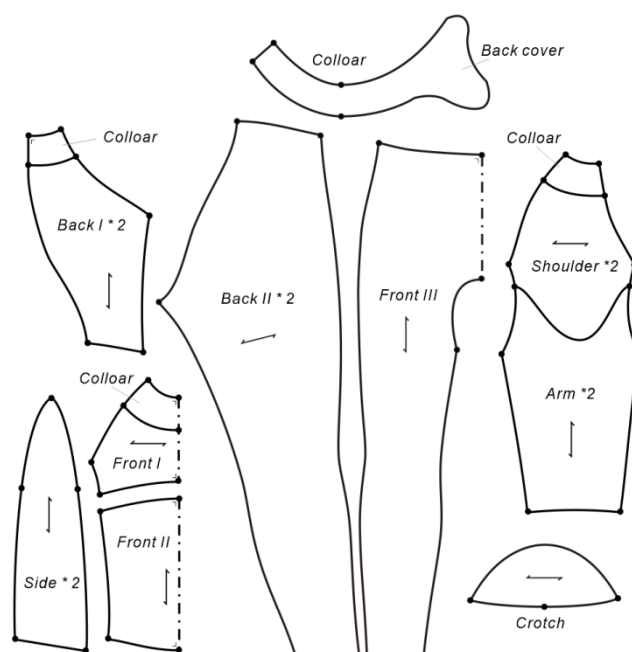


Figure 5.15 – The designed wetsuit pattern blocks

Figure 5.16 shows the final virtual try on performance of 6 postures, and other diving postures are shown in Appendix D, Figure D.11.

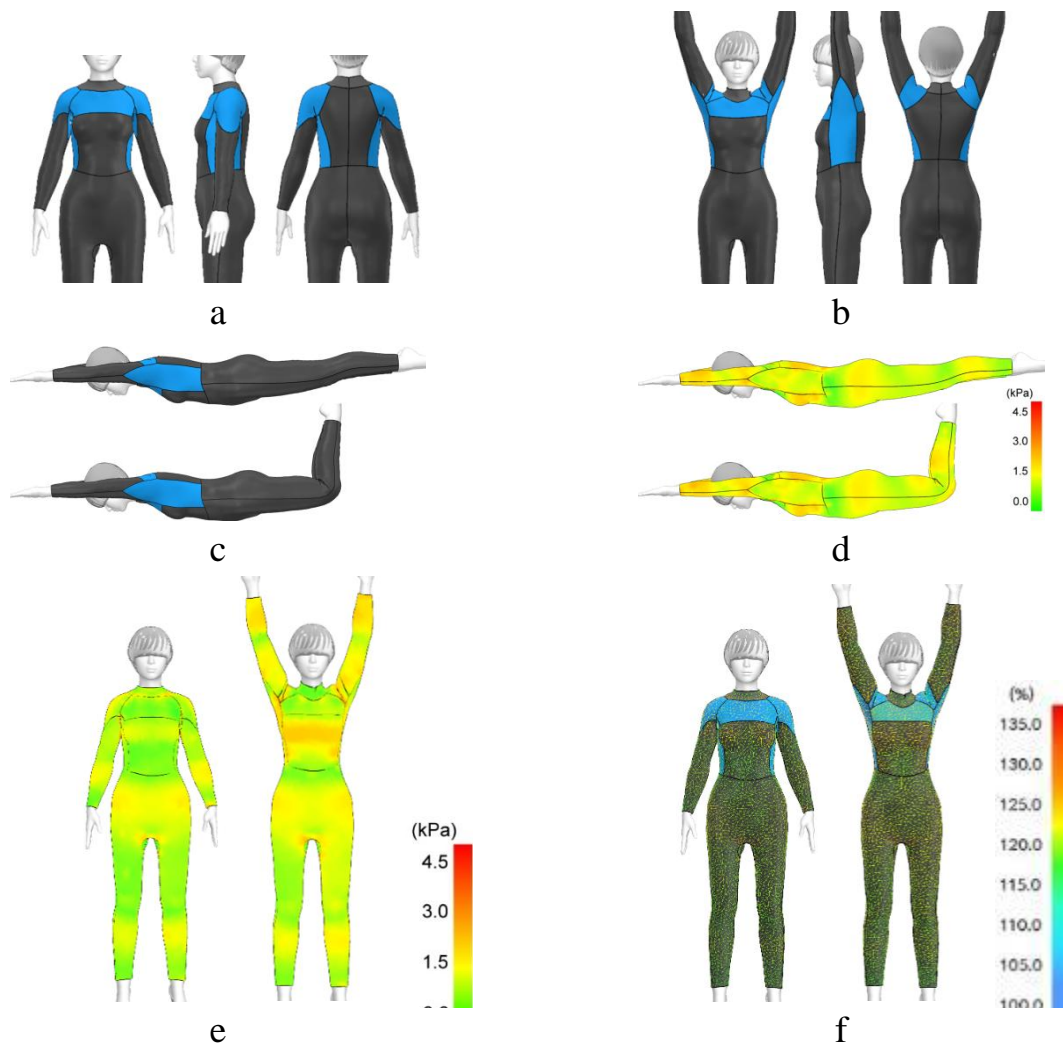


Figure 5.16 – Simulation of designed wetsuit: a – try on in P1; b – try on in P2; c – try on in P3, P4 (P5, P6); d, e – pressure maps; f – material strain mesh maps

The designed wetsuits are verified by the virtual try on tests, and can obtain reasonable pressure in dynamic and obviously improve fit performance. Reasonable pressure change and material strain of the CLO “pressure/strain maps” in dynamic and static show our design is rational.

The virtual results will help wetsuit designers respond to rapid modification, evaluation, and omit actual repetitive manufacture works for optimizing pattern design, enhancing productivity, and further improving customers' wearing experience.

5.4. Evaluation of the finished product

5.4.1. Comparison of developed designs with existing products

Three young Chinese female testers with body sizes Y1, A1, and B1 were selected for the following test of wetsuits. The detailed body sizes of volunteers are in Appendix D, TableD.14.

Five mass production wetsuits of three popular styles of regular structure sold by JINMING apparel company (Wuhan, China) in M2 material, 3 mm thick, the sizes (trade group S - small, M - medium, L - large) were selected. Mass-production wetsuits were designated PW1-S, PW2-S, PW3-S, PW1-M, and PW1-L (Figure 5.17 a and b). With the same fabric and gluing technology, three suits were made for three volunteers, which roughly corresponds to the fullness: Y1 – small size, A1 – medium size, B1 – large size. They were designated as DW-Y1, DW-A1, and DW-B1. Based on the new method, two materials M2 and M3 were chosen for the production of DW (wetsuit design).

Figures 5.17 and 5.18 show the try on performance of static standing (try on in dynamic postures are in Appendix D, FigureD.5...10).

Figure 5.17c shows that the PW does not fit well, especially at the shoulder, arm and crotch, but the DW fits well.

Figure 5.18 shows that the two-material DW has a good fit and provides the necessary freedom of movement (Appendix D, Figure D.11).





Figure 5.17 – The appearance of the existing PW factory-made wetsuits (a – in the Y1 body; b – in the A1 and B1 bodies) and the appearance of problem areas on the existing PW and the developed DW wetsuit (c)



Figure 5.18 – Appearance of the new wetsuits: a – for body Y1 made of material M2; b – for body Y1 from material M3

Figure 5.18 shows the traditional wetsuits of general size are poor fit when natural standing, the similar design defects exist in the same parts when three testers trying on. The extra ease exists on armpit, thigh, and crotch obviously. When lifting hands, the armpit and waist side obviously have low extensibility, which will influence the arm lifting degree.

The static and dynamic subjective evaluation of try on feeling was carried out according to the Likert Scale 7-level evaluation, including a set number of responses for testee to choose, respectively:

- 1 - extremely dissatisfied (material is sagging, very loose, does not fit the body, or there are other uncomfortable sensations, for example, a feeling of strong pressure or restriction of movement)
- 2 - quite dissatisfied (the material of the clothing is very relaxed, does not fit the body well, or has another unpleasant feeling; a feeling of squeezing and restriction of movement)
- 3 - dissatisfied (the material of the clothing is loose, feeling of a bad fit or other unpleasant feeling; feeling of squeezing of areas of the body and restriction of movement)
- 4 - partially satisfied (material fits the body, but it can be better; some movements with an average amplitude can be performed)
- 5 - satisfied (fits the body, but can be a little tighter; you can perform most movements with an average amplitude)
- 6 - quite satisfied (feeling tight and comfortable pressure; easy to perform most movements with a large amplitude)
- 7 - very satisfied (very tight fit, very comfortable pressure; easy to perform all kinds of movements with a large amplitude)

The feelings of uncomfortable and comfortable felt by the tester himself refer to the weak and strong pressure feelings produced by wetsuit materials. Uncomfortable feeling also refers to the misfit caused by pattern design defects. Pressure sensitivity and comfort scores are subjective and also depend on the area of the body, so the results of the survey varied with such a small sample.

The results of subjective evaluation in static and dynamic are shown in Figures 5.19 and 5.20.

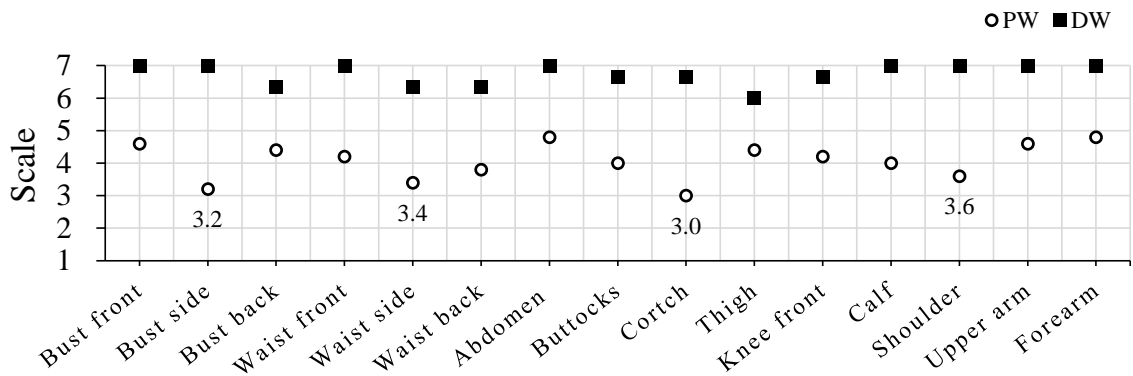


Figure 5.19 – The static subjective evaluation results



Figure 5.20 – The dynamic subjective evaluation results

The static and dynamic (hands up) subjective evaluation results indicate that the lower satisfaction ranking (average are 4.1 in static and 3.0 in dynamic) of PW are mainly found at front knee (squatting), bust side, waist side, back, shoulder and upper arm.

The average score for DW was 6.7 in static and dynamic. A positive rating means that the comfort of the new wetsuit is significantly higher than the PW rating, between 6 "quite satisfied" and 7 "very satisfied".

The objective evaluation results are shown in Figure 5.21.

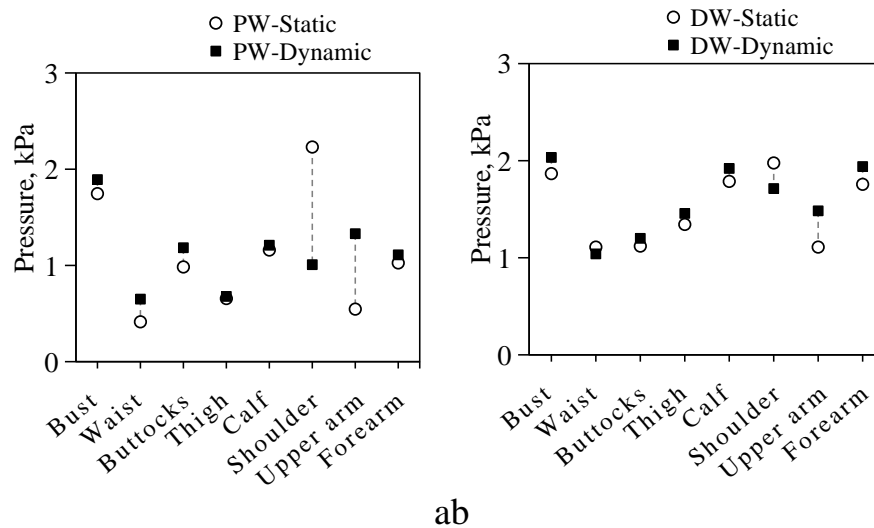


Figure 5.21 – Results of body pressure measurements: a – industrial wetsuits PW; b – developed wetsuit

The static and dynamic (hands up) objective evaluation results (in Appendix D, Table D.14) indicate that the significant pressure ΔP_{PW} difference measured on the shoulder is -54.8% (-1.22 kPa), on the upper arm is 143.6.2% (0.78 kPa), and on the waist is 57.0% (0.24 kPa). The ΔP_{DW} range is only -13.3...33.6% (during -0.26...0.37 kPa).

Thus, objective (pressure measurement) and subjective (wearing feeling) evaluation showed that the existing wetsuit does not meet the requirements of consumers. The developed DW design eliminates dynamic pressure changes, optimizes important structural elements: side part, shoulder area, sleeve, groin area, solves the problems of comfort of movement and functionality during operation.

5.4.2. Underwater test and evaluation

The test project address is located in the professional diving training center – Wuhan Diving Center (Wuhan, China) cooperates with PADI® Dive Center. In order to test the performance of DW in all aspects, the test project needs to choose equipped with scuba from SCUBAPRO® professional equipment. Two testers Y1 and A1 conduct the test.

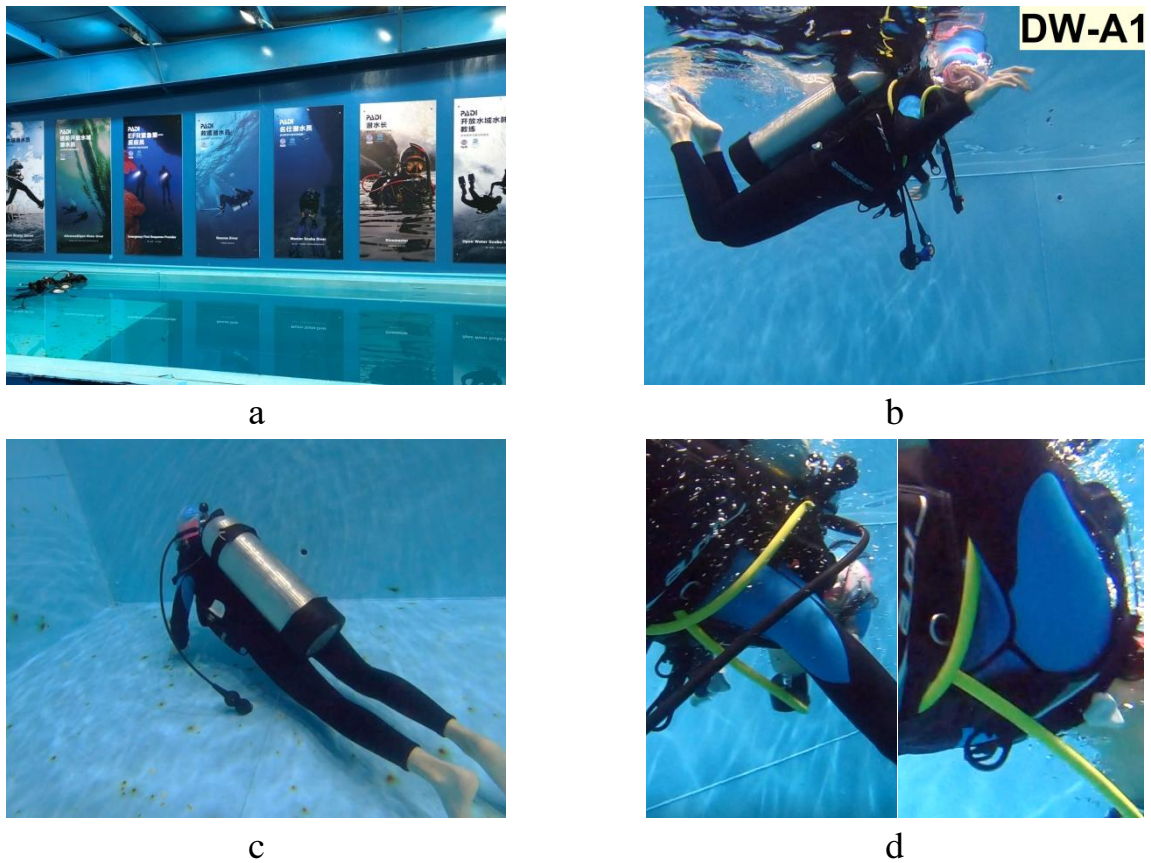


Figure 5.22 – Diving experiment: a –the appearance of the “Wuhan diving center”;
b, c, d – scuba diver in different poses

Under the guidance of professional instructors, the diver dived, performing freestyle swimming and diving and squats. The maximum diving depth was 6 meters. The results of the subjective assessment, obtained by interviewing two divers, are shown in Figure 5.23.

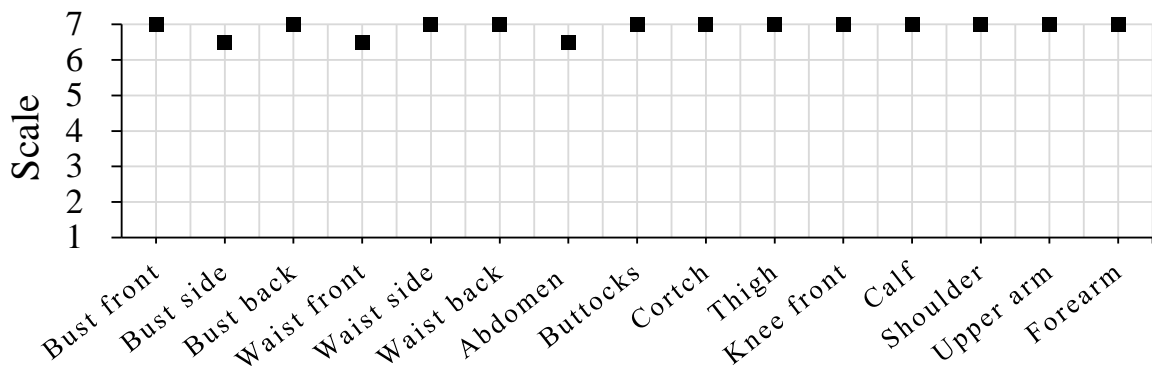


Figure 5.23 –Results of subjective assessment of the fit of DW wetsuits during underwater testing

Both divers noted that they did not have any obstacles to movement underwater and experienced a feeling of good body fit.

5.4.3. Verification of theoretical and actual pressure values

The manufactured wetsuits were used to check the correctness of the theoretical conclusions we made earlier. For three wetsuits DW for types Y1, A1 and B1 made of M2 middle-end material, the pressure was measured according to the experimental scheme (the same seven body parts in Chapter 3 – bust, waist, buttocks, thigh, calf, upper arm, and forearm). The average of actual P_{\max} on 7 body parts is 1.44 kPa in static and 1.58 kPa in dynamic. In parallel, P_{\max} was calculated according to the Equations (4.3) to (4.7) given in Chapter 4 using different indicators of material properties M2. Table 5.2 shows the P_{\max} comparison between the calculated and the measured P_{\max} .

Table 5.2 – Absolute difference value between calculated and measured material pressure M2 on seven body parts

Equation	Material property index M2	Predicted \hat{P}_{\max} , kPa	Absolute difference value between theoretical and actual pressure	
			Static / Dynamic, kPa	Static / Dynamic, %
(4.3)	F15 _c	1.69	0.25 / 0.11	17.5 / 7.1
(4.4)	WT _c	1.70	0.26 / 0.12	17.8 / 7.4
(4.5)	WT _w	2.29	0.85 / 0.71	59.4 / 45.2
(4.6)	LT _w	2.16	0.72 / 0.28	50.2 / 36.9
(4.7)	2HG _w	2.24	0.80 / 0.66	55.5 / 41.7
Avg.			<i>0.58 / 0.44</i>	<i>40.1 / 27.7</i>

It can be seen from Table 5.2 that the smallest difference between the theoretical and actual pressure values is 7.1%.

After comparing the predicted pressure with the real measured pressure, we found that the average difference calculated by five equations is 0.44 kPa. Equation (4.3) has the smallest error of 0.11 kPa when wetsuit made of material M2

even in different postures, so this equation is

$$\hat{P}_{\max} = 0.86 + 2.45 / WT_w$$

Its use in the selection of materials for wetsuits will ensure that the maximum effect of the new wetsuit is obtained.

Conclusion of chapter 5

1. A new flat design method for a wetsuit to keep dynamic fit is proposed, and the virtual fitting and objective pressure comparison shows that the basic wetsuit pattern drawing method is rational and variable, and the basic pattern has a good fit.

2. The deformed digital replicas of the female body are constructed in the virtual system to test wetsuit design and the material strain and compression ability are identified. The digital replicas based on real data transformation are feasible and practical, and the process of establishing digital replicas with 3D body scanning technology is valid and accurate.

3. Based on the digital replicas, all design cutting lines are checked in the virtual system, then dynamic fit and material strain of the wetsuit is evaluated in advance, and the final optimized wetsuit pattern is obtained. A new virtual working process of wetsuit simulation, pre-design, and evaluation can be completed.

4. The static and dynamic subjective evaluation of try on feeling was carried out according to the Likert scale 7-level evaluation, DW obtained a higher ranking than the wetsuit in the market.

5. Through the comparison between the objective data measurement of the real samples and the data obtained in the virtual system, a positive correlation exists between real and virtual values.

6. This DW pattern has passed the factory check, it is applicable to different female body types.

CONCLUSION AND SUGESSTION

RESULTS OF THE COMPLETED STUDY

1. Based on the analysis of the functional and aesthetic characteristics of wetsuits, modern methods of designing them and an expert survey of diving enthusiasts, the main design directions in the direction of increasing comfort, including from the standpoint of studying changes in anthropometric data and functional structural optimization, were determined.

2. A new grouping of female bodies has been developed and a database has been formed in the form of anthropometric measurements, which includes dynamic changes in the size of bodies when swimming underwater. The areas of the greatest dynamic changes in the size of the bodies when performing movements during swimming are established.

3. The relative changes in the dimensional characteristics of female figures under the action of hydraulic pressure were measured, which made it possible to calculate the allowable ranges of structural increases in wetsuits.

4. A new indicator characterizing the compression ability of wetsuit materials is proposed. Recommendations have been developed for calculating the constructive dynamic gains of clothing for eight types of bodies.

5. Dependences for calculating the upper limits of the allowable comfortable pressure of a wetsuit on the indicators of the deformation properties of the material used have been established.

6. The found relationships between the deformation of the clothing material and the change in the dimensional features of the body are used to generate digital twins of the bodies. Digital Twin bodies are created in dynamic positions corresponding to swimming conditions for virtual modeling of the dynamic system "body-wetsuit" underwater, fitting and evaluation of the wetsuit.

7. In a virtual environment, the design of the raglan sleeve was optimized from the standpoint of optimizing the configuration and achieving reasonable pressure in dynamics.

RECOMMENDATIONS, PROSPECTS FOR FURTHER DEVELOPMENT OF THE THEME

The results of the work should be used in the process of higher education for the preparation of bachelors and masters specializing in the design of compression clothing, in related areas of designing light industry products; Wetsuit industries need to improve the current design concept of CAD elements to develop and optimize new diving products.

Thanks to the improvement of anthropometric measurement programs, it is possible to identify morphological differences in female bodies, in order to customize products and improve the quality of clothing in conditions of mass consumption, to eliminate the shortage of products in the existing market.

Further development of the "digital twin" concept can be developed simultaneously in two directions - for an expanded set of standard bodies in mass production (ready-to-wear), as well as for an individual approach (e-bespoke).

The results of the work can be used in the field of practical artistic and industrial design, education and advanced training for a qualitative change in existing concepts and the development of new economies focused on digitalization.

REFERENCES

- [1] Abteu, M.A. Development of comfortable and well-fitted bra pattern for customized female soft body armor through 3D design process of adaptive bust on virtual mannequin / M.A. Abteu, P. Bruniaux, B. François, et al // *Computers in Industry*, 2018, 100, pp. 7–20.
- [2] Ancutienė, K. The influence of textile materials mechanical properties upon virtual garment fit / K. Ancutienė, D. Sinkevičiūtė // *Materials science*, 2011, 17(2), pp. 160–167.
- [3] Ashdown, S.P. An investigation of the structure of sizing systems / S.P. Ashdown // *International Journal of Clothing Science & Technology*, 2013, 10(5), pp. 324–341.
- [4] Avădanei, M. 3D pattern design of products with special destination / M. Avădanei, C. Loghin, I. Dulgheriu // *TEXTILE. PIELĂRIE*, 2013, pp. 19–30.
- [5] Aldrich, W. *Metric pattern cutting for women's wear (5th Edition)* / W. Aldrich // Blackwell Publishing, 2007. – 218p.
- [6] Bai, Q. Application of stitching design in sportswear / Q. Bai // *Modern Business Industry*, 2015, 36(25), pp. 116–116.
- [7] Ballester, A. 3D-based resources fostering the analysis, use, and exploitation of available body anthropometric data / A. Ballester, E. Parrilla, J. Uriel // *Proceedings of the 7th International Conference on 3D Body Scanning Technologies*, Lugano, Switzerland, 21-22 October, 2014, –C. 237–247.
- [8] Berry, M.J. The effects of elastic tights on the post-exercise response. *Canadian journal of sport sciences* / M.J. Berry, S.P. Bailey, L.S. Simpkins, et al. // *Journal canadien des sciences du sport*, 1991, 15(4), pp. 244–248.
- [9] Brown, F. Compression garments and recovery from exercise: a meta-analysis / F. Brown, C. Gissane, G. Howatson, et al. // *Sports Medicine*, 2017, 47(11), pp. 2245–2267.
- [10] Chen, D. *Clothing Hygiene* / D. Chen // Beijing: China Textile Press, 2000, p. 64.
- [11] Chen, D. Development of garment pressure testing system / D. Chen, L. Cui // *Journal of Textile Research*, 2008, 29(3), pp. 72–75.
- [12] Chen, G. Research on virtual simulation technology of men's shirt for personalized customization / G. Chen, Q. Li, D. Chen // *Textile Industry and Technology*, 2018, 47(11), pp. 29–31.
- [13] Cheng, Z. A digital replica of male compression underwear / Z. Cheng, V.E. Kuzmichev, D.C. Adolphe // *Textile Research Journal*, 2020, 90(7-8), pp. 877–895.
- [14] Cheng, Z. Development of knitted materials selection for compression underwear / Z. Cheng, V.E. Kuzmichev, D.C. Adolphe // *Autex Research Journal*, 2017, 17(2), pp. 177–187.
- [15] Cheng, Z. Research on the male lower torso for improving underwear design / Z.

Cheng, V.E. Kuzmichev, D.C. Adolphe // *Textile Research Journal*, 2019, 89(9), pp. 1623–1641.

[16] Choi, J.H. A Study about reduction rate of wetsuit patterns for men in their 30s / J.H. Choi // *Journal of the Korean Society of Clothing and Textiles*, 2011, 35(9), pp. 1039–1048.

[17] Choi, J.H. Development of the men's scuba diving suit pattern by using 3D body-scanned data / J.H. Choi // *Journal of the Korean Home Economics Association*, 2011, 49(4), pp. 105–113.

[18] Choi, J.H. The production condition and consumer satisfaction of men's scuba diving suits / J.H. Choi, J.A. Jeong // *Journal of the Korean Society of Clothing and Textiles*, 2009; 33(11), pp. 1683–1695.

[19] Choi, M.S. Comparison of body measurements between korean and the us women aged over 55 / M.S. Choi, P.A. Susan, H.J. Cho // *Fashion Business*, 2002, 6(6), pp. 34–42.

[20] Chun, J. Sizing in Clothing, Communication of sizing and fit / J. Chun // *Woodhead Publishing Series in Textiles*, 2007, pp. 220–245

[21] Coltman, C.E. Three-dimensional scanning in women with large, ptotic breasts: implications for bra cup sizing and design / C.E. Coltman, D.E. McGhee, J.R. Steele // *Ergonomics*, 2017, 60(3), pp. 439–445.

[22] Daanen, H.A. 3D body scanning. Automation in garment manufacturing / H.A. Daanen, A. Psikuta // *Cambridge: Woodhead Publishing*, 2018, 1, pp. 237–252.

[23] Danckaers, F. Evaluation of 3D body shape predictions based on features / F. Danckaers, T. Huysmans, D. Lacko, et al. // *Proceeding of 6th International Conference on 3D Body Scanning Technologies*, Lugano, Switzerland, 27-28 October 2015. –C. 27–28.

[24] Davis, L.R. Swimsuit issue and sport, the: hegemonic masculinity in sports illustrated / L.R. Davis // *SUNY Press*, 1997. – 163 p.

[25] Denton, M.J. Fit stretch comfort 3rd shirley international seminar / M.J. Denton // *England Manchester: Textile for Comfort*, 1970, pp. 15–17.

[26] Ding, X. The relationship between the stretch elasticity of knitted knitted beam pants and garment pressure / X. Ding, N. Chen, X. Wu // *Journal of Donghua University (Natural Science Edition)*, 2010, 1, pp. 47–51.

[27] Duan, L. Automatic three-dimensional-scanned garment fitting based on virtual tailoring and geometric sewing / L. Duan, Z. Yueqi, W. Ge // *Journal of Engineered Fibers and Fabrics*, 2019, 14, pp. 1–16.

[28] Ernst, M. Investigation on body shaping garments using 3D-body scanning technology and 3D-simulation tools / M. Ernst, U. Detering-Koll, D. Gützel // *Proceedings of the 3rd International Conference on 3D Body Scanning Technologies*, Lugano, Switzerland, 16-17 October 2012. –C. 64–73.

- [29] Fei Y. Correlation of free movement of hands and garment ease / Y. Fei, Y. Guanluo, W. Chunyan // *Journal of Textile Research*, 2006, 27(7), pp. 40–43.
- [30] Gao, X. Research and optimization of the structure of women's body-fitting yoga track pants (dissertation) / X. Gao // Donghua University, 2012. – 101 p.
- [31] GB/T 1335.2-1997, Standard sizing systems for garments-women (China), 1997. – 40 p.
- [32] Geršak, J. The complex design concept for functional protective clothing / J. Geršak, M. Marčič // *Tekstil*, 2013, 62(1-2), pp. 38–44.
- [33] Gill, S. Sizing in clothing: developing effective sizing systems for ready - to - wear clothing / S. Gill // *Journal of Fashion Marketing & Management*, 2015, 12(4), pp. 579–581.
- [34] Goto, K. Efficacy of wearing compression garments during post-exercise period after two repeated bouts of strenuous exercise: a randomized crossover design in healthy, active males / K. Goto, S. Mizuno, A. Mori // *Sports Medicine*, 2017, 3(1), pp. 25.
- [35] Grogan, S. Whole body scanning as a tool for clothing sizing: effects on women's body satisfaction / S. Grogan, E. Storey, K. Brownbridge, et al. // *The Journal of The Textile Institute*, 2020, 111(6), pp. 862–868.
- [36] Gu, J. Application of laminated fabric in diving suit / J. Gu, G. Shi // *Shanghai Textile Science and Technology*, 2005, 33(7), pp. 36–38.
- [37] Gu, J. Characteristics and development trend of diving suit / J. Gu, P. Ni // *Personal Protective Equipment in China*, 2006, 2, pp. 45–47.
- [38] Guo Z. Test experiment on the effects of body-shaping underwear on human physiology / Z. Guo, J. Xu, X. Liu // *Journal of Xi'an University of Technology*, 2012, 2, pp. 168–173.
- [39] Hagggar, A. Pattern design for underwear, swimwear, beachwear and casual wear / A. Hagggar // China Textile Press, 2001. – 264 p.
- [40] Han, H. Automatic body landmark identification for various body figures / H. Han, Y. Nam // *International Journal of Industrial Ergonomics*, 2011, 41(6), pp. 592–606.
- [41] He, X. On the application of fabric stitching in the design of casual sportswear / X. He, H. Yuan, Y. Tian // *Modern Decoration (Theory)*, 2012, 11, pp. 209–210.
- [42] Hrženjak, R. Sizing system for girls aged 13–20 years based on body types / R. Hrženjak, K. Doležal, D. Ujević // *Textile research journal*, 2015, 85(12), pp. 1293–1304.
- [43] <https://nl.oneill.com/pages/wetsuit> (дата обращения 2019-12-15).
- [44] <http://thedivingblog.com/how-many-active-divers-are-there/> (дата обращения 2020-2-2).
- [45] <http://www.chyxx.com/industry/201610/459676.html> (дата обращения 2019-10-23).

- [46] <http://www.ewetsuits.com/acatalog/How-Wetsuits-Work.html> (дата обращения 2019-3-5).
- [47] <http://www.madehow.com/Volume-4/Wet-Suit.html> (дата обращения 2020-01-20).
- [48] <http://www.navalunderseamuseum.org/mk-v/> (дата обращения 2019-09-19).
- [49] <http://www.stats.gov.cn/tjsj/tjgb/rkpcgb/> (дата обращения 2019-4-29).
- [50] <https://us.aqualung.com>(дата обращения 2019-7-27).
- [51] <http://www.techweb.com.cn/news/2013-07-20/1311247.shtml> (дата обращения 2019-7-20).
- [52] <https://www.doc88.com/p-9863831651193.html> (дата обращения 2019-2-12).
- [53] <https://en.wikipedia.org/wiki/Neoprene> (дата обращения 2019-01-20).
- [54] https://en.wikipedia.org/wiki/Wallace_Carothers (дата обращения 2020-5-22).
- [55] <https://perfectwetsuit.com/wetsuit-thickness-and-temperature-guide/>(дата обращения 2020-2-7).
- [56] <https://surfing-waves.com/equipment/wetsuit-temperature-guide.htm>(дата обращения 2019-10-27).
- [57] <https://surfing-waves.com/wetsuit-thickness.htm> (дата обращения 2019-2-12).
- [58] <https://wetsuitwarehouse.com.au/blogs/news/seams-wetsuit-stitching>(дата обращения 2019-7-25).
- [59] https://www.arenawaterinstinct.com/en_global/woman-sams-carbon-wetsuit.html (дата обращения 2019-2-12).
- [60] <https://www.cleanlinesurf.com/wetsuit-guide> (дата обращения 2019-2-12).
- [61] <https://www.divesmartgozo.com/> (дата обращения 2019-10-23).
- [62] <https://www.enjoy-swimming.com/swimming-breast-stroke.html> (дата обращения 2019-8-11).
- [63] <https://www.kingofwatersports.com/wetsuit-buying-guide?group=US> (дата обращения 2019-2-12).
- [64] <https://www.padi.com/about/who-we-are> (дата обращения 2020-2-15).
- [65] <https://www.scubapro.com/blog/article/diving-semi-dry-wetsuit> (дата обращения 2019-5-10).
- [66] https://www.sfia.org/reports/796_Scuba-Diving-Participation-Report-2019 (дата обращения 2019-2-12).
- [67] <https://www.terrapinwetsuits.com/materials.html> (дата обращения 2020-2-1).
- [68] Hu, M. Research on the setting of the prototype gap of the close-fitting thoracolumbar structure / M. Hu, Z. Lei // Progress in Textile Science and Technology, 2007, 4, pp. 77–80.
- [69] Huang, L. Research on tight-fitting sportswear based on three-dimensional

anthropometry / L. Huang, L. Song // *Industrial Design*, 2016, 2, pp. 69–70.

[70] Huang, M. Research on the tight-fitting prototype of knitted female tops based on the comfort of wearing pressure / M. Huang, X. Chai, B. Ke, et al. // *Wool Textile Technology*, 2016, 44(1), pp. 60–64.

[71] Hur, H.J. Investigation of wetsuit wearing condition and size system for product development—comparison between domestic brands and imported brands / H.J. Hur, S. Kim, J. Lee // *Journal of the Korean Society of Clothing and Textiles*, 2015, 39(3), pp. 408–418.

[72] Jolly, K. Kinematic modeling of a motorcycle rider for design of functional clothing / K. Jolly, S. Krzywinski, et al. // *International Journal of Clothing Science and Technology*, 2019, pp. 1–19.

[73] JIS L 4005:2001, JATRA/JSA adult women's clothing size system, 2001. –25p.

[74] Jishuang, Y. High-tech swimsuits promote the development of swimming sports / Y. Jishuang, W. Ping, W. Yang, et al. // *Chinese Invention and Patent*, 2012, 9, pp. 26–27.

[75] Karakashian, K. Computational investigation of the Laplace law in compression therapy / K. Karakashian, C. Pike, R.L. Van // *Journal of biomechanics*, 2019, 85, pp. 6–17.

[76] Kim, J.M. A study on the visual image of windsurfing suits / J.M. Kim // *Fashion & Textile Research Journal*, 2012, 14(5), pp. 713–719.

[77] Kobayashi, T. Analysis of clothing pressure on the human body / T. Kobayashi, O. Shuya // *SIMULIA Customer Conference*, 2011, 5, pp. 1–15.

[78] Korycki, R. Optimisation of thermal conditions in a composite wet diving suit / R. Korycki // *Fibres & Textiles in Eastern Europe*, 2011, 19(6), pp. 89.

[79] Kuzmichev, V.E. Sizing and fit for pressure garments / V.E. Kuzmichev, Z. Cheng // *Anthropometry, Apparel Sizing and Design*. Woodhead Publishing, 2020, pp. 331–370.

[80] Labat, K. L. Body cathexis and satisfaction with fit of apparel / K.L. Labat, M.R. Delong // *Clothing & Textiles Research Journal*, 1990, 8(2), pp. 43–48.

[81] Lee, H.J. 3D pattern development of ergonomic outdoor pants based on skin deformation in trekking postures / H. Lee, Y. Lee, K. Hong // *Korean Society of Human Engineers Conference Papers*, 2013, 1, pp. 458–462.

[82] Lee, H.J. Selection and design of functional area of compression garment for improvement in knee protection / H.J. Lee, N.Y. Kim, K.H. Hong // *Korean Journal of Human Ecology*, 2015, 24(1), pp. 97–109.

[83] Lee, W. Heuristic misfit reduction: A programmable approach for 3D garment fit customization / W. Lee, H.S. Ko // *Computers & Graphics*, 2018, 71, pp. 1–13.

[84] Li, D. Analysis of wet diving suit / D. Li // *World Textile Herald*, 2016, 44 (5), pp. 60–65.

- [85] Li, D. Research progress and discussion of wearing pressure comfort / D. Li, T. Xia, J. Li // *Textile Herald*, 2007, 11, pp. 98–100.
- [86] Li, M. Research on underwear structure and digital design based on female body analysis / M. Li // *Journal of Donghua University*, 2001, 18(3), pp. 23–25.
- [87] Liang, Z. New Olympic Siamese tight sportswear / Z. Liang // *Tianjin Textile Science and Technology*, 2001, 3, pp. 50–52.
- [88] Lin, Y. Analysis and research on clothing comfort and its evaluation method / Y. Lin // *Bilingual Learning*, 2007, 12, pp. 220–222.
- [89] Lin, Y.L. The development of a clothing fit evaluation system under virtual environment / Y.L. Lin, M.J. Wang // *Multimedia Tools and Applications*, 2016, 75(13), pp. 7575–7587.
- [90] Liu, H. An investigation into the bust girth range of pressure comfort garment based on elastic sports vest / H. Liu, D. Chen, Q. Wei, et al. // *Journal of the Textile Institute*, 2013, 104(2), pp. 223–230.
- [91] Liu, K. 3D interactive garment pattern-making technology / K. Liu, X. Zeng, P. Bruniaux, et al // *Computer-Aided Design*, 2018, 104, pp. 113–124.
- [92] Liu, K. Fit evaluation of virtual garment try-on by learning from digital pressure data / K. Liu, X. Zeng, P. Bruniaux, et al // *Knowledge-Based Systems*, 2017, 133, pp. 174–182.
- [93] Liu, Y. Study of optimum parameters for Chinese female underwire bra size system by 3D virtual anthropometric measurement / Y. Liu, J. Wang, C.L. Istook // *The Journal of The Textile Institute*, 2017, 108(6), pp. 877–882.
- [94] Loercher, C. Motion-oriented 3D analysis of body measurements / C. Loercher, S. Morlock, A. Schenk // *IOP Conference Series: Materials Science and Engineering*, IOP Publishing, 2017, 254, p.172016
- [95] Machado, A.A. Post-exercise effects of graduated compression garment use on skeletal muscle recovery and delayed onset muscle soreness: a systematic review / A.A. Machado, C.R. Kohn, A.J. Rombaldi // *Motricidade*, 2018, 14, pp.2–3.
- [96] Mah, T. Investigation of the contribution of garment design to thermal protection. Part 1: characterizing air gaps using three-dimensional body scanning for women’s protective clothing / T. Mah, G. Song // *Textile Research Journal*, 2010, 80(13), pp. 1317–1329.
- [97] Makabe, H. Effect of covered area at the waist on clothing pressure / H. Makabe, H. Momota, T. Mitsuno, et al. // *SeniGakkaishi*, 1993, 49(10), pp. 513–521.
- [98] Matsuda, A. 3-dimensional joint torque calculation of compression sportswear using 3D-CG human model / A. Matsuda, H. Tanaka, H. Aoki, et al. // *Procedia Engineering*, 2015, 112, pp. 40–45.

[99] McMaster, D.T. The efficacy of wrestling-style compression suits to improve maximum isometric force and movement velocity in well-trained male rugby athletes / D.T. McMaster, C.M. Beaven, B. Mayo, et al. // *Frontiers in Physiology*, 2017, 8, p. 874.

[100] Meixner, C. Development of a method for an automated generation of anatomy-based, kinematic human models as a tool for virtual clothing construction / C. Meixner, S. Krzywinski // *Computers in Industry*, 2018, 98, pp.197–207.

[101] Monji, K. Changes in insulation of wetsuits during repetitive exposure to pressure / K. Monji, K. Nakashima, Y. Shogabe, et al. // *Undersea Biomed Research*, 1989, 16(4), pp. 313–319.

[102] Morgan, A. Can scuba diving offer therapeutic benefit to military veterans experiencing physical and psychological injuries as a result of combat? A service evaluation of Depthrapy UK / A. Morgan, H. Sinclair, et al. // *Disability and rehabilitation*, 2019, 41(23), pp. 2832–2840.

[103] Naebe, M. Assessment of performance properties of wetsuits / M. Naebe, N. Robins, X.Wang, et al. // *Proceedings of the Institution of Mechanical Engineers, Part P: Journal of Sports Engineering and Technology*, 2013, 227(4), pp. 255–264.

[104] Naglic, M. and Petrak, S. 2017 Analysis of dynamics and fit of diving suits / M. Naglic, S. Petrak // *IOP Conference Series: Materials Science and Engineering*, IOP Publishing, 2017, 254, p.152007.

[105] Naglic, M.M. Analysis of 3D construction of tight fit clothing based on parametric and scanned body models / M.M. Naglic, S. Petrak, Z. Stjepanović // *Proceedings of the 7th International Conference on 3D Body Scanning Technologies*, Lugano, Switzerland, 30 Nov.-1 Dec. 2016. –C. 302–313.

[106] Naglic, M.M. Analysis of dynamics and fit of diving suits / M.M. Naglic, S. Petrak, J. Gersak, et al. // *IOP Conference Series: Materials Science and Engineering*, IOP Publishing, 2017, 254(15), p.152007.

[107] Nakashima, M. 3D-CG based musculoskeletal simulation for a swimmer wearing competitive swimwear / M. Nakashima, T. Hasegawa, A. Matsuda, et al. // *Procedia Engineering*, 2013, 60(10), pp. 367–372.

[108] Nazakat, A. Effect of different types of seam, stitch class and stitch density on seam performance / A. Nazakat, et al. // *Journal of applied and emerging sciences*, 2014, 5(1), pp. 32–43.

[109] Ni, H. Pressure testing of women's elastic stockings and research on their pressure comfort / H. Ni, Y. Gan, D. Chen, S. Liang // *Journal of Xi'an University of Technology*, 2009, 1, pp. 35–38.

- [110] Novak, H.F. Scuba diving as a rehabilitation approach in paraplegia / H.F. Novak, G. Ladurner // *Die Rehabilitation*, 1999, 38(3), pp. 181–184.
- [111] Oh, H. A study of the improvement of foam material sealing technology for wetsuits / H. Oh, K.W. Oh, S. Park // *Fashion and Textiles*, 2019, 6(1), pp. 1–15.
- [112] Peng, T. Research on the classification of young women's body based on front and back body differences (dissertation) / T. Peng // Wuhan Textile University, 2016.– 53p.
- [113] Petrak, S. Dynamic anthropometry-defining protocols for automatic body measurement / S. Petrak, M. Naglic // *Tekstilec*, 2017, 4, pp. 254–262.
- [114] Petrak, S. Impact of male body posture and shape on design and garment fit / S. Petrak, M. Mahnic, D. Rogale, et al. // *Fibers and Textiles in Eastern Europe*, 2015, 23(6), pp. 150–158.
- [115] Petrak, S. Research of 3D body models computer adjustment based on anthropometric data determined by laser 3D scanner / S. Petrak, M. Mahnic, D. Ujevic, et al. // *Proceeding of 3rd International Conference on 3D Body Scanning Technologies*, Lugano, Switzerland, 16-17 Oct. 2012. – C. 115–126.
- [116] Petrak, S. Sizing and fit for swimsuits and diving suits / S. Petrak, M.M. Naglič, et al. // *Anthropometry, Apparel Sizing and Design*, Woodhead Publishing, 2020, pp. 255–287.
- [117] Porterfield, A. Examining the effectiveness of virtual fitting with 3D garment simulation. *International Journal of Fashion Design* / A. Porterfield, T.A. Lamar // *Technology and Education*, 2017, 10(3), pp. 320–330.
- [118] Prabir, J. Assembling technologies for functional garments - An overview / J. Prabir // *Indian Journal of Fiber & Textile Research*, 2011, 36(12), pp. 380–387.
- [119] Pratt, J. Pressure garments: a manual on their design and fabrication / J. Pratt, G. West // *Butterworth-Heinemann*, 1995. –130 p.
- [120] Rainey, C. Wet suit pursuit: hugh bradner's development of the first wet suit / C. Rainey // *Scripps Institution of Oceanography SIO Reference*, 1998, 11, pp. 1–10.
- [121] Rudolf, A. Study regarding the virtual prototyping of garments for paraplegics / A. Rudolf, et al. // *Fibers and Polymers*, 2015, 16(5), pp. 1177–1192.
- [122] Shenzhen Shengshihuayan Business Management Co., Ltd. 2019-2025 Research report on technology development trends of china's marine diving equipment industry, 2019, 1, pp. 7–8.
- [123] Shimana, T. A new method for designing sportswear by using three dimensional computer graphic based anisotropic hyperelastic models and musculoskeletal simulations / T. Shimana, M. Nakashima, A. Matsuda, et al. // *Procedia Engineering*, 2013, 60, pp. 331–336.
- [124] Shiue, M.C. Finishing method for manufacturing wetsuits non-stitch / M.C. Shiue //

U.S. Patent Application 11/281, 118.(2007-5-17).

[125] Staal, T. A 3D anthropometric approach for designing a sizing, system for tight fitting garments / T. Staal, T. huysmans, et al. // 2nd International Comfort Congress, August 29-30 2019, Delft, 2019. – C. 1–6.

[126] Staples, M.L. A system for the sizing of women's garments / M.L. Staples, D.B. Delury // Textile Research Journal, 1949, 19(6), pp. 346–354.

[127] Stjepanovic, Z. Construction of adapted garments for people with scoliosis using virtual prototyping and CASP method / Z. Stjepanovic, A. Cupar, S. Jevšnik, et al. // Industria Textila, 2016, 67(2), pp. 141–148.

[128] Su, J. Development of individualized pattern prototype based on classification of body features / J. Su, G. Liu, B. Xu // International Journal of Clothing Science & Technology, 2015, 27(6), pp. 895–907.

[129] Sybilska, W. Analysis of body measurements using a 3d contactless scanning method / W. Sybilska, L. Napieralska, E. Mielicka // Autex Research Journal, 2010, 10(3), pp. 77–79.

[130] Tanaka, H. 3-dimensional stress calculation of competitive swimwear using anisotropic hyperelastic model considering stress softening / H. Tanaka, T. Shimana, A. Matsuda // Procedia Engineering, 2014, 72, pp. 261–266.

[131] Van, G.E. Comparing swimsuits in 3D / G.E. Van, J. Molenbroek, S. Schreven, et al. // Work, 2012, 41(1), pp. 4025–4030.

[132] Vuruskan, A. Modeling of half-scale human bodies in active body positions for apparel design and testing / A. Vuruskan, S.P. Ashdown // International Journal of Clothing Science and Technology, 2017, 29(6), pp. 807–821.

[133] Wang X., Yao Mu. Discussion on the pressure comfort and sports function of sports protective equipment / X. Wang, M. Yao // Journal of Northwest Textile University, 2001, 15(2), pp. 56–59.

[134] Wang, G. Diving suit with automatic temperature adjustment / G. Wang // Chinese Personal Protective Equipment, 2002, 6, pp. 33.

[135] Wang, J. A review of the research on the application of digital clothing based on 3D measurement / J. Wang, X. Li // Textile Herald, 2011(11), pp.82–84.

[136] Wang, S. Research on thermal and wet comfort of golf clothing based on ergonomics / S. Wang, H. Xie, B. Hu, et al. // Shanghai Textile Science and Technology, 2014, 42(11), pp. 11–14.

[137] Wang, X. Study on the difference in skin surface hardness of adult males with different body fat rates / X. Wang, W. Bu, S. Liu, et al. // Chinese Journal of Aerospace

Medicine, 2013, 24(3), pp. 204–209.

[138] Wang, Y. Pressure comfort sensation and discrimination on female body below waistline / Y. Wang, Y. Liu, S. Luo, et al. // *Journal of the Textile Institute*, 2018, 109(8), pp. 1067–1075.

[139] Wang, Y. The Pressure comfort sensation of female's body parts caused by compression garment / Y. Wang, Y. Liu, S. Luo, et al. // *Advances in Intelligent Systems and Computing*, 2018, 608, pp. 94–104.

[140] Wang, Z. 3d human body data acquisition and fit evaluation of clothing / Z. Wang, Y.Q. Zhong, K.J. Chen, et al. // *Advanced Materials Research*, 2014, 989, pp. 4161–4164.

[141] Wang, Z. Preparation and performance study of composite phase change material loaded with fatty acid supported by expanded perlite for thermal insulation diving / Z. Wang // Shanghai:East China University of Science and Technology, 2013, – 56 p.

[142] Williams, G. Exposure suits: a review of thermal protection for the recreational diver / G. Williams, C.J. Acott // *Rubicon Research Repository*, 2003, 3, pp. 37–40.

[143] Wu, X. Development of female torso classification and method of patterns shaping / Xinzhou Wu, V.E. Kuzmichev, Peng T. // *Autex Research Journal*, 2018, 18(4), pp. 419–428.

[144] Wu, X. Analysis of diving sports mechanics and key points of diving suit design / Xinzhou Wu, Jinsong Du // *Journal of Wuhan Textile University*, 2015, 28(5), pp. 29–33

[145] Wu, X. Study on the body girth dynamic size for wetsuit ease design / Xinzhou Wu, V.E. Kuzmichev // *IOP Conference Series: Materials Science and Engineering*. IOP Publishing, 2018, 459(1), p. 012085.

[146] Wu, X. Prediction of wet diving suit comfortability / Wu Xinzhou, V.E. Kuzmichev // 18th AUTEX International conference, Istanbul, 20–22 June, Turkey. 2018. – C. 494–499.

[147] Wu, X. Design and dynamic simulation of 3d virtual wetsuit / Xinzhou Wu, V.E. Kuzmichev // *DEStech Transactions on Computer Science and Engineering*, 2018, 9, pp. 142–145.

[148] Wu, X. Research on the trousers with zero loose quantity pattern / Xinzhou Wu, Jingsong Du, Yunxiang Lu // *Journal of Beijing Institute of Fashion Technology: Natural Science Edition*, 2015, 35(3), pp. 33–39.

[149] Wu, X. A design of wetsuit based on 3D body scanning and virtual technologies / Xinzhou Wu, V.E. Kuzmichev // *International Journal of Clothing Science and Technology*, 2020, 33(4), pp: 477–494.

[150] Wu, X. Computer technologies for designing close-fitting apparel with specific properties / Xinzhou Wu, V.E. Kuzmichev // *DEStech Transactions on Computer Science and Engineering*, 2020, 9, pp. 30–35.

- [151] Xiaoxia, S. The relationship between clothing pressure and human comfort / S. Xiaoxia, F. Xunwei. // *Textile Journal*, 2006, 27(3): 103–105.
- [152] Xie, J. A comparative study of donghua prototype, new japanese buka prototype and russian mgutd women's prototype / J. Xie // *International Textile Herald*, 2014, 3, pp. 71–72.
- [153] Xu D. Research on pressure comfort of women's one-piece swimwear / Daifang X., Dongyun L., Zhiming W. // *Knitting Industry*, 2013(6): 65–67.
- [154] Xu, D. Design and optimization of women's swimwear wide margin based on pressure comfort / D. Xu, D. Liu, Z. Wu // *Journal of Beijing Institute of Clothing Technology*, 2012, 3, pp. 16–25.
- [155] Xu, D. On the particularity of swimwear structure design /D. Xu // *Journal of Tianjin Polytechnic University*, 2000, 19(5), pp. 66–69.
- [156] Xu, J. Study on the pressure comfort of women's beach volleyball clothing based on sports biomechanics / J. Xu, L. Zhang, F. Zhang, et al. // *Journal of Tianjin Polytechnic University*, 2009, 4(1), pp. 462–468.
- [157] Yan, Y. The effect of women's basketball underwear pressure on heart rate variability index / Y. Yan, J. Gao, J. Jin, et al. // *Journal of Textiles*, 2014, 35(6), pp. 100–104.
- [158] Yeung, K.W. A 3D biomechanical human model for numerical simulation of garment–body dynamic mechanical interactions during wear / K.W. Yeung, Y. Li, X. Zhang // *The Journal of The Textile Institute*, 2004, 95(1-6), pp. 59–79.
- [159] Yuan, J. Contrast test of thickness and thermal performance of two wet diving suit materials under pressure / J. Y, J. Gu, X. Gu // *Chinese Journal of Nautical Medicine and Hyperbaric Medicine*, 2008, 15(4), pp. 240–241.
- [160] Yuan, S. Discussion on waterproof and breathable clothing and its processing technology / S. Yuan // *Shanghai Textile Science and Technology*, 2009, 37(1), pp. 1–2.
- [161] Yuan, X. Study on the comfort of female tights / X. Yuan, Y. Gan, D. Chen // *Journal of Xi'an University of Technology*, 2009, 3, pp. 31–35.
- [162] Zhang, F. Dynamic ease evaluation for 3D garment design / F. Zhang, T.J. Little // *Journal of Fashion Marketing and Management: An International Journal*, 2018, 22(2), pp. 209–222.
- [163] Zhang, J. Upper garment 3d modeling for pattern making / J. Zhang, N. Innami, K.O. Kim, M. Takatera // *International Journal of Clothing Science & Technology*, 2015, 27(6), pp. 852–869.
- [164] Zhang, L. The effect of clothing pressure on upper limb fatigue in men's basketball / L. Zhang, Y. Yan // *Journal of Zhejiang University of Science and Technology: Social Science Edition*, 2017, 38(2), pp. 133–138.

[165] Zhang, W. Ergonomics of clothing / W. Zhang, F. Fang // Shanghai: Donghua University Press, 2008, 1, pp. 183–190.

[166] Zhang, X. Research on comfortable pressure range of female one-piece swimsuit / X. Zhang, H. Mu // Modern Silk Science and Technology. 2012, 27(1), pp. 5–7.

[167] Zhao, L. Analysis of men's neck pressure comfort based on changes in neck blood flow / L. Zhao, D. Chen // Journal of Clothing, 2018, 3(6), pp. 487–491.

[168] Zhang Qiyue, Lu Xin. Analysis of research status of clothing pressure comfort [J]. Liaoning Silk, 2018(1): 29–30.

[169] Zhao, L. Study of an arm model for compression sleeve design and garment pressure measurement / L. Zhao, J. Yu, S. Zhang, et al. // Journal of Engineered Fibers and Fabrics, 2019, 14, №. 1558925019872656.

[170] Zhao, M. Study on the pressure comfort of warp-knit seamless fit women's tops / M. Zhao, Z. Wu, Z. Dong // Journal of Tianjin Polytechnic University, 2011, 2, pp. 35–39.

[171] Сеницкий И.А. Моделирование мягких тканей виртуального манекена для проектирования корсетных изделий и белья / И.А. Сеницкий, Д.А. Васильев, А.Е. Горелова, et al. // Программные продукты и системы, 2015, 1(109), pp. 167–172.

[172] У Синьчжоу. The influence of squatting postures on the tight pants pattern block / У Синьчжоу, В. Е. Кузьмичев // Информационная среда вуза. Иваново: ИВГПУ, 2017, 9, с.151–154

[173] У Синьчжоу. Инструментальное исследование деформации фигур под влиянием костюма для подводных видов спорта / У Синьчжоу, В. Е. Кузьмичев // II Международная научно-практическая конференция "Модели инновационного развития текстильной и легкой промышленности на базе интеграции университетской науки и индустрии. Образование-наука-производство": сборник статей. 23-25 марта 2016 г. - Казань: Изд-во КНИТУ, 2016, с. 462–465.

[174] У Синьчжоу. Алгоритм проектирования костюма для подводного плавания / У Синьчжоу, В. Е. Кузьмичев // Технология текстильной промышленности, 2019, 38(3), pp. 121–127.

[175] У Синьчжоу. Моделирование деформации фигур под влиянием водной среды и костюма для подводных видов спорта / У Синьчжоу, В. Е. Кузьмичев, Доминик С. Адольф // Инновационное развитие легкой и текстильной промышленности (ИНТЕКС-2016) сборник материалов Всероссийской научной студенческой конференции. МГУДТ. Москва, 2016, 5-6 апреля, с. 32–35.

[176] Чен, Ч. Усовершенствованная технология проектирования мужского белья / Ч. Чен, В.Е. Кузьмичев // Информационная среда вуза, 2017, 1(24), pp. 154–159.

RESULTS OF ANTHROPOMETRIC MEASUREMENTS

Table A.1 – Primary body measurements with a 3D body scanner

Category	No.	ID	Measurements interpretation	Symbols	Average, S.D., cm
1	2	3	4	5	6
Distance	1	0510	Distance 7CV (BNP) to vertical	-	27.0 ± 1.8
	2	0515	Distance neck front (FNP) to vertical	-	36.6 ± 2.0
	3	0550	Distance waist to vertical	-	44.2 ± 3.0
	4	0530	Distance waist back to vertical	-	26.1 ± 2.9
	5	0600	Distance bust to vertical	-	46.3 ± 3.1
	6	0610	Distance back in bust height to vertical	-	23.1 ± 2.4
Width	7	3020	Cross shoulder width	-	41.6 ± 4.1
	8	4030	Bust points (BP) width	-	17.2 ± 1.8
	9	4010	Across/bust front width	-	32.7 ± 4.4
	10	5020	Across back width	-	33.1 ± 2.9
Girth	11	4510	Bust girth	BG	83.9 ± 4.7
	12	6510	Waist girth	WG	69.5 ± 7.5
	13	7520	Buttock/hip girth	HG	90.5 ± 5.3
	14	9510	Thigh	TG	51.2±3.3
Height	15	0030	Neck (7CV/BNP) height	H _{BNP}	136.9 ± 8.0
	16	0170	Bust (BP) height	H _{BP}	115.7 ± 7.8
Length	17	2010/ 2020	Side upper torso length	SL	19.0 ± 2.1
	18	4050	Neck front (FNP) to waist	FNP-WL	31.1 ± 3.3
	19	5040	Neck to waist centre back	BNP-WL	36.1 ± 3.2
	20	6011	Crotch length, front	-	36.1 ± 3.2
	21	6012	Crotch length, back	-	38.0 ± 2.7
	22	6010	Crotch length	-	74.1 ± 5.7
Additional measurements	23	-	Bust front girth	BG _F	42.3 ± 4.5
	24	-	Bust back girth	BG _F	38.8 ± 4.6
	25	-	Waist front girth	WG _F	35.0 ± 4.2
	26	-	Waist back girth	WG _B	34.5 ± 4.3
	27	-	Hip front girth	HG _F	43.9 ± 3.1

End of Table A.1

1	2	3	4	5	6
Additional measurements	28	-	Hip back girth	HG _B	46.6 ± 3.5
	29	-	Mid-waist girth	-	79.9 ± 6.1
	30	-	Mid-waist front girth	-	42.7 ± 3.9
	31	-	Mid-waist back girth	-	37.2 ± 2.0
	32		Upper arm girth	-	25.1 ± 2.3
	33	8530/85 31	Elbow girth	-	22.5 ± 2.2
	34	8555	Wrist girth	-	15.3 ± 1.1
	35	9550/95 51	Ankle girth	-	25.1 ± 2.9
	36	9540/95 41	Calf girth	-	34.5 ± 2.7
	37	8040/80 41	Upper arm length	-	30.0 ± 1.7
	38	3030/30 31	Shoulder length	-	12.5 ± 1.1
	39	8030/80 31	Arm length	-	52.5 ± 3.1
	40	9010/90 11	Inseam length	-	63.2 ± 3.8
	41	9040/90 41	Outside seam length	-	91.1 ± 6.4
42	0010	Height	-	161.5 ± 5.6	

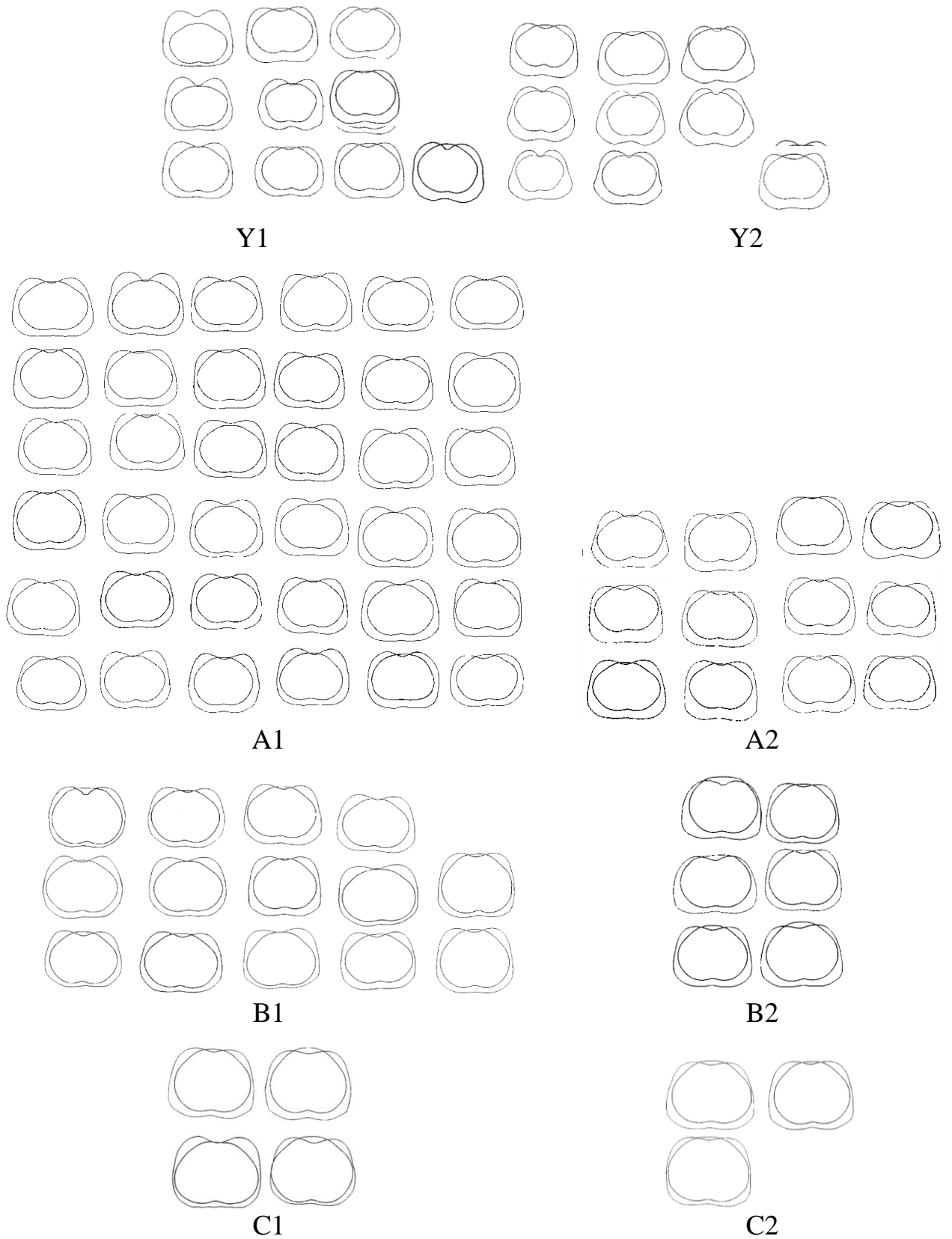


Figure A.1 – Waist and hip cross-sections of 8 body types

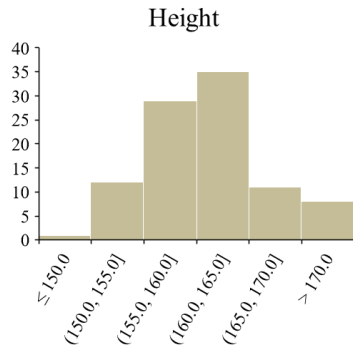


Figure A.2 – Data distribution of height

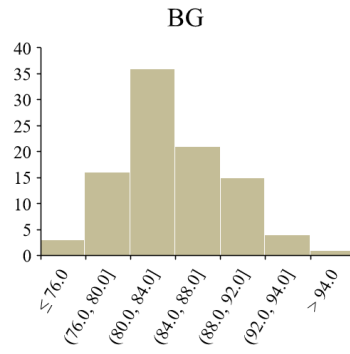


Figure A.3 – Data distribution of BG

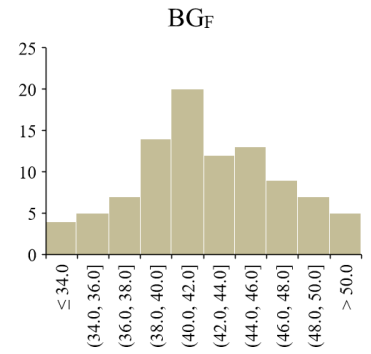


Figure A.4 – Data distribution of BGF

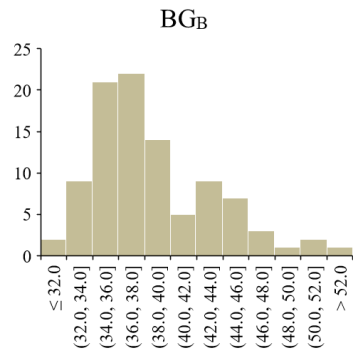


Figure A.5 – Data distribution of BGB

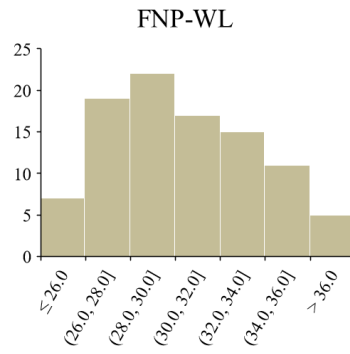


Figure A.6 – Data distribution of FNP-WL

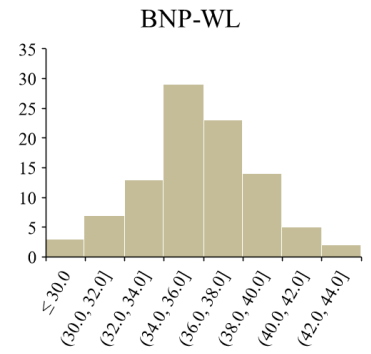


Figure A.7 – Data distribution of BNP-WL

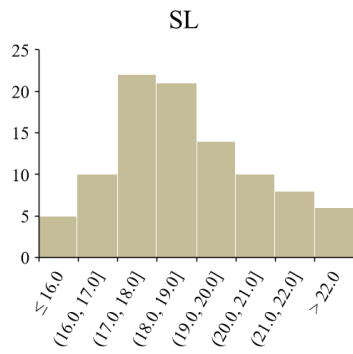


Figure A.8 – Data distribution of SL

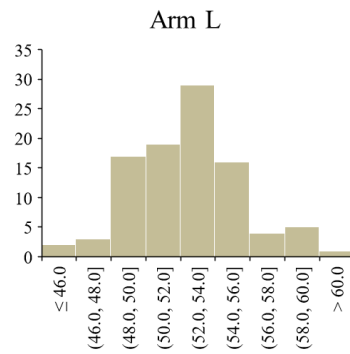


Figure A.9 – Data distribution of arm L

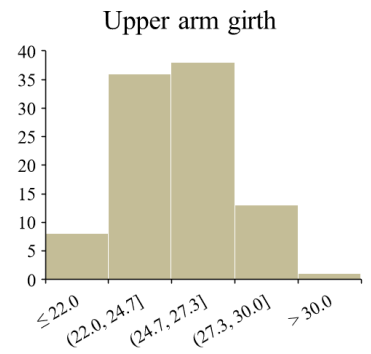


Figure A.10 – Data distribution of upper arm G

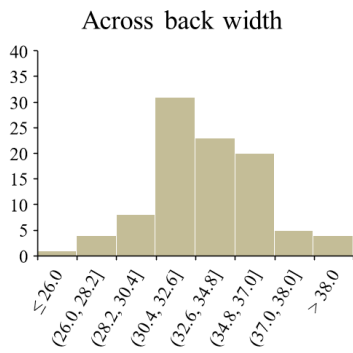


Figure A.11 – Data distribution of back width

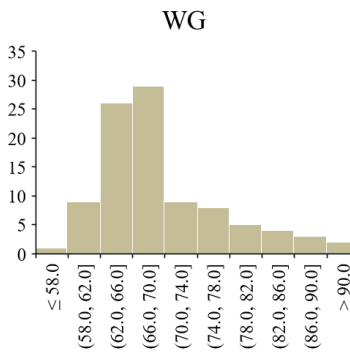


Figure A.12 – Data distribution of WG

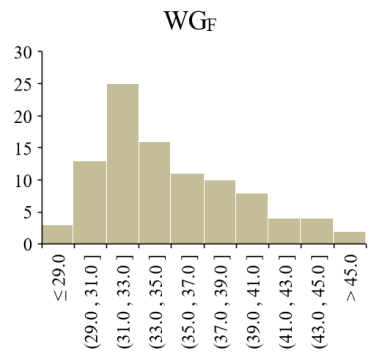


Figure A.13 – Data distribution of WGF

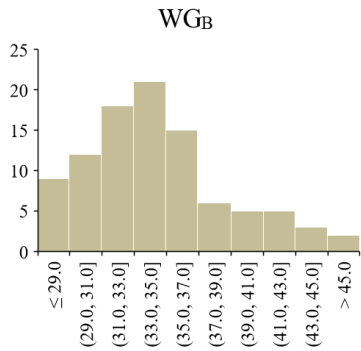


Figure A.14 – Data distribution of WGB

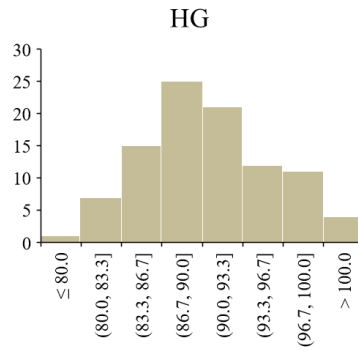


Figure A.15 – Data distribution of HG

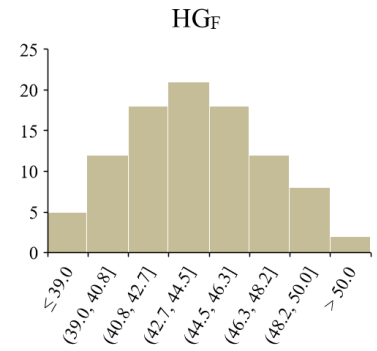


Figure A.16 – Data distribution of HGF

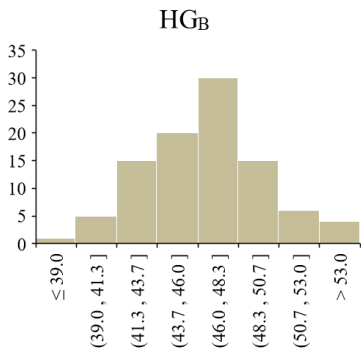


Figure A.17 – Data distribution of HGB

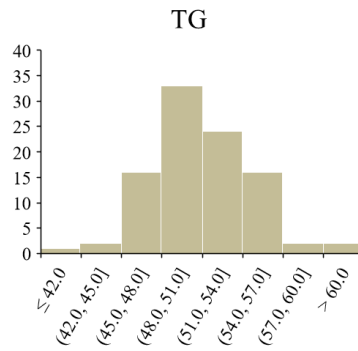


Figure A.18 – Data distribution of TG

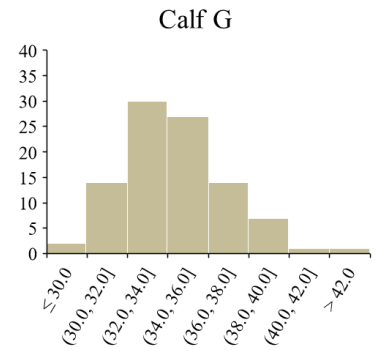


Figure A.19 – Data distribution of calf girth

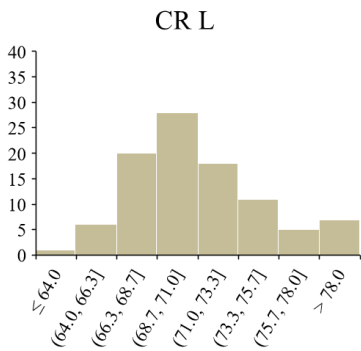


Figure A.20 – Data distribution of crotch length

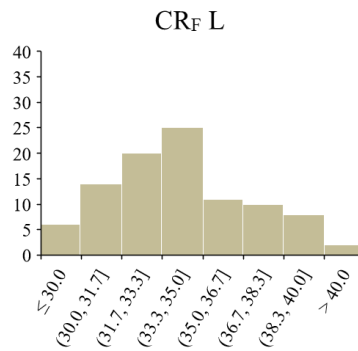


Figure A.21 – Data distribution of crotch front length

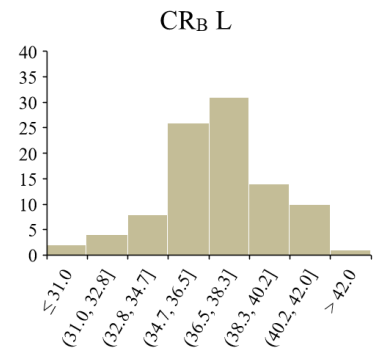


Figure A.22 – Data distribution of crotch back length

**RESULTS OF MEASURING PRESSURE AND STRETCH OF
MATERIALS**

TableB.1 – Measurements of materials elongation E_{\max} on key body parts, %

Body position	Measured in material course direction				
	M1	M2	M3	M4	Avg.
1	2	3	4	5	6
Upper arm	20.4	18.5	12.6	19.5	17.8
Forearm	20.0	18.5	14.0	19.5	18.0
Bust	27.2	21.4	15.5	22.8	21.7
Waist	27.7	19.6	14.1	20.2	20.4
Hip	33.5	22.5	20.9	22.7	24.9
Thigh	24.6	16.9	12.5	18.8	18.2
Calf	25.5	15.8	13.1	19.0	18.4
Avg.	25.6	19.0	14.7	20.4	19.9
	Measured in material wale direction				
Body position	M1	M2	M3	M4	Avg.
Upper arm	15.2	12.5	10.1	13.8	12.9
Forearm	15.0	12.6	11.0	12.0	12.7
Bust	17.7	12.0	10.5	14.0	13.6
Waist	16.2	10.4	9.7	10.7	11.8
Hip	19.5	12.5	10.2	16.2	14.6
Thigh	18.4	10.2	9.0	16.8	13.6
Calf	19.7	9.8	9.7	15.9	13.8
Avg.	17.4	11.4	10.0	14.2	13.3

Table B.2 – The P_{\max} on key body parts, kPa

	Measured in material course direction				
Body position	M1	M2	M3	M4	<i>Avg.</i>
Upper arm	2.01	1.95	2.38	1.84	<i>2.05</i>
Forearm	2.17	1.91	2.46	1.89	<i>2.11</i>
Bust	1.84	1.72	2.09	1.72	<i>1.84</i>
Waist	1.75	1.70	2.02	1.64	<i>1.78</i>
Hip	1.66	1.59	2.14	1.50	<i>1.72</i>
Thigh	1.38	1.34	2.02	1.22	<i>1.49</i>
Calf	2.19	1.80	2.52	1.78	<i>2.07</i>
<i>Avg.</i>	<i>1.86</i>	<i>1.72</i>	<i>2.23</i>	<i>1.66</i>	<i>1.87</i>
	Measured in material wale direction				
Body position	M1	M2	M3	M4	<i>Avg.</i>
Upper arm	2.10	2.45	2.65	2.26	<i>2.37</i>
Forearm	2.21	2.34	2.88	2.25	<i>2.42</i>
Bust	1.95	2.26	2.46	2.19	<i>2.22</i>
Waist	1.80	2.14	2.35	2.10	<i>2.10</i>
Hip	1.73	2.01	2.40	2.00	<i>2.04</i>
Thigh	1.45	1.98	2.21	2.10	<i>1.94</i>
Calf	2.32	2.45	2.80	2.39	<i>2.49</i>
<i>Avg.</i>	<i>1.94</i>	<i>2.23</i>	<i>2.54</i>	<i>2.18</i>	<i>2.22</i>

Table B.3 – Index of RC_b on key body parts, kPa/%

	Measured in material course direction				
Body position	M1	M2	M3	M4	Avg.
Upper arm	0.21	0.20	0.25	0.19	0.21
Forearm	0.23	0.20	0.26	0.20	0.22
Bust	0.13	0.12	0.14	0.12	0.13
Waist	0.12	0.12	0.14	0.11	0.12
Hip	0.21	0.20	0.27	0.19	0.22
Thigh	0.11	0.11	0.16	0.10	0.12
Calf	0.28	0.23	0.32	0.23	0.27
Avg.	<i>0.18</i>	<i>0.17</i>	<i>0.22</i>	<i>0.16</i>	<i>0.18</i>
	Measured in material wale direction				
Body position	M1	M2	M3	M4	Avg.
Upper arm	0.22	0.26	0.28	0.24	0.25
Forearm	0.23	0.25	0.30	0.24	0.26
Bust	0.13	0.16	0.17	0.15	0.15
Waist	0.12	0.15	0.16	0.14	0.14
Hip	0.22	0.25	0.30	0.25	0.25
Thigh	0.12	0.16	0.18	0.17	0.16
Calf	0.30	0.31	0.36	0.31	0.32
Avg.	<i>0.19</i>	<i>0.22</i>	<i>0.25</i>	<i>0.21</i>	<i>0.22</i>

Table B.4 – Index of RC_m on key body parts, %

	Measured in material course direction				
Body position	M1	M2	M3	M4	<i>Avg.</i>
Upper arm	2.13	1.93	1.31	2.03	<i>1.85</i>
Forearm	2.11	1.95	1.47	2.05	<i>1.89</i>
Bust	1.88	1.48	1.07	1.57	<i>1.50</i>
Waist	1.87	1.32	0.95	1.36	<i>1.38</i>
Hip	3.88	2.81	2.61	2.84	<i>3.03</i>
Thigh	1.97	1.35	1.00	1.50	<i>1.46</i>
Calf	3.27	2.03	1.68	2.44	<i>2.35</i>
<i>Avg.</i>	<i>2.44</i>	<i>1.84</i>	<i>1.44</i>	<i>1.97</i>	<i>1.92</i>
	Measured in material wale direction				
Body position	M1	M2	M3	M4	<i>AVG.</i>
Upper arm	1.58	1.30	1.05	1.44	<i>1.34</i>
Forearm	1.58	1.33	1.16	1.26	<i>1.33</i>
Bust	1.22	0.83	0.72	0.97	<i>0.93</i>
Waist	1.09	0.70	0.66	0.72	<i>0.79</i>
Hip	2.75	1.56	1.28	2.03	<i>1.90</i>
Thigh	1.47	0.82	0.72	1.34	<i>1.09</i>
Calf	2.53	1.26	1.24	2.04	<i>1.77</i>
<i>Avg.</i>	<i>1.75</i>	<i>1.11</i>	<i>0.98</i>	<i>1.40</i>	<i>1.31</i>

Table B.5 – The average minimum design ease of M1 on key body parts, %

Body position	Y1	Y2	A1	A2	B1	B2	C1	C2	Avg.
BGF	-17.4	-17.5	-22.9	-24.0	-18.6	-23.7	-19.4	-18.1	-20.2
WG	-1.2	-1.3	-4.1	-4.6	-3.6	-3.7	-3.3	-3.4	-3.1
WGF	-6.5	-3.4	-5.6	-7.1	-6.1	-4.9	-7.3	-10.8	-6.5
HG	-5.0	-5.6	-8.6	-7.3	-9.0	-4.3	-8.6	-6.6	-6.9
HGB	-22.9	-17.2	-25.5	-18.2	-22.2	-18.9	-19.6	-24.5	-21.1
Thigh	-2.4	-2.2	-2.1	-3.0	-0.9	-2.8	-4.1	-4.0	-2.7
Calf	-5.5	-4.6	-4.9	-4.6	-5.8	-2.9	-8.4	-6.1	-5.4
Upper arm	0.6	1.5	2.4	1.9	1.7	1.1	1.3	1.9	1.5
Forearm	0.9	1.5	2.2	2.2	2.2	1.8	2.6	2.2	2.0

Table B.6 – The average minimum design ease of M2 on key body parts, %

Body position	Y1	Y2	A1	A2	B1	B2	C1	C2	Avg.
BGF	-12.9	-13.1	-17.1	-17.9	-13.9	-17.7	-14.4	-13.5	-15.1
WG	-0.8	-0.9	-2.8	-3.1	-2.4	-2.5	-2.2	-2.3	-2.1
WGF	-4.7	-2.5	-4.1	-5.2	-4.4	-3.5	-5.3	-7.8	-4.7
HG	-3.3	-3.7	-5.7	-4.8	-5.9	-2.8	-5.7	-4.4	-4.5
HGB	-15.1	-11.4	-16.8	-12.0	-14.6	-12.5	-12.9	-16.2	-13.9
Thigh	-1.5	-1.4	-1.3	-1.9	-0.5	-1.7	-2.6	-2.5	-1.7
Calf	-3.1	-2.6	-2.8	-2.6	-3.3	-1.6	-4.8	-3.5	-3.0
Upper arm	0.5	1.3	2.1	1.6	1.5	1.0	1.1	1.6	1.3
Forearm	0.8	1.3	2.0	2.0	2.0	1.6	2.3	2.0	1.7

Table B.7 – The average minimum design ease of M3 on key body parts, %

Body position	Y1	Y2	A1	A2	B1	B2	C1	C2	Avg.
BGF	-10.0	-10.1	-13.2	-13.9	-10.7	-13.7	-11.2	-10.5	<i>-11.7</i>
WG	-0.6	-0.7	-2.3	-2.5	-1.9	-2.0	-1.8	-1.9	<i>-1.7</i>
WGF	-3.5	-1.9	-3.1	-3.9	-3.3	-2.7	-3.9	-5.9	<i>-3.5</i>
HG	-2.9	-3.3	-5.1	-4.3	-5.3	-2.5	-5.1	-3.9	<i>-4.0</i>
HGB	-13.4	-10.1	-15.0	-10.7	-13.0	-11.1	-11.5	-14.4	<i>-12.4</i>
Thigh	-1.2	-1.1	-1.0	-1.5	-0.4	-1.4	-2.1	-2.0	<i>-1.3</i>
Calf	-2.7	-2.3	-2.4	-2.3	-2.9	-1.4	-4.2	-3.0	<i>-2.7</i>
Upper arm	0.4	1.0	1.7	1.3	1.2	0.8	0.9	1.3	<i>1.1</i>
Forearm	0.7	1.1	1.7	1.7	1.7	1.4	1.9	1.7	<i>1.5</i>

Table B.8– The average minimum design ease of M4 on key body parts, %

Body position	Y1	Y2	A1	A2	B1	B2	C1	C2	Avg.
BGF	-14.2	-14.4	-18.8	-19.7	-15.2	-19.4	-15.9	-14.9	<i>-16.6</i>
WG	-0.9	-1.0	-3.1	-3.4	-2.6	-2.8	-2.4	-2.5	<i>-2.3</i>
WGF	-4.8	-2.5	-4.2	-5.3	-4.5	-3.6	-5.4	-8.0	<i>-4.8</i>
HG	-7.4	-8.4	-12.8	-10.8	-13.3	-6.4	-12.8	-9.8	<i>-10.2</i>
HGB	-33.9	-25.6	-37.9	-27.1	-33.0	-28.0	-29.0	-36.4	<i>-31.4</i>
Thigh	-2.5	-2.3	-2.1	-3.1	-0.9	-2.8	-4.3	-4.1	<i>-2.8</i>
Calf	-7.8	-6.6	-7.0	-6.6	-8.2	-4.1	-11.9	-8.6	<i>-7.6</i>
Upper arm	0.7	1.9	3.0	2.3	2.1	1.4	1.6	2.3	<i>1.9</i>
Forearm	1.1	1.8	2.7	2.7	2.7	2.2	3.1	2.7	<i>2.4</i>

Table B.9– The average minimum design ease of M1...M4 in course, %

Body position	Y1	Y2	A1	A2	B1	B2	C1	C2	Avg.
BGF	-16.8	-17.0	-22.2	-23.3	-18.0	-23.0	-18.8	-17.6	-19.6
WG	-1.1	-1.3	-3.9	-4.4	-3.4	-3.5	-3.1	-3.2	-3.0
WGF	-6.2	-3.2	-5.3	-6.7	-5.8	-4.6	-6.9	-10.3	-6.1
HG	-6.4	-7.3	-11.1	-9.4	-11.5	-5.6	-11.1	-8.6	-8.9
HGB	-29.5	-22.2	-32.9	-23.5	-28.7	-24.4	-25.2	-31.7	-27.3
Thigh	-2.3	-2.1	-2.0	-2.9	-0.8	-2.6	-3.9	-3.8	-2.5
Calf	-6.2	-5.2	-5.6	-5.2	-6.5	-3.3	-9.5	-6.9	-6.0
Upper arm	0.6	1.7	2.8	2.1	1.9	1.3	1.5	2.1	1.8
Forearm	1.1	1.8	2.6	2.6	2.6	2.2	3.1	2.6	2.3

Table B.10– The average minimum design ease of M1...M4 in wale, %

Body position	Y1	Y2	A1	A2	B1	B2	C1	C2	Avg.
BGF	-10.5	-10.6	-13.8	-14.5	-11.2	-14.3	-11.7	-10.9	-12.2
WG	-0.6	-0.7	-2.2	-2.5	-1.9	-2.0	-1.7	-1.8	-1.7
WGF	-3.6	-1.9	-3.1	-4.0	-3.4	-2.7	-4.0	-6.0	-3.6
HG	-2.9	-3.2	-5.0	-4.2	-5.1	-2.5	-5.0	-3.8	-4.0
HGB	-13.1	-9.9	-14.7	-10.5	-12.8	-10.9	-11.2	-14.1	-12.1
Thigh	-1.5	-1.4	-1.3	-1.9	-0.5	-1.7	-2.6	-2.5	-1.7
Calf	-3.4	-2.8	-3.0	-2.8	-3.6	-1.8	-5.2	-3.7	-3.3
Upper arm	0.4	1.1	1.8	1.4	1.3	0.8	1.0	1.4	1.2
Forearm	0.7	1.1	1.6	1.6	1.6	1.4	1.9	1.6	1.4

RESULTS OF TESTING MATERIALS ON THE KES-F COMPLEX

Stretch charts

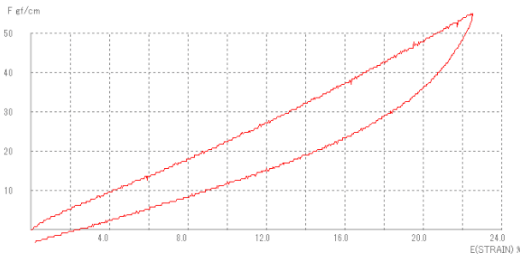


Figure C.1 – KES tension (50 cN/cm) test M1 in course

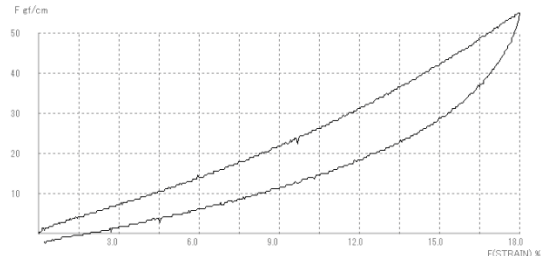


Figure C.2 – KES tension (50 cN/cm) test M1 in wale

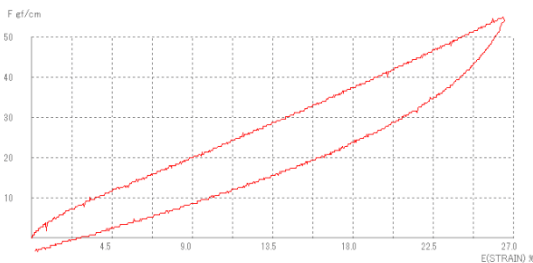


Figure C.3 – KES tension (50 cN/cm) test M2 in course

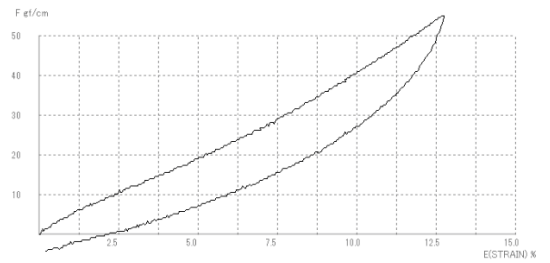


Figure C.4 – KES tension (50 cN/cm) test M2 in wale

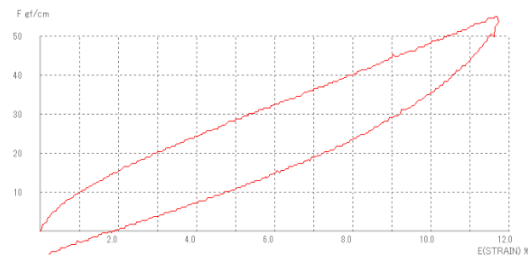


Figure C.5 – KES tension (50 cN/cm) test M3 in course

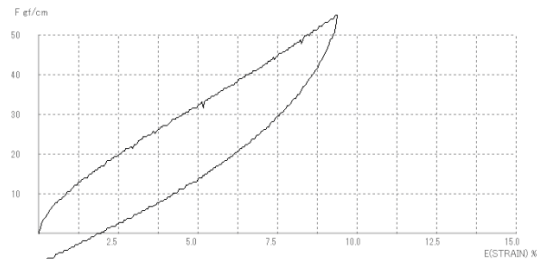


Figure C.6 – KES tension (50 cN/cm) test M3 in wale

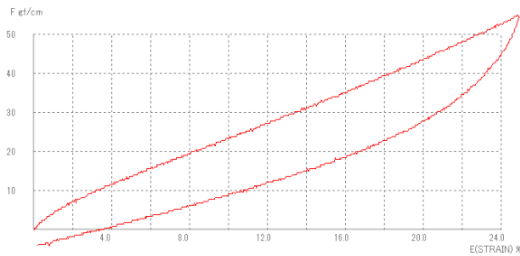


Figure C.7 – KES tension (50 cN/cm) test M4 in course

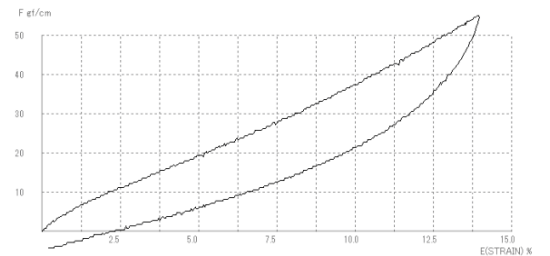


Figure C.8 – KES tension (50 cN/cm) test M4 in wale

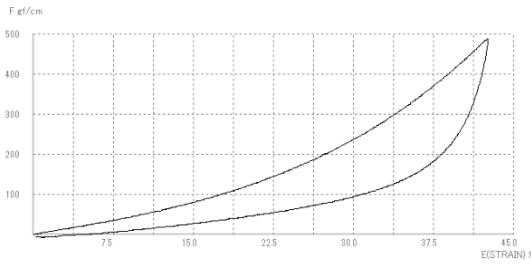


Figure C.9 – KES tension (500 cN/cm) test M1 in course

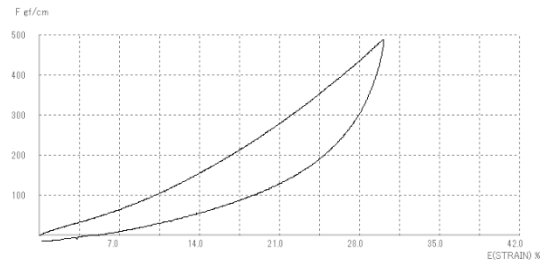


Figure C.10 – KES tension (500 cN/cm) test M2 in course

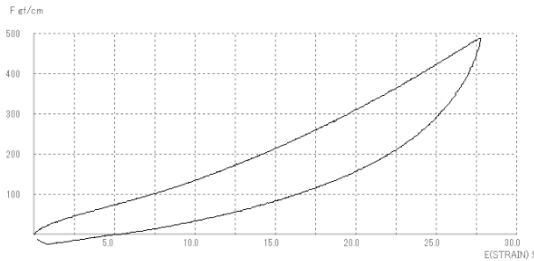


Figure C.11 – KES tension (500 cN/cm) test M3 in course

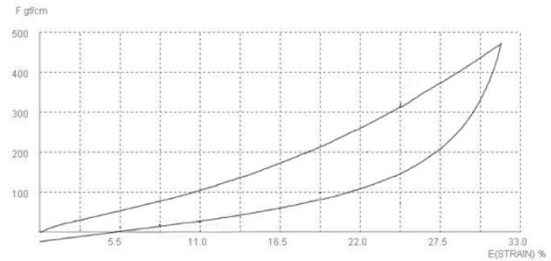


Figure C.12 – KES tension (500 cN/cm) test M4 in course

Table C.1 – KES-FB1-4 indexes

Indexes	Direction	M1	M2	M3	M4
LC	-	0.603	0.550	0.473	0.664
WC (gf/cm ²)	-	0.330	0.469	0.220	0.397
RC (%)	-	51.520	58.000	53.640	57.430
T _M (mm)	-	2.681	2.847	2.705	3.120
T ₀ (mm)	-	2.900	3.188	2.891	3.359
MIU	<i>Wale</i>	0.290	0.236	0.242	0.256
	<i>Course</i>	0.398	0.368	0.341	0.428
MMD	<i>Wale</i>	0.007	0.006	0.008	0.010
	<i>Course</i>	0.012	0.010	0.010	0.012

1	2	3	4	5	6
SMD	<i>Wale</i>	3.490	1.410	1.975	5.160
	<i>Course</i>	2.175	1.775	3.315	2.320
High load 500 gf/cm					
LT	<i>Course</i>	0.684	0.796	0.870	0.799
WT(cN.cm / cm ²)	<i>Course</i>	72.750	59.800	60.200	60.800
RT(%)	<i>Course</i>	47.010	50.920	50.080	45.720
EMT(%)	<i>Course</i>	42.650	30.170	27.800	30.560
Low load 50 gf/cm					
LT	<i>Wale</i>	0.473	0.52	0.614	0.541
	<i>Course</i>	0.533	0.561	0.625	0.575
WT(cN.cm / cm ²)	<i>Wale</i>	2.120	1.650	1.430	1.880
	<i>Course</i>	2.990	3.700	1.820	3.570
RT(%)	<i>Wale</i>	61.79	58.79	50.35	54.79
	<i>Course</i>	62.880	61.890	53.850	54.060
EMT(%)	<i>Wale</i>	18.030	12.690	9.320	13.910
	<i>Course</i>	22.450	26.400	11.640	24.840
G	<i>Wale</i>	2.520	3.590	7.310	3.140
	<i>Course</i>	2.490	3.570	7.080	3.620
2HG	<i>Wale</i>	5.280	8.750	19.200	7.850
	<i>Course</i>	4.150	7.350	18.900	8.130
2HG5	<i>Wale</i>	5.400	8.630	19.980	7.280
	<i>Course</i>	4.400	7.500	19.300	8.250

Table C.2– Tension load and the pressure in the course

Materials	Tension load F_x (cN/cm) under x , %				
	3%	6%	9%	12%	15%
M1	18.32	34.20	50.07	68.39	86.71
M2	21.98	36.64	50.07	64.73	78.16
M3	51.29	81.83	111.14	139.84	168.91
M4	23.20	39.08	53.74	68.39	83.05

Table C.3 – Tension load and the pressure in the wale

Materials	Tension load F_x (cN/cm) under x , %		
	3%	6%	9%
M1	14.66	29.31	43.97
M2	29.31	54.96	87.93
M3	52.52	85.49	120.91
M4	35.45	62.29	91.60

Table C.4 – Correlation coefficients between P_{\max} , E and KES results

KES indexes	P_{\max}		E_{\max}	
	Course	Wale	Course	Wale
<i>LT</i>	0.693	0.973	-0.937	-0.834
<i>WT</i>	-0.988	-0.967	0.496	0.989
<i>RT</i>	-0.350	-0.914	0.667	0.740
<i>EMT</i>	-0.925	-0.868	0.563	0.912
<i>G</i>	0.828	0.941	-0.908	-0.801
<i>2HG</i>	0.822	0.956	-0.904	-0.818
<i>2HG5</i>	0.829	0.940	-0.899	-0.799
<i>LC</i>	-0.831	-0.738	0.693	0.727
<i>WC</i>	-0.918	-0.469	0.335	0.158
<i>RC</i>	-0.599	0.205	-0.342	-0.436
<i>TM</i>	-0.689	-0.066	-0.026	0.016
<i>TO</i>	-0.802	-0.119	0.000	-0.030
<i>MIU</i>	-0.773	-0.794	0.671	0.943
<i>MMD</i>	-0.478	0.114	0.792	0.087
<i>SMD</i>	0.883	-0.456	-0.625	-0.628
F3	0.893	0.970	-	-
F6	0.914	0.971	-	-
F9	0.930	0.968	-	-
F12	0.948	-	-	-
F15	0.959	-	-	-

**LT* is tensile rigidity, *WT* is tension energy, gf.cm/cm²; *RT* is recoverability, %; *EMT* is tensile strain, %; *G* is Shear rigidity, gf/cm; *2HG* is elasticity for minute shear, gf/cm; *2HG5* is elasticity for large shear, gf/cm; *WC* is work of compression, gf.cm/cm²; *MIU* is Frictional coefficient; *MMD* is Mean deviation of coefficient of friction; *SMD* is surface roughness

CURVEFIT
 /VARIABLES= Pmax WITH F15c
 /CONSTANT
 /MODEL=INVERSE

Pmax
Inverse

Model Summary

R	R Square	Adjusted R Square	Std. Error of the Estimate
.965	.931	.897	.082

The independent variable is F15c.

Coefficients

	Unstandardized Coefficients		Standardized Coefficients	t	Sig.
	B	Std. Error	Beta		
1 / F15c	-78.805	15.137	-.965	-5.206	.035
(Constant)	2.699	.165		16.335	.004

Figure C.13 – SPSS equation 4.3

CURVEFIT
 /VARIABLES= Pmax WITH WTc
 /CONSTANT
 /MODEL=INVERSE

Pmax
Inverse

Model Summary

R	R Square	Adjusted R Square	Std. Error of the Estimate
.987	.975	.962	.050

The independent variable is WTc.

Coefficients

	Unstandardized Coefficients		Standardized Coefficients	t	Sig.
	B	Std. Error	Beta		
1 / WTc	1.945	.222	.987	8.773	.013
(Constant)	1.169	.083		14.029	.005

Figure C.14 – SPSS equation 4.4

CURVEFIT
 /VARIABLES= Pmax WITH WTw
 /CONSTANT
 /MODEL=INVERSE

Pmax
Inverse

Model Summary

R	R Square	Adjusted R Square	Std. Error of the Estimate
.973	.947	.921	.069

The independent variable is WTw.

Coefficients

	Unstandardized Coefficients		Standardized Coefficients	t	Sig.
	B	Std. Error	Beta		
1 / WTw	2.445	.407	.973	6.003	.027
(Constant)	.811	.238		3.414	.076

Figure C.15 – SPSS equation 4.6

CURVEFIT
 /VARIABLES= Pmax WITH LTW
 /CONSTANT
 /MODEL=INVERSE

Pmax
Inverse

Model Summary

R	R Square	Adjusted R Square	Std. Error of the Estimate
.972	.944	.916	.071

The independent variable is LTW.

Coefficients

	Unstandardized Coefficients		Standardized Coefficients	t	Sig.
	B	Std. Error	Beta		
1 / LTW	-1.194	.205	-.972	-5.811	.028
(Constant)	4.465	.388		11.519	.007

Figure C.16 – SPSS equation 4.7

CURVEFIT

/VARIABLES= Pmax WITH 2HGw

/CONSTANT

/MODEL=S

Pmax**Inverse****Model Summary**

R	R Square	Adjusted R Square	Std. Error of the Estimate
.999	.999	.998	.005

The independent variable is 2HGw.

Coefficients

	Unstandardized Coefficients		Standardized Coefficients	t	Sig.
	B	Std. Error	Beta		
1 / 2HGw	-1.961	.050	-.999	-39.140	.001
(Constant)	1.031	.007		157.993	.000

Figure C.17 – SPSS equation 4.8

ALGORITHM FOR CONSTRUCTION OF THE BASIC DESIGN OF A WETSUIT AND TEST RESULTS

TableD.1 – Structural drawing of back piece

Segment	Rules of construction	Illustration
00	Draw a horizontal line to the right, and a vertical line down	
/00–02/	$BG / 12 = 6.7$ cm, half neck width; vertical line from 02	
/01–11/	$/00–10/ / 3 = 2.2$ cm, back neck depth, downward from point 00 ; draw a horizontal line from point 10 to the right; /10–01/ half neck back curve	
/10–30/	Equal to /01–11/ ; horizontal line from point 30 to the right	
/30–33/	Back width to SP, SP is 33	
/02–42/	Shoulder length, SNP-SP, 12.2 cm	
/10–90/	Back centre length, BNP-WL, neck back to waist, 38cm; draw a horizontal line from point 90 to the right waist line	
/10–80/	$BG / 3 + 7 = 20.3$ cm, BNP-BL; draw horizontal line from point 80 to the right	
/80–84/	$BG / 4 = 20.0$ cm, middle point 84 at side	
/60–80/	Point 60 on midway of /30–80/ ; draw horizontal line from point 60 to the right	
/60–62/	Back width, $BWB / 2 = 32.9 / 2 = 16.5$ cm, equal to /80–82/	

Table D.2 – Structural drawing of front piece

Segment	Rules of construction	Illustration
/27–28/	Lower back /00–01/ than 0.5 cm, /27–28/ = /00–01/ - 0.2 = 6.5 cm, neck front width	
/28–58/	/00–01/ + 1 = 7.7 cm, neck front depth; /27–58/ is half neck front curve	
/28–48/	/00–10/ * 2 = 4.4 cm	
/27–45/	Shoulder length, SNP-SP, 12.2 cm, SP is 45 in front	
/45–48/	Front width to SP	
/78–88/	Point 78 on midway of /58–88/, horizontal line to the left	
/76–78/	Equal to /88–86/, half front horizontal width FWB / 2 = 30.9 / 2 = 15.5 cm	
/84–88/	BG / 4 = 20.0 cm, middle point 84 at side	

Table D.3 – Structural drawing of armseye part

Segment	Rules of construction	Illustration
/80–88/	BG / 2 = 40.0 cm, half length of the bust girth, point 24 in the middle	
/90–98/	Distance of point 90 to 98 equal to /80–88/, point 94 in the middle	
/62–84/	Draw curve, (/82–84// 2 + 0.5) = 4 cm off from the vertex 82 of ∠(62-82-84) angle bisector	
/76–84/	Draw curve, (/82–84// 2) = 3.5 cm off from the vertex 86 of ∠(76-86-84) angle bisector	
/90'–98'/	Half waist girth = 33.3 cm	

Table D.4 – Structural drawing of lower piece

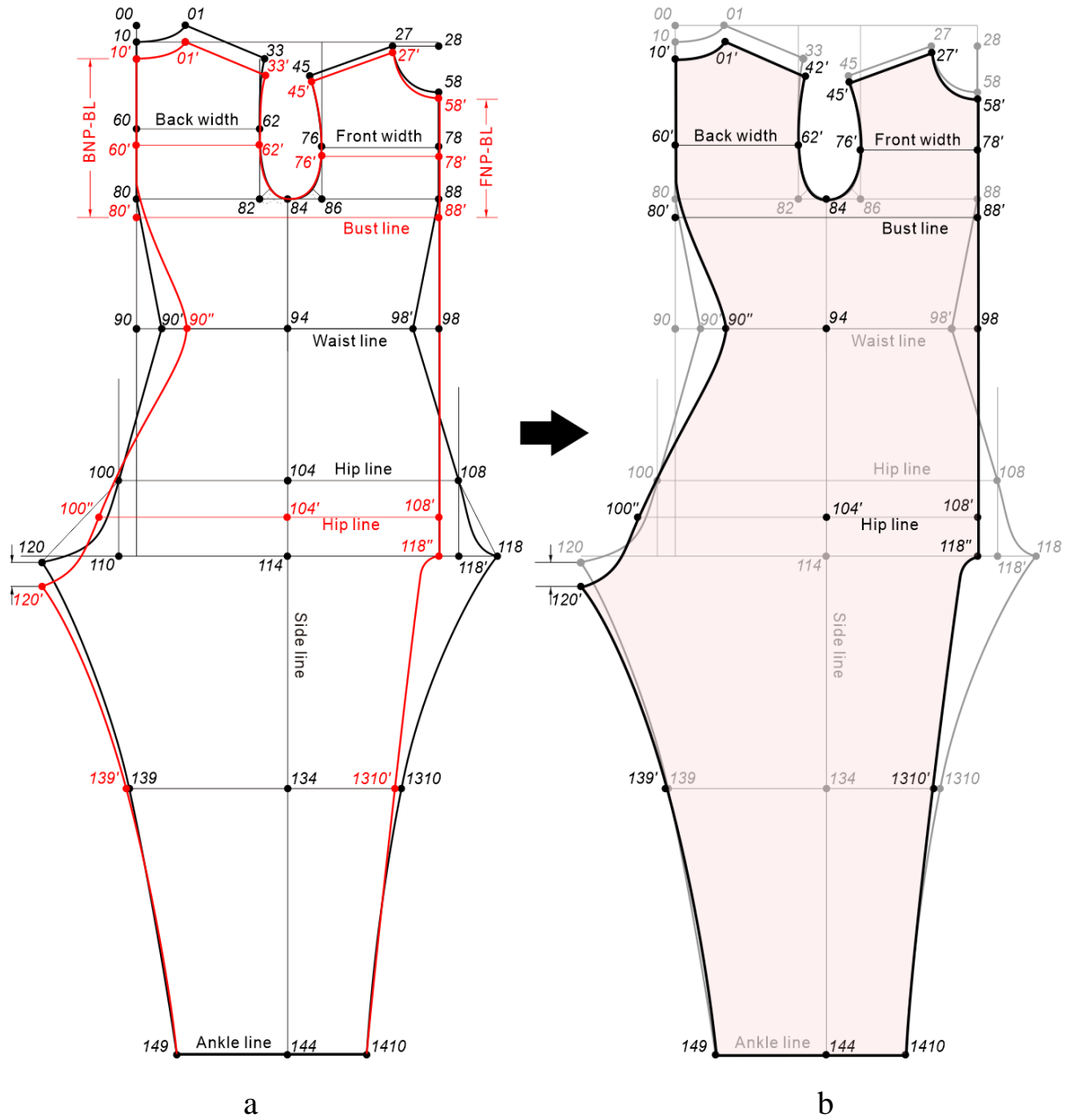
Segment	Rules of construction	Illustration
/94–114/	Square down from 94 to 114 , body rise 30.2 cm. $/110-114/=114-118'$	
/100–108/	half hip girth = 44.8 cm, 110' on two-third of /94–114/	
/118–118'/	$HG / 16 - 0.5 = 5.1$ cm	
120, 110	120 lower 0.5cm. Distance between 120 and 110 , $HG/8-0.5 = 10.7$ cm, crotch back width; (or $/118-118'/* 2 + 0.5$)	
/90'–100– 120/	Curve across the middle of altitude of triangle \angle $/100-110-120/$, off from the vertex 110	
/98–108–1 18/	Curve across the two-thirds of altitude of triangle \angle $/108-118'-118'/$, off from the vertex 118'	
/94–144/	Vertical line from waist to ankle 88.9 cm	
/114–134/	Half the /94–144/ minus 2 cm	
/139–1310/	Mid-knee girth, $/82-81/ + 3$ cm = $/8-82/$	
/149–1410/	Ankle girth, $/144-1410/ + 2$ cm = $/149-144/$	

Table D.5 – Structural drawing of sleeve piece

Segment	Rules of construction	Illustration
/S01–S51/	Square down from S01 , sleeve length, SP to wrist, 49.8 cm	
/S01–S31/	One-third length of armscye curve /33–84–45/	
/S30–S32/	Horizontal line, upper arm girth, 25.7 cm, S31 in the middle	
/S01–S30/	Straight, equal to /S01–S32/	
/S32–S12/	Armscye front, S12 on half of /S01–S32/ and move 1 cm to the point S32 ; the curve fall 1.3 cm in middle of /S12–S32/	
/S01–S12/	Armscye front, the curve rises 1.8 cm in middle of /S01–S12/	
/S20–S30/	Armscye back, S20 on the half of the (/S01–S30/ - □), /S01–S32// 4 = □, as the figure shows; the curve fall 0.7 cm in middle	
/S01–S20/	The curve rises 2 cm in middle	
/S01–S41/	Upper arm length, 30.1 cm	
/S40–S42/	Elbow girth, S41 in the middle	
/S50–S52/	Wrist girth, S51 in the middle, 14.8 cm	
/S30–S50/	Inseam of sleeve, equal to /S32–S52/	

Table D.6 – Rules of basic wetsuit construction (FigureD.1)

Sign	Rules of construction
/10'-80'/	BNP-BL, for wetsuit shorten back length equal to the body measurement, 21.2 cm
/10'-90''/	Make curve start from point 60'
/58'-88'/	FNP-BL, for wetsuit shorten front length equal to the body measurement, 15.8 cm
33', 45'	Lower bust line and SP 33' and 45' , SNP 01' and 27' , decrease armscye depth
/90''-98/	Half WG, equal to /90'-98'/
/94-104'/	Equal to /98-108''/ , the waist height to hip height by measured, 25.5 cm; lower the hip line to draw the back centre
/100''-108'/	Half HG, equal to the /100-108/
/98-108''/	Vertical line, shorten front crotch width, /33-61/ was shortened,
/98-118''/	Vertical line, equal to the /98'-118/ , the front crotch length
/90''-120'/	Equal to the $CrL_B = 39.2$ cm, 120' lower than 120 (2.3 cm) and move to the left (1.8 cm); equal to the Full CrL minus CrL_F /98-118''/ , and longer than the curve /90'-120/ ; distance between point 120 to 120' is balance value



FigureD.1– Graphic of the structure: a –modification based on the initialprototype; b – basic type wetsuit pattern (red color block)

Table D.7 – Pressure comparison between two patterns

Measured position		Prototype, kPa	Basic, kPa
Bust	<i>Front</i>	2.88	1.68
	<i>Side</i>	0.35	1.38
	<i>Back</i>	0.12	1.54
Waist	<i>Front</i>	1.00	0.80
	<i>Side</i>	0.50	0.77
	<i>Back</i>	0.80	1.61
Hip	<i>Front</i>	0.78	1.27
	<i>Side</i>	0.40	1.77
	<i>Back</i>	1.97	2.18
Shoulder		0.82	1.83
Upper arm		0.78	1.68
Forearm		2.11	2.14
Wrist		0.12	0.67
Thigh		0.75	1.14
Knee front		1.07	0.92
Calf		1.68	1.45
Ankle		0.30	0.65
S.D., \pm		0.77	0.49

Table D.9 – Pressure difference (value order is SP, BP and Side point), %

Front Back	-3 cm			-2 cm			-1 cm			0 cm			1 cm			2 cm			3 cm		
-3 cm	-14.0	13.5	44.4	-16.4	8.5	18.8	-13.3	6.9	48.4	-25.0	-2.2	37.0	-15.6	-6.1	28.5	-24.9	-6.1	44.9	-30.4	-4.2	39.8
-2 cm	-16.1	15.1	29.4	-18.9	2.7	29.1	-15.3	5.0	53.2	-22.4	-3.0	34.1	-17.3	-1.3	16.2	-24.9	-0.4	44.0	-24.2	-4.6	43.1
-1 cm	-21.3	12.5	35.8	-20.7	1.3	23.8	-14.7	5.5	56.2	-18.9	-1.7	41.3	-17.8	-1.7	36.2	-20.8	-0.9	50.9	-24.2	-5.4	34.9
0 cm	-23.8	7.5	26.6	-24.7	0.4	16.4	-21.1	3.1	49.6	-20.9	-2.1	38.6	-24.7	-5.7	31.5	-25.7	-7.7	36.1	-24.3	-8.8	43.1
1 cm	-27.9	8.5	25.2	-21.0	-1.7	29.7	-19.0	2.7	50.0	-22.3	-2.1	33.8	-25.6	-5.3	24.4	-26.4	-10.9	38.5	-29.1	-8.7	50.9
2 cm	-25.5	6.5	24.8	-22.7	-3.4	32.1	-19.0	2.7	53.7	-22.8	-2.5	54.5	-22.1	-4.9	20.7	-27.1	-7.3	35.8	-28.1	-9.8	44.5
3 cm	-21.6	6.8	24.8	-20.7	-3.4	33.1	-15.1	2.2	54.4	-22.9	-2.5	49.2	-26.6	-6.1	16.5	-27.4	-5.7	34.7	-27.6	-9.7	39.7

Table D.10 – Pressure on waist side, kPa

Front Back	1 cm	2 cm	3 cm	4 cm	5 cm
	1 cm	0.22	0.20	0.26	0.27
2 cm	0.21	0.20	0.25	0.24	0.23
3 cm	0.20	0.23	0.24	0.20	0.24
4 cm	0.22	0.21	0.23	0.22	0.23
5 cm	0.23	0.25	0.24	0.25	0.22

Table D.11– Pressure difference on waist side point and SP

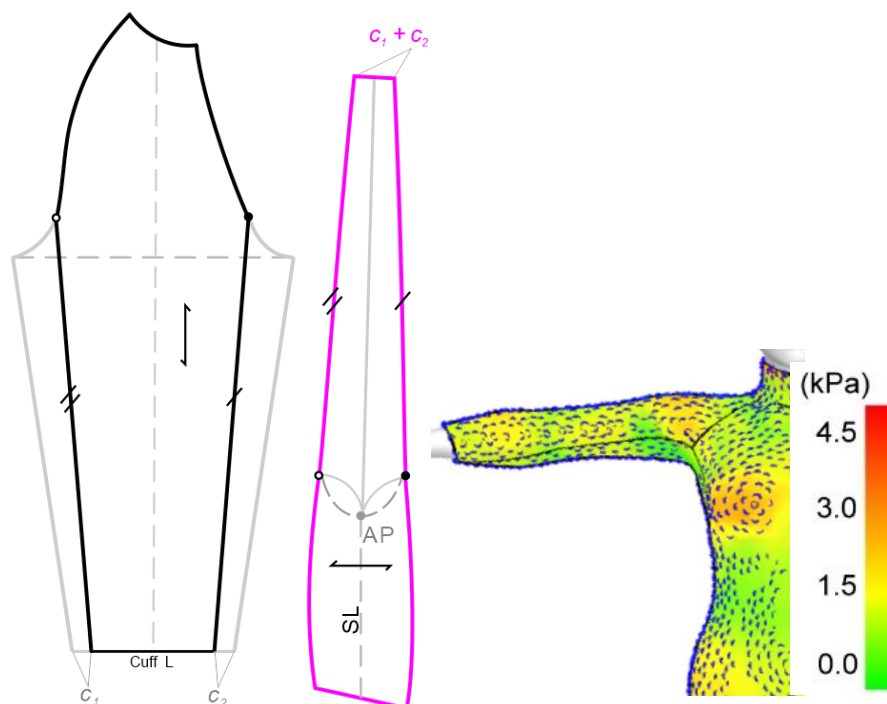
<i>h</i>	Pressure difference, %				
	7 cm	9 cm	11 cm	13 cm	15 cm
Δ SP	-17.5	-20.0	-16.0	-15.2	-14.3
Δ Waist side point	26.7	27.3	25.0	19.7	13.0

Table D.12– Pressure on waist side point and SP

<i>x</i>	$C_1+C_2=x$				
	2 cm	4 cm	6 cm	8 cm	10 cm
	Pressure, kPa				
SP	1.77	1.65	1.56	1.47	1.45
Waist side point	0.17	0.15	0.17	0.16	0.17

Table D.13 –Pressure on 2 parts

	Pressure measured upper BL				
Upper than BL	1 cm	2 cm	3 cm	4 cm	5 cm
BP, kPa	1.98	1.94	1.92	1.85	1.77
Lower WL	2 cm	4 cm	6 cm	8 cm	10 cm
Lower navel points, kPa	0.46	0.40	0.55	0.67	0.32

**Figure D.2 –Verification of two-piece sleeve**

*The sum of C1 and C2 is the cuff width of the small piece. We take the small cuff width from 2...10 cm to test (average wrist girth is 14.8 cm)

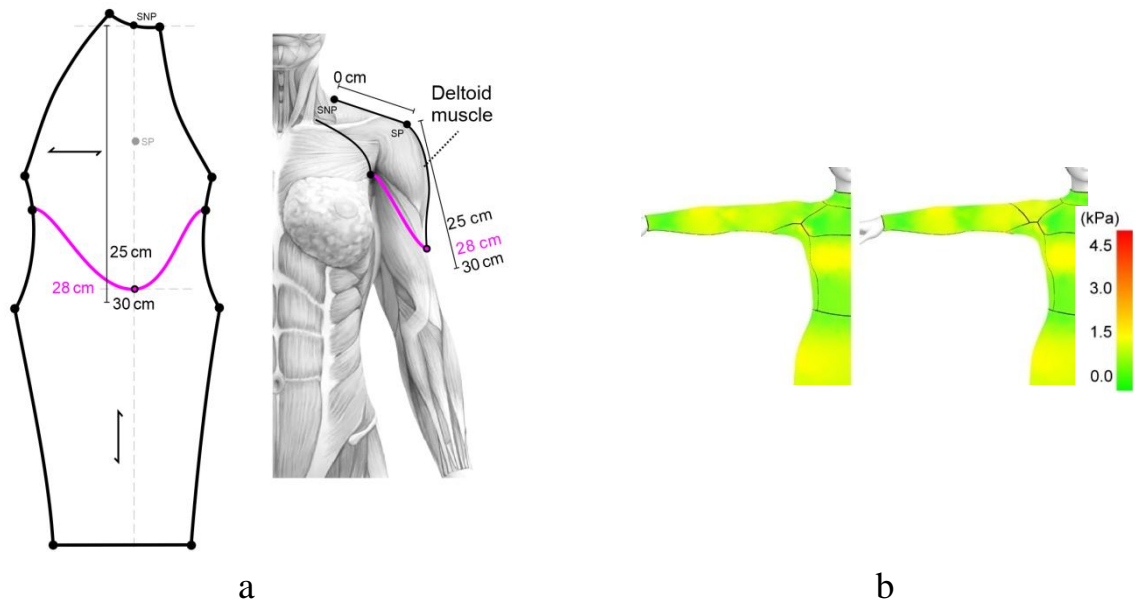


Figure D.3 – Shoulder design: a – cutting on sleeve; b – (left)traditional design, (right) separated shoulderdesign

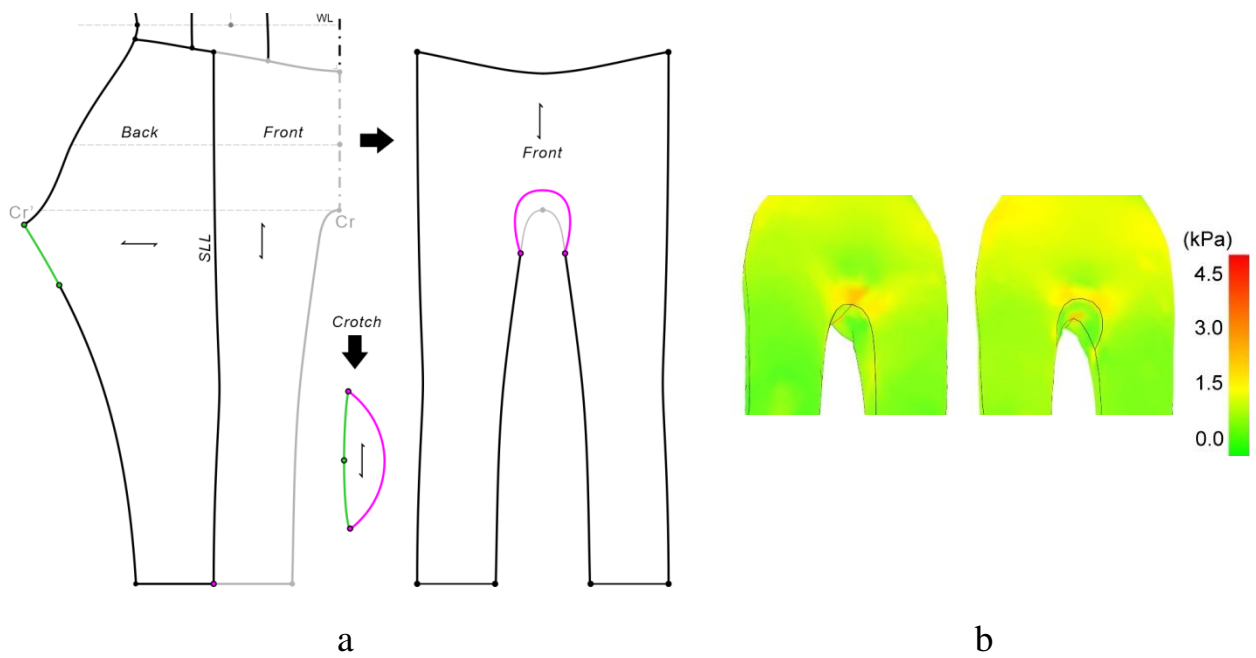


Figure D.4–Crotch part design: a – cutting on crotch; b – (left)traditional crotch design, (right) separated crotch

*Figure shows a separated crotch – width 6...12 cm, length 20...26 cm. In general, the female tight clothing of crotch width cannot too wide, usually during 6...8 cm.

Table D.14 – Tester size, cm

	Type	Hight	BG	BG _F	WG	HG	Thigh G	FullcrotchL
Testee 1	Y1	158	81	43	62	86	46	66
Testee 2	A1	157	82	44	67	91	52	68.5
Testee3	B1	160	88	47	71	89.5	49	67



**FigureD.5– PW1-S with Y1
sizedestee**



FigureD.6 – PW1-MwithA1 sizedestee



FigureD.7 – PW1-LwithB1 sizedestee



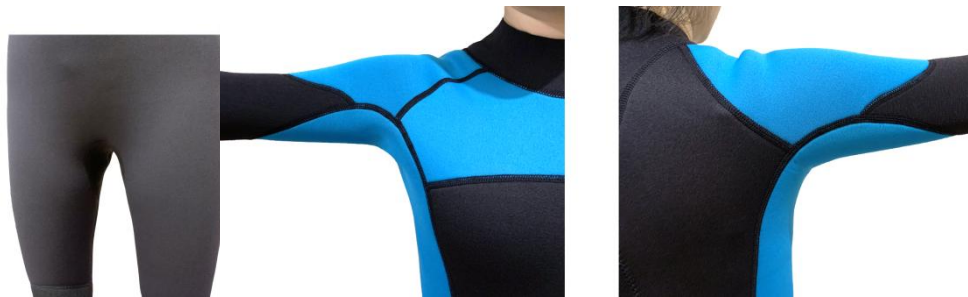
FigureD.8 – Squatting test



FigureD.9 – DW1-A1 with A1
sizedestee



FigureD.10 – DW1-B1 with B1 sizedestee



FigureD.11 – Wetsuit details

TableD.15 –Pressure difference between PW and DW

Position	PW		DW	
	Percentage difference	Pressure difference	Percentage difference	Pressure difference
Bust	8.4%	0.15	8.9%	0.17
Waist	57.0%	0.24	23.4%	0.26
Buttocks	20.3%	0.20	7.1%	0.08
Thigh	3.4%	0.02	8.4%	0.11
Shoulder	-54.8%	-1.22	-4.9%	-0.10
Upper arm	143.6%	0.78	33.6%	0.37
Avg.	29.6%	0.03	12.8%	0.15

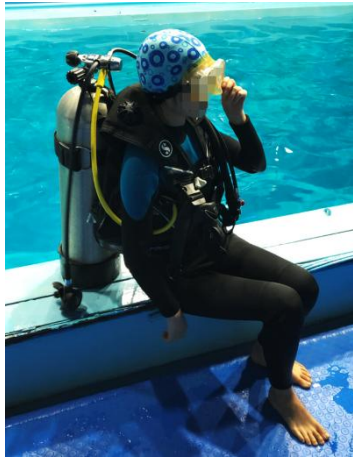


Figure D.12 – Y1 tester scuba diving



Figure D.13– A1 tester scuba diving

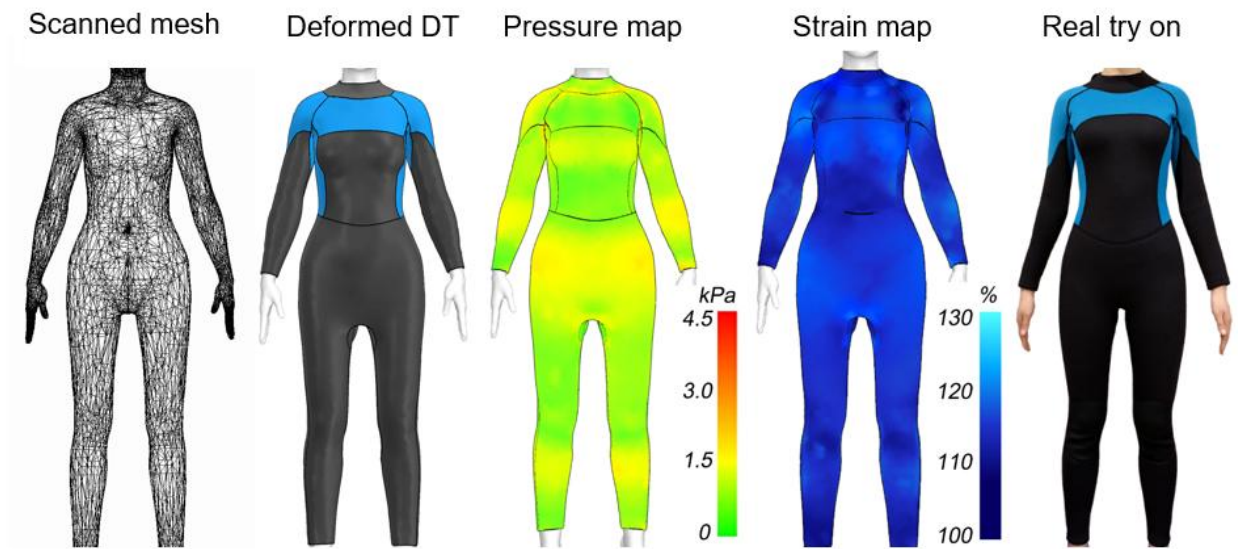


Figure D.14– Virtual and real try on

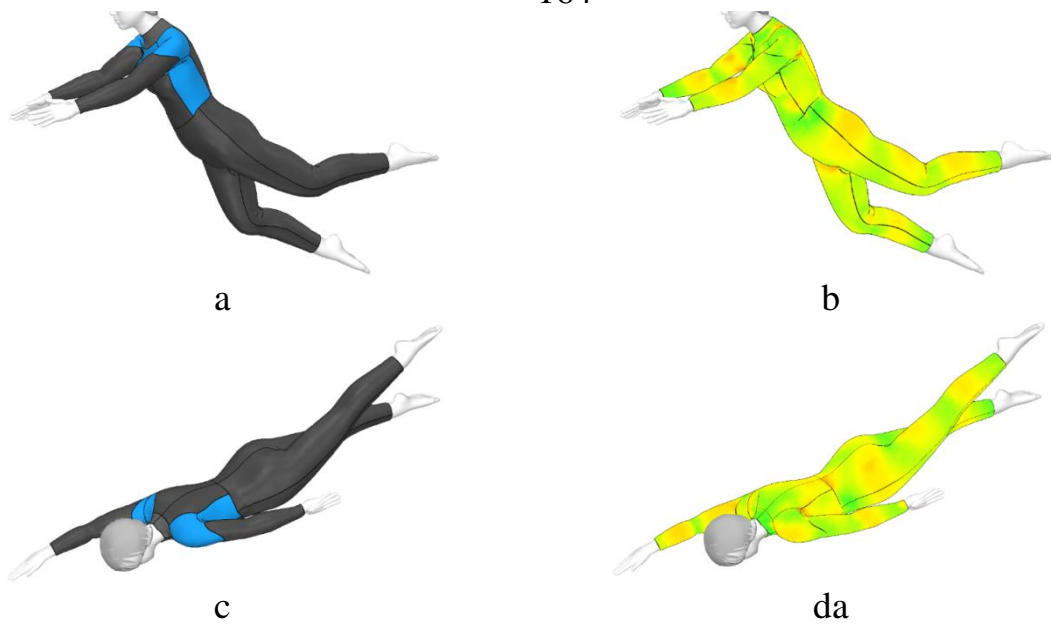


Figure D.15 – Screenshot of DW dynamic swimming actions simulations

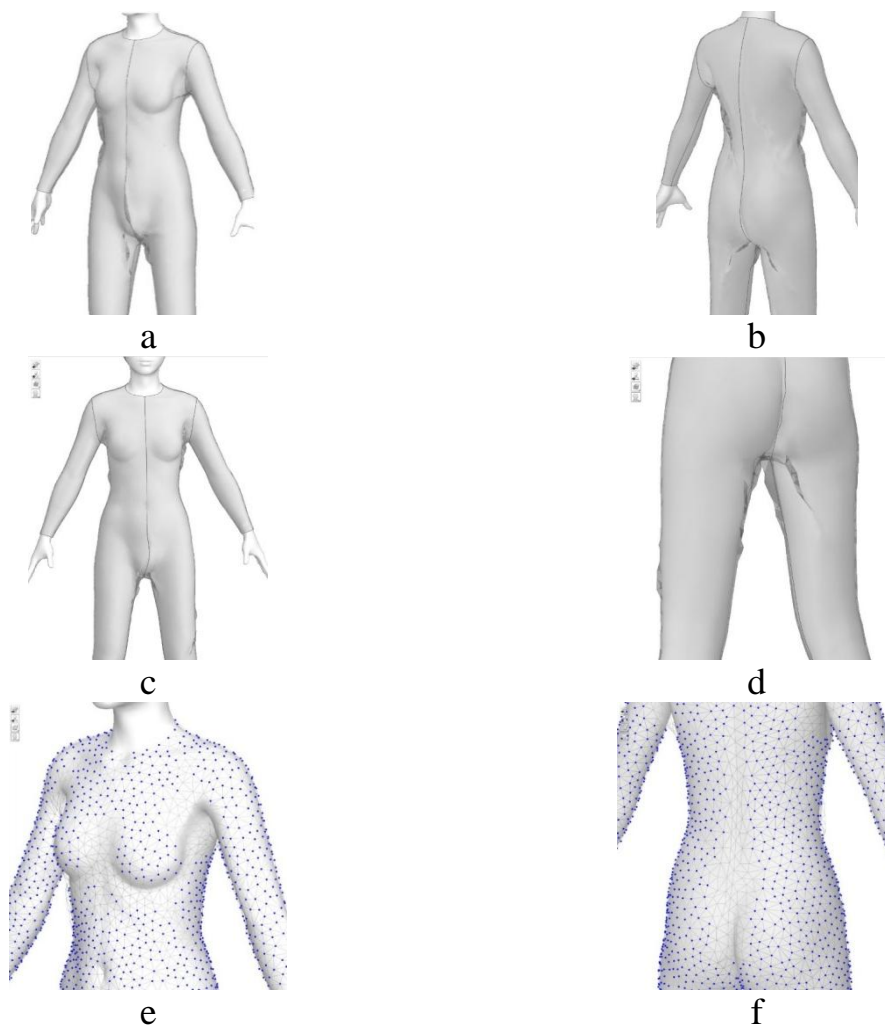


Figure D.16 – Screenshot of prototyping: a, b, c, d – some misfit parts; e, f – contact pressure points on basic wetsuit mesh

APPROVEMENT

Director of JINMING Apparel Company (China) Tianhui

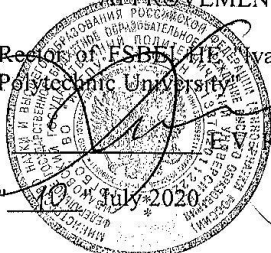
" 9 " July 2020



APPROVEMENT

Recto of FSBEI HE Ivanovo State Polytechnic University Rummyantsev

" 10 " July 2020



ACT production verification of the results
obtained in the dissertation of Wu Xinzhou

We, the undersigned, designer L. Li, technologist X. Weiguo from JINMING apparel company, on the one hand, and head of the department of clothing design V. Kuzmichev and graduate student Wu Xinzhou from FSBEI HE "IVGPU", on the other hand, have compiled this production act verification of the results obtained during the dissertation "Development of female wetsuit design process".

Date of verification – April 2020 – July 2020.

The object of implementation is the design technique for female wetsuit for scuba diving type DW.

Implementation conditions – design and manufacture of models of female wetsuits made of special styrene-chloroprene rubber (composition: polyester + 30% chloroprene rubber + intermediate adhesive bonding layer + 70% butylene-styrene rubber + polyester).

The enterprise was given 8 sets of drawings in 8 sizes.

10 suits of type DW were made using the equipment of the enterprise.


All suits were tested by trying on diving enthusiasts, whose reviews of the ergonomics of the suits and their fit included positive ratings without comments.

CONCLUSION. The developed design drawings meet the requirements of the enterprise, and the manufactured samples have high consumer properties.

From JINMIN

From IVGPU

Designer

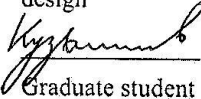
 L. Li

Technologist


 X. Weiguo

JINMING Apparel Company (China)

Head of the Department of clothing design

 V.E. Kuzmichev

Graduate student

 Wu Xinzhou

www.ivgpu.com